ANTIPROTON ANNIHILATION AND PION INTERACTIONS IN COMPLEX NUCLEI

by

Hans Mes

Submitted in partial fulfillment of
the requirements for the degree of
Doctor of Philosophy.

Department of Physics,
Faculty of Pure and Applied Science,
University of Ottawa,
Ottawa, Canada.

May, 1968

to Lynne.

ABSTRACT

The annihilation of stopped antiprotons in nuclear emulsion involves two distinct steps. The antiproton first annihilates with a nucleon of one of the nuclei of the emulsion, to produce pions: these pions may then interact with the nucleus, so that the final product of annihilation consists of pions and nucleons.

The annihilation into pions is a strong interaction and thus isospin should be conserved. Isospin conservation was applied in a statistical manner, to the annihilation process, so that the frequency of certain pionic final states, not observable experimentally, could be predicted. The results were found to compare well with a simple Fermi-statistical model having $\Omega = 8\,\Omega_0$.

The second step in the annihilation, involving the interaction of the pions with the nucleus, was simulated by a Monte Carlo calculation. For the calculation it was assumed that the pions interact with individual nucleons to form an isobar. This isobar could then de-excite by colliding with another nucleon, thus absorbing the pion, or by decaying back to a pion and a nucleon, which corresponds to pion-nucleon scattering.

The Monte Carlo calculations were also applied to

negative pion capture in several nuclei.

In both cases satisfactory agreement could be obtained.

Finally an experiment with mono-energetic pions was started, in the hope of obtaining more information on pion-nucleus interactions. For this purpose a stack of nuclear emulsion was exposed to a beam of 250 Mev positive pions. The flux of pions inside the stack was measured at several places and compared to expected values. From the attenuation of the flux, the pion interaction cross-section in emulsion was estimated and found to agree well with previous experimental results, and with the cross-section expected on the basis of the isobar model.

ACKNOWLEDGEMENTS

I wish to express my gratitude to Professor J.Hébert for his interest and guidance, to Miss Barbara Mills for her invaluable help in the analysis of the data, and to my wife, Lynne, for her encouragement throughout.

I wish to thank Dr. D. Tycko for communicating to us data compiled at Columbia University, Dr. N.W. Tanner, Dr. G. Charpak, Dr. P. Cüer and his research group, and Mr. A. Cordaillat for help in the preparation and irradiation of the emulsion stack, and Dr. I. Ahmad for useful discussion and the use of his data.

I also wish to thank the staff of the computing centre of the University of Ottawa, and, in particular, Mrs. D. Toop, for their consideration.

I wish to acknowledge helpful discussion with Mr. K. Crouch, Dr. J. Kos, Dr. D. Brown, Mr. S. Chakravartty, Mr. R. Molloy, and Mr. A. Filion.

I am grateful to Mrs. J. Hébert and to Miss Lorraine Matte for help in the preparation of this manuscript.

Finally, I am indebted to the National Research Council of Canada for financial assistance in the form of scholarships.

Table of Contents.

List of Illustrations

List of Tables

List of Symbols and Abbreviations.

p	proton
n	neutron
N	nucleon
N^*	isobar, resonance or excited nucleon
$\bar{p}$	antiproton
$\bar{n}$	antineutron
π	pi-meson or pion
ρ	rho-meson
L	relative angular momentum of two particles
S	total spin of a compound state.
J	intrinsic angular momentum of a particle or system of particles
P	parity
T	isotopic spin or isospin
C	C-parity or charge parity
G	G-parity
α	states having isospin one
β	states having isospin zero
Ω_o	theoretically expected volume from which pions are emitted in the Fermi statistical model
Ω	experimentally required volume for the Fermi statistical model
$\langle N_\pi \rangle$	pion multiplicity or average number of pions emitted per annihilation

Mev	million electron volts
f	fermi = 10^{-13} centimeters
μ	microns = 10^{-6} meters
r_o	1.3 fermis
A	Atomic mass number
PEP	Pauli exclusion principle
BSW	model by which a pion is absorbed on a correlated nucleon pair
R	random number
λ	mean free path
$\sigma_{\pi N}$	pion-nucleon cross-section
σ_θ	angular dispersion of beam of particles
$\sigma_\perp$	dispersion of beam of particles
t	distance traversed by beam of particles in target material

Statement of Originality

To the best of the author's knowledge, the following contributions are original:

- The application of isospin conservation in a statistical manner, to supplement the Fermi Statistical model. (This allows a more complete comparison of the theory with experimental data.)
- Application of the above to $\bar{p}p$ and $\bar{p}n$ annihilation to determine the branching ratios, of the various charge configurations for specific pion multiplicities; and to determine the average neutral and charged pion multiplicities.
- The analysis of $\bar{p}$ annihilation data available in the literature to give the following:
  1. The average number of neutral pions emitted per $\bar{p}p$ annihilation, assuming that the neutral pions have the same average energy as charged pions. This showed that, contrary to what had been assumed, on the average more neutral pions are produced than either positive or negative pions.
  2. Furthermore, the analysis sets a lowest experimentally permissible limit for the average neutral pion multiplicity, which is still slightly larger than the positive or negative pion multiplicities.

3. The probability for pion absorption by emulsion nuclei as a function of energy (this is at present the best indication that pion absorption occurs through isobar formation; it also indicates that pions see a potential well when they enter the nucleus).

- A programme to simulate $\bar{p}$ annihilation on complex nuclei (complicated by the fact that only an IBM 1620 was conveniently available).
- The consideration of $\bar{p}$ annihilation as a source of charged and neutral pions, having a definite energy spectrum, in place of many beams of mono-energetic pions. The pions from annihilation have the advantage that they do not have to overcome a coulomb barrier. (It should be noted that neutral pions have a very short life, thus this may be one of very few methods for investigating the behaviour of neutral pions in nuclear matter).
- The use of the isobar model in a Monte Carlo calculation to simulate the interaction of pions with complex nuclei.
- Demonstration that the isobar model easily explains the observed ratio of n-n to n-p pairs produced in π^- capture by complex nuclei.
- From the calculation an indication was obtained that in π^- capture, the pions are absorbed at, or near, the centre of the nucleus.

- The use of a tilted stage to do scanning of emulsion. (A tilted stage allows for a rate of scanning, two or three times faster than a conventional stage . A simple way of modifying a conventional microscope was found).
- The method employed for the analysis of the flux of pions inside a finite emulsion stack based upon multiple coulomb scattering.
- The method of analysis allowed a determination of the actual pion flux attenuation due to pion interactions only.
- An improved value for the positive pion cross-section in emulsion for pion energies from 100 to 230 Mev. This cross-section compared favourably to the cross-section calculated on the basis of the isobar model.

Chapter I

INTRODUCTION

When an antiproton annihilates, it does so generally with a nucleon. The product, or final state of the annihilation is a number of mesons, predominantly pions. The annihilation process is a strong interaction, and thus various quantum numbers are conserved; in particular, it is expected that isospin (isotopic spin) is a good quantum number in the annihilation process. If this is so, then the probability of certain final states may be calculated.

Fermi [1] proposed a statistical model, based on phase space calculations, to explain the annihilation into mesons. With modification, by Cerulus [2], this model can predict the probability of occurrence of certain groups of final states. These groups contain subgroups of different charge states. By including isospin conservation, and applying it in a statistical manner, the model can be expanded to predict the probability of occurrence of these subgroups [3]. Since experimentally, only some of these subgroups, but none of the complete groups, can be observed, the introduction of isospin invariance should allow for a better comparison between theory and experiment.

When antiprotons are allowed to annihilate in

nuclear emulsions, they generally do so by annihilating with one nucleon at the surface of a nucleus [4]. The annihilation centre then radiates pions isotropically, so that approximately half must pass through the nucleus. As it passes through the nucleus, a pion may be scattered off a nucleon, generally producing a fast nucleon which also leaves the nucleus, or it may be absorbed by the nucleus, which then rids itself of the excess energy by emitting energetic nucleons. Exactly how these processes occur is at present not at all certain. It is generally assumed that the pion-nucleon scattering process inside and outside the nucleus are identical except for the Pauli exclusion principle. In 1951, Brueckner, Serber and Watson [5] proposed that the pion is absorbed on a pair of nucleons, present as such in the nucleus. This process (BSW model), however, is not well suited to the absorption of fast pions, since the probability of a pion meeting a pair of nucleons which are sufficiently close, is too small. In 1963, Fraenkel [6] proposed the following method of absorption: the pion (π) when interacting with a nucleon (N), in the nucleus, forms a meta-stable state (N^*), known as an isobar, resonance or excited nucleon, which lives sufficiently long (10^{-23} to 10^{-22} seconds) to allow it to interact with another nucleon, and thus de-excite on

this nucleon. Schematically:

$$\pi + N \longrightarrow N^*$$
$$N^* + N \longrightarrow N + N$$

and thus the pion is absorbed. If the scattering of a pion is then also assumed to occur through the isobar formation, that is:

$$\pi + N \longrightarrow N^*$$
$$N^* \longrightarrow \pi + N$$

then the two processes will have the first step in common.

If one further assumes that the cross-section for the first step is the same pion-nucleon cross-section as measured outside the nucleus, (that is on free nucleons), then the model becomes rather simple; in particular, it lends itself well to a Monte Carlo type of calculation (7). To accomplish this, pions having the energy distribution typical of antiproton-nucleon annihilation were considered to be emitted isotropically at the surface of a nucleus; these pions were then followed through the nucleus and allowed to react according to the isobar model. The energy

of the pions and protons thus obtained were compared to the experimentally determined spectra.

The model was then also used to simulate negative pion capture at rest in several heavy nuclei [8]. In this case both neutron and proton spectra could be compared.

The interaction of energetic pions was also simulated, but in this case little experimental data is available . This group, thus, started a study of pion interactions in nuclear emulsions. In this thesis a preliminary experiment in the energy region of 100 to 250 Mev. is described.

Chapter II

ANTIPROTON-NUCLEON ANNIHILATION INTO PIONS

II-1 Introduction

An antiproton ($\bar{p}$) is a particle having the same mass as a proton (p), but opposite charge (-1), parity (-1) and baryon number (-1). The antiproton and proton both have spin (J) 1/2, and together with the antineutron ($\bar{n}$) and neutron (n), respectively form two isospin doublets.

In a nucleon-antinucleon collision, the combined state has a baryon number of zero, making it identical to a very heavy meson, which in this case is highly unstable; in 96% of all cases, it breaks up into pions[9,10] through strong interactions. The other 4% contains kaons, which also eventually decay into pions, but through weak interactions. Since the kaons form only a small fraction of the total, they can be neglected.

The antinucleon-nucleon system has a total mass of about 1880 Mev, while the pion mass is about 140 Mev, so that a maximum of 13 pions can be produced. In reality, though, one finds that the production of 4,5 and 6 pions accounts for approximately 80% of all annihilations,

and that the production of more than 7 pions is rare.

The antinucleon-nucleon system can have an isospin (T) of 0 or 1, and a charge of 1, 0 or -1, depending on which nucleon-antinucleon pair is used. The particular case of interest here is the antiproton-proton system, also called protonium. The antiproton 'replaces' the electron in a hydrogen atom, and from this atomic state the annihilation occurs. It appears that the majority of annihilations occur from an S atomic state; that is, either a triplet ($^3S_1$) or singlet ($^1S_0$) state. The principal quantum number may, however, be quite large.[11]

The annihilation into pions is reasonably well described by a modified Fermi-statistical* model. The centre of annihilation can be pictured as an extremely hot cloud which expands, and emits pions in the process. Since this is a statistical process, the energy distribution and the pion multiplicities can be calculated from phase-space integrals. Good agreement with experiment can, however,

---

*For this model one calculates the number of available states in a volume (Ω) and a momentum space limited by the available energy. The interaction volume is generally assumed to be determined by the Compton wave length of pions, however, in practice it is found that this volume (Ω_o) is too small to give the expected results.

only be obtained if one takes into consideration the emission of heavier meta-stable mesons. The model can predict the frequency with which a certain number of pions are produced, but not the frequency of a certain charge configuration; for example, it can predict the frequency with which five pions are produced, but not specifically the frequency for $\pi^0 2\pi^+ 2\pi^-$ production. Experimentally only this latter case can be observed*, but the five pion state also contains the $5\pi^0$ and $3\pi^0\pi^+\pi^-$ charge configurations, so that a direct comparison cannot be made. In general only the overall multiplicity and the energy distribution of the pions are compared.

Since the annihilation proceeds through strong interactions, the conservation of isospin should apply. The antinucleon-nucleon system has a definite isospin at annihilation; if one then assumes that after a pion is emitted the remaining centre still has a definite isospin, the relative rates may be predicted. Such calculations have been performed.

---

*Neutral pions can not at present be detected efficiently, so that their presence is only known from the missing mass in a kinematic fit.

II-2 Experimental Data

For the calculation, pion multiplicities up to seven only were considered. Table 1 shows the possible modes (charge configurations) and their experimental frequency[9,10,12], when known. From the six values marked with an asterisk (*) the remaining ones are to be calculated and compared to the experimental values.

Also shown in table 1 are the total, neutral and charged pion multiplicites ($\langle N_\pi \rangle$, $\langle N_{\pi^0} \rangle$ and $\langle N_{\pi^\pm} \rangle$ respectively) for annihilations having 0,2,4 and 6 charged pions, and for all annihilations. The charged pion multiplicity is simply the number of charged pions multiplied by the fraction of annihilations having this number of charged pions; this can easily be calculated from the available data. This same procedure cannot be used for the neutral pions; instead, one has to assume that the neutral pions have the same energy distribution as the charged pions, and thus their multiplicity can be calculated from the average energy of the charged pions. For example, in the case of two charged pions and more than one neutral pion ($\pi^+\pi^-X^0$), the average charged pion energy[13] is 381.3 Mev (estimated to be accurate to better than 1%). Since, per annihilation, 1878 Mev is available, from the ratio the average number of pions per annihilation in this case is 4.93. Since two charged pions accompany the annihilation,

Table 1

Observed Frequencies (%) and Pion Multiplicities of Various Pionic Final States in Antiproton-proton Annihilation.

No. of Pions.	No. of Charged Pions				
	0	2	4	6	
2	$2\pi^0$	$\pi^+\pi^-$ 0.36 ± 0.04 *			
3	$3\pi^0$	$\pi^0\pi^+\pi^-$ 6.3 ± 0.6 *			
4	$4\pi^0$	$2\pi^0\pi^+\pi^-$	$2\pi^+2\pi^-$ 5.8 ± 0.2 *		
5	$5\pi^0$	$3\pi^0\pi^+\pi^-$	$\pi^0 2\pi^+ 2\pi^-$ 20.2 ± 0.8 *		
6	$6\pi^0$	$4\pi^0\pi^+\pi^-$	$2\pi^0 2\pi^+ 2\pi^-$ 12.5 ± 1.6	$3\pi^+3\pi^-$ 1.9 ± 0.2 *	
7	$7\pi^0$	$5\pi^0\pi^+\pi^-$	$3\pi^0 2\pi^+ 2\pi^-$ 4.8 ± 0.9	$\pi^0 3\pi^+ 3\pi^-$ 1.7 ± 0.2 *	Total
Total†	3.2 ± 0.5	42.6 ± 1.1	45.8 ± 1.0	3.8 ± 0.2	95.4 ± 1.6
$\langle N_{\pi^0} \rangle$	$0.16 \pm .02$	$1.05 \pm .04$	$0.65 \pm .03$	$.020 \pm .004$	$1.88 \pm .05$
$\langle N_{\pi^\pm} \rangle$	0.0	$0.85 \pm .02$	$1.83 \pm .04$	$.23 \pm .01$	$2.95 \pm .04$
$\langle N_{\pi} \rangle$	$0.16 \pm .02$	$1.90 \pm .05$	$2.48 \pm .05$	$.25 \pm .01$	$4.83 \pm .07$

*These six values were used in the calculations.

†Including more than 7 pions.

the average number of neutral pions is 2.93. From table 1, this case occurs with a frequency of 34.8± 1.2 %, so that the contribution to the neutral pion multiplicity for all annihilations is the product, or 1.02± .04. (The error comes from the uncertainty in the value of the frequency). To obtain the neutral pion multiplicity due to annihilations having two charged pions, the contribution from $\pi^+\pi^-\pi^o$ must be added: also a correction, amounting to about 3%, must be made for electromagnetic decays*. The values thus obtained (table 1) agree well with those compiled by Apostolakis et al.[12], from earlier experiments.

The total pion multiplicity is simply the sum of the charged and neutral pion multiplicities. Table 1 also shows the multiplicities for all annihilations. These values are based on all experimental data available [9,10,12,13,14,15].

An examination of the multiplicities for all annihilations shows that more neutral pions are produced, than either positive or negative ones. This can also be seen, if it is assumed that no annihilation leads to more

---

*We are indebted to Professor J. Vandermeulen (from Université de Liège) for bringing this to our attention.

than two neutral pions; in this case a lower limit of 1.47 is obtained for the neutral pion multiplicity; since this is also the multiplicity of positive and negative pions, there will be more neutral pions produced than either negative or positive ones.

The fact that the multiplicities are not equal indicates that the charge is not selected at random, but that there is a definite process by which the charges are determined.

II-3 Application of Isospin Conservation to Antiproton-proton Annihilation

The antiproton-proton system is assumed to annihilate predominantly from a $^1S_0$ and $^3S_1$ state, in which case table 2 lists the quantum numbers* and the allowed pionic final states[18]. It may be observed, that starting from a T=1 state, an even number of neutral pions only cannot be obtained due to either C- or G-parity conservation. Applying isospin conservation imposes this same restriction. A similar case is found starting from a T=0 state† . Since all other modes are allowed, isospin conservation alone imposes all necessary restrictions.

For further discussion it is convenient to denote the three states having T=1 by α^+,α^0 and α^-, and the state having T=0 by β. The following four schemes may then be written for the breaking up of an α or β state:

---

*See appendix 1 for an explanation of the quantum numbers.
† The two neutral pion final state is forbidden from all S states, however it is allowed from either a $^3P_0$ or $^3P_2$ state having T=0. For the calculations, since the contribution from two neutral pions is small, it was assumed that it could occur through these P states.

Table 2

Selection Rules for Antiproton-proton and Antineutron-neutron Annihilation from an S Atomic State.

	$^1S_0$	$^1S_0$	$^3S_1$	$^3S_1$
J^P	0^-	0^-	1^-	1^-
T^{CG}	0^{++}	1^{+-}	0^{--}	1^{-+}
$2\pi^0$	P	PG	GC	C
$\pi^+\pi^-$	P	PG	G	
$3\pi^0$	G		C	GC
$\pi^0\pi^+\pi^-$	G			G
$4\pi^0$		G	GC	C
$2\pi^0\pi^+\pi^-$		G	G	
$2\pi^+2\pi^-$		G	G	
$5\pi^0$	G		C	GC
$3\pi^0\pi^+\pi^-$	G			G
$\pi^0 2\pi^+ 2\pi^-$	G			G
$6\pi^0$		G	GC	C
$4\pi^0\pi^+\pi^-$		G	G	
$2\pi^0 2\pi^+ 2\pi^-$		G	G	
$3\pi^+ 3\pi^-$		G	G	
$7\pi^0$	G			GC
$5\pi^0\pi^+\pi^-$	G			G
$3\pi^0 2\pi^+ 2\pi^-$	G			G
$\pi^0 3\pi^+ 3\pi^-$	G			G

P,C,G indicate parity, C-parity and G-parity forbidden respectively.

$$\alpha \longrightarrow \alpha\,\alpha \qquad \ldots\ldots (1)$$

$$\alpha \longrightarrow \alpha\,\beta \qquad \ldots\ldots (2)$$

$$\beta \longrightarrow \alpha\,\alpha \qquad \ldots\ldots (3)$$

$$\beta \longrightarrow \beta\,\beta \qquad \ldots\ldots (4)$$

Processes 3 and 4 should statistically be equally probable; processes 1 and 2, however, differ in that process 1, like 3 and 4, produces two indistinguishable particles. Thus process 2 may be written either as $\alpha \longrightarrow \alpha\beta$ or $\alpha \longrightarrow \beta\alpha$; these are equally probable and it was assumed that each is as probable as process 1.

Processes 1,2 and 3 may be considered as the emission of a pion, in accord with the Fermi-model, and process 4 would have to be considered as the splitting up of the centre into two new centres.

With the help of Clebsch-Gordan coefficients* the probability for different charge states may be computed. Table 3 shows all possible combinations and their probabi-

---

*See appendix 2

Table 3

Relative Frequency of Decay Products.

Initial State	Final State	Probability
α^0	$\pi^+ \alpha^-$	1/6
α^0	$\pi^- \alpha^+$	1/6
α^0	$\pi^0 \beta$	2/3
α^+	$\pi^+ \alpha^0$	1/6
α^+	$\pi^0 \alpha^+$	1/6
α^+	$\pi^+ \beta$	2/3
α^-	$\pi^- \alpha^0$	1/6
α^-	$\pi^0 \alpha^-$	1/6
α^-	$\pi^- \beta$	2/3
β	$\pi^+ \alpha^-$	1/6
β	$\pi^0 \alpha^0$	1/6
β	$\pi^- \alpha^+$	1/6
β	$\beta \beta$	1/2

lity of occurrence. From experimental data [9,10] it appears that all of these combinations are possible; there is, however no way of observing a $\beta\beta$ state since this would result in at least two neutral pions.

By allowing the centre to emit pions, or break up, with the probabilities just calculated, the relative rates of different charge configurations may be found. Since we are, however only interested in pionic final states, any mode containing a β state should not be counted. Thus the associated pion states have to be renormalized.

For example, the case of antiproton-proton annihilating through the T=1 state to two pions:

$$\alpha^o \longrightarrow \pi^+\pi^- \qquad \text{Probability } 1/3$$
$$\longrightarrow \pi^o\,\beta \qquad \text{Probability } 2/3$$

but $\pi^o\beta$ is not a two pion state, and thus:

$$\alpha^o \longrightarrow \pi^+\pi^- \quad 100\%$$

Similarly for the antiproton-proton annihilating through the T=1 state to three pions:

	Probability		Probability	Renormalized Probability
$\alpha^\circ \longrightarrow$	$\pi^-\alpha^+$ (1/6)	$\longrightarrow$	$\pi^-\pi^+\pi^\circ$ (1/18)	(1/6)
		$\longrightarrow$	$\pi^-\pi^+\beta$ (2/18)	0
$\longrightarrow$	$\pi^+\alpha^-$ (1/6)	$\longrightarrow$	$\pi^+\pi^-\pi^\circ$ (1/18)	(1/6)
		$\longrightarrow$	$\pi^+\pi^-\beta$ (2/18)	0
$\longrightarrow$	$\pi^\circ\beta$ (2/3)	$\longrightarrow$	$\pi^\circ\pi^+\pi^-$ (2/9)	(4/9)
		$\longrightarrow$	$\pi^\circ\pi^\circ\pi^\circ$ (1/9)	(2/9)
		$\longrightarrow$	$\pi^\circ\beta\beta$ (1/3)	0

so that one obtains: $3\pi^\circ/\pi^+\pi^-\pi^\circ = 2/7$. Since $\pi^+\pi^-\pi^\circ$ occurs with a frequency of $(6.3\pm.6)\%$, the charge configuration $3\pi^\circ$ should occur with a frequency of $(1.8\pm.2)\%$, provided the antiproton-proton system annihilates through the T=1 state.

This procedure becomes tedious for more pions, and will not be shown. Instead the final results for the antiproton-proton system to annihilate through the T=1 or T=0 state are shown in tables 4 and 5, respectively. Only the neutral pion multiplicity is shown for comparison, since the other two multiplicities are contained implicitly in the total charged prong frequency and the neutral pion multiplicity. For comparison, the prediction of the simple Fermi-statistical model having $\Omega=8\Omega_o$ is shown [19]; this particular case was chosen because it has approximately the

Table 4

Calculated Frequencies (%) for Antiproton-proton Annihilation through a T=1 State.

No. of Pions.	No. of Charged Pions				Total	Predicted Total from Fermi Model $\Omega=8\Omega_o$
	0	2	4	6		
2	0.0	0.36 ± 0.04 *			0.4 ± 0.04	0.3
3	1.8	6.3 ± 0.6 *			8.1 ± 0.8	5.4
4	0.0	22.7	5.8 ± 0.2 *		28.5 ± 1.0	26.2
5	2.1	12.3	20.2 ± 0.8 *		34.6 ± 1.4	38.7
6	0.0	4.5	11.6 ± 1.2 (12.5 ± 1.6) *	1.9 ± 0.2 *	18.0 ± 1.9	21.4
7	0.03	0.4	4.3 ± 0.5 (4.8 ± 0.6) *	1.7 ± 0.2 *	6.4 ± 0.8	3.4
Total	3.9 ± 0.3	46.6 ± 1.2	41.9 ± 1.5	3.6 ± 0.3	96.0 ± 2.8	95.4
Observed Total	3.2 ± 0.5	42.6 ± 1.1	45.8 ± 1.0	3.8 ± 0.2	95.4 ± 1.6	
$\langle N_{\pi^0} \rangle$	.16 ± 0.01	1.09 ± 0.03	0.58 ± 0.03	.017 ± .002		
Observed $\langle N_{\pi^0} \rangle$	.16 ± 0.02	1.05 ± 0.04	0.65 ± 0.03	.020 ± .004		

*Observed values.

Table 5

Calculated Frequencies (%) for Antiproton-proton Annihilation through a T=0 State.

No. of Pions.	No. of Charged Pions				Total	Predicted Total from Fermi Model $\Omega=8\Omega_o$
	0	2	4	6		
2	0.18	0.36 ± 0.04 *			0.5 ± 0.06	0.3
3	0.0	6.3 ± 0.6 *			6.3 ± 0.6	5.4
4	1.3	6.6	5.8 ± 0.2 *		13.7 ± 0.6	26.2
5	0.0	10.2	20.2 ± 0.8 *		30.4 ± 1.2	38.7
6	0.2	1.5	7.0 ± 0.7 (12.5 ± 1.6) *	1.9 ± 0.2 *	10.6 ± 1.0	21.4
7	0.0	0.5	1.9 ± 0.2 (4.8 ± 0.6) *	1.7 ± 0.2 *	4.1 ± 0.5	3.4
Total	1.7 ± 0.2	25.5 ± 0.8	34.9 ± 1.1	3.6 ± 0.3	75.6 ± 1.8	95.4
Observed Total	3.2 ± 0.5	42.6 ± 1.1	45.8 ± 1.0	3.8 ± 0.2	95.4 ± 1.6	
$\langle N_{\pi^o} \rangle$	.07 ± .01	0.59 ± 0.02	0.40 ± 0.02	.017 ± .002		
Observed $\langle N_{\pi^o} \rangle$	.16 ± .02	1.05 ± 0.04	0.65 ± 0.03	.020 ± .004		

* Observed values.

right total pion multiplicity for all annihilations.

The agreement for T=1 state is very reasonable, however it is expected that the antiproton-proton annihilates at equal rates through both isospin states [11,12]; in that case the agreement is poor. This leads us to believe that some channels are strongly dominated by a specific resonance; in particular, from antiproton-neutron data[20], it appears that in the 5 pion case the T=1 centre emits a pion to leave a T=0 state. If it is assumed that this occurs in all cases, the results shown in table 6 are obtained.

Finally table 7 shows the experimental pion multiplicities for all annihilations and the calculated multiplicities for all three cases.

Table 6

Calculated Frequencies (%) for Antiproton-proton Annihilation through a T=1 or a T=0 State with Equal Probability. (Modified scheme)

No. of Pions.	No. of Charged Pions				Total	Predicted Total from Fermi Model $\Omega = 8\Omega_0$
	0	2	4	6		
2	0.18	0.36 ± 0.04 *			0.5 ± 0.1	0.3
3	1.3	6.3 ± 0.6 *			7.6 ± 0.7	5.4
4	1.3	20.8	5.8 ± 0.2 *		27.9 ± 1.0	26.2
5	1.7	15.1	20.2 ± 0.8 *		37.0 ± 1.3	38.7
6	0.2	5.0	14.0 ± 1.4 (12.5 ± 1.6) *	1.9 ± 0.2 *	21.1 ± 2.2	21.4
7	0.0	0.7	3.2 ± 0.4 (4.8 ± 0.6) *	1.7 ± 0.2 *	5.6 ± 0.6	3.4
Total	4.7 ± 0.3	48.3 ± 1.3	43.2 ± 1.7	3.6 ± 0.3	99.7 ± 2.9	95.4
Observed Total	3.2 ± 0.5	42.6 ± 1.1	45.8 ± 1.0	3.8 ± 0.2	95.4 ± 1.6	
$\langle N_{\pi^0} \rangle$	.19 ± .02	1.17 ± 0.05	0.58 ± 0.06	.017 ± .002		
Observed $\langle N_{\pi^0} \rangle$	.16 ± .02	1.05 ± 0.04	0.65 ± 0.03	.020 ± .004		

* Observed values.

Table 7

Calculated and Observed Pion Multiplicities for Antiproton-proton Annihilation.

	Calculated			Observed
	T = 1	T = 0	Combined (Modified scheme)	
$\langle N_{\pi^0} \rangle$	1.83 ± 0.04	1.06 ± 0.03	1.95 ± 0.04	1.88 ± 0.05
$\langle N_{\pi^\pm} \rangle$	2.82 ± 0.04	2.12 ± 0.03	2.91 ± 0.04	2.95 ± 0.04
$\langle N_{\pi} \rangle$	4.65 ± 0.07	3.19 ± 0.06	4.86 ± 0.07	4.83 ± 0.07

II-4 Antiproton-neutron Annihilation

In the case of antiproton-neutron annihilation, the same procedure may be used; in this case, however, the system can only be in a T=1 state. The experimental data [12,20] is shown in table 8*. The pion multiplicities were calculated in the same manner as for the antiproton-proton annihilation. The neutral pion multiplicity was calculated from some of the antiproton-proton data [13], on the assumption that the antiproton-proton and antiproton-neutron annihilation produce comparable energy spectra; the calculated multiplicities were found to compare well with data from Apostolakis et al.[12], and to improve statistics, were combined with it.

The experimental data was obtained from antiproton annihilation on deuterium, and thus it would again be reasonable to assume that annihilation occurs from an S atomic state [21]. Table 9 gives the relevant quantum numbers, and lists the allowed and forbidden decay channels. No channel is forbidden if annihilation occurs from an S atomic state.

Application of the simplest version of the mo-

---

* In this case, kaons were not separated.

Table 8

Observed Frequencies (%) and Pion Multiplicities of Various Pionic Final States in Antiproton-neutron Annihilation.

No. of Pions.	No. of Charged Pions				
	1	3	5	7	
2	$\pi^0\pi^-$ 0.7 ± 0.3				
3	$2\pi^0\pi^-$	$2\pi^-\pi^+$ 1.6 ± 0.2 *			
4	$3\pi^0\pi^-$	$\pi^0 2\pi^-\pi^+$ 21.8 ± 2.2 *			
5	$4\pi^0\pi^-$	$2\pi^0 2\pi^-\pi^+$	$3\pi^- 2\pi^+$ 5.2 ± 0.5 *		
6	$5\pi^0\pi^-$	$3\pi^0 2\pi^-\pi^+$	$\pi^0 3\pi^- 2\pi^+$ 15.1 ± 1.0 *		
7	$6\pi^0\pi^-$	$4\pi^0 2\pi^-\pi^+$	$2\pi^0 3\pi^- 2\pi^+$	$4\pi^- 3\pi^+$ 0.4 ± 0.1 *	Total
Total.	16.4 ± 0.5	59.7 ± 1.2	23.4 ± 0.7	0.4 ± 0.1	99.9 ± 1.5
$\langle N_{\pi^0} \rangle$	$0.64 \pm .03$	$1.05 \pm .07$	$0.23 \pm .02$	0.0	$1.92 \pm .08$
$\langle N_{\pi^+} \rangle$	0.0	$0.60 \pm .01$	$0.47 \pm .02$	$.012 \pm .003$	$1.08 \pm .03$
$\langle N_{\pi^-} \rangle$	$.164 \pm .005$	$1.19 \pm .02$	$0.70 \pm .02$	$.016 \pm .004$	$2.07 \pm .03$
$\langle N_{\pi} \rangle$	$0.80 \pm .03$	$2.84 \pm .07$	$1.40 \pm .03$	$0.03 \pm .01$	$5.07 \pm .09$

Note- In this case K-mesons have not been separated.
* These five values were used in the calculations.

Table 9

Selection Rules for Antiproton-neutron and Antineutron-proton Annihilation from an S Atomic State.

	$^1S_0$	$^3S_1$
J^P	0^-	1^-
T^G	1^-	1^+
$\pi^0\pi^-$	PG	
$2\pi^0\pi^-$		G
$2\pi^-\pi^+$		G
$3\pi^0\pi^-$	G	
$\pi^0 2\pi^-\pi^+$	G	
$4\pi^0\pi^-$		G
$2\pi^0 2\pi^-\pi^+$		G
$3\pi^- 2\pi^+$		G
$5\pi^0\pi^-$	G	
$3\pi^0 2\pi^-\pi^+$	G	
$\pi^0 3\pi^- 2\pi^+$	G	
$6\pi^0\pi^-$		G
$4\pi^0 2\pi^-\pi^+$		G
$2\pi^0 3\pi^- 2\pi^+$		G
$4\pi^- 3\pi^+$		G

P and G indicate parity and G-parity forbidden respectively.

del yields the results shown in table 10; the agreement is found to be poor. A re-examination of the table shows that only the five pion case disagrees badly with the simple Fermi-model, thus suggesting that it may be responsible for the poor result. Bettini et al.[20] did in fact find that the $3\pi^-2\pi^+$ is strongly dominated by a resonance. That is, they found that the antiproton-neutron emits a negative pion to leave either a T=0 or T=2 state, which subsequently splits into two ρ-mesons. (a ρ-meson decays into two pions) It seems highly unlikely that the intermediate state has $T = 2^*$; thus it will be assumed that it is a T=0 state.

In that case several schemes can be worked out which will give better results. None of them are, however, entirely satisfactory. One example is the following:

$$\alpha^- \longrightarrow \pi^- \beta \longrightarrow \pi^- \rho\rho \longrightarrow 5\pi \qquad 37\%$$
$$\alpha^- \longrightarrow \alpha^- \beta \longrightarrow \pi^0 \alpha^- \beta \longrightarrow 5\pi \qquad 63\%$$

The results for this is shown in table 11.

---

*The inclusion of a T=2 state gives the ratio $3\pi^-2\pi$: $2\pi^0 2\pi^- \pi^+$ = 1:14 which leads to absurd results.

Table 10

Calculated Frequencies (%) for Antiproton-neutron Annihilation.

No. of Pions.	No. of Charged Pions				Total	Predicted Total from Fermi Model $\Omega=8\Omega_o$
	1	3	5	7		
2	0.7 ± 0.3 *				0.7 ± 0.3	0.3
3	1.0	1.6 ± 0.2 *			2.6 ± 0.3	5.6
4	2.6	21.8 ± 2.2 *			24.4 ± 2.3	27.4
5	1.3	9.9	5.2 ± 0.5 *		16.4 ± 1.5	40.6
6	0.6	9.7	15.1 ± 1.0 *		25.4 ± 1.7	22.4
7	0.1	0.6	1.9	0.4 ± 0.1 *	3.0 ± 0.8	3.6
Total	6.3 ± 0.5	43.6 ± 2.5	22.2 ± 1.3	0.4 ± 0.1	72.5 ± 3.4	99.9
Observed Total	16.4 ± 0.5	59.7 ± 1.2	23.4 ± 0.7	0.4 ± 0.1	99.9 ± 1.5	
$\langle N_{\pi^o} \rangle$	0.19 ± 0.01	0.73 ± 0.04	0.19 ± 0.02	0.0		
Observed $\langle N_{\pi^o} \rangle$	0.64 ± 0.03	1.05 ± 0.07	0.23 ± 0.02	0.0		

* Observed values.

Table 11

Calculated Frequencies (%) for Antiproton-neutron Annihilation.
(Modified scheme)

No. of Pions.	No. of Charged Pions				Total	Predicted Total from Fermi Model $\Omega=8\Omega_o$
	1	3	5	7		
2	0.7 ± 0.3 *				0.7 ± 0.3	0.3
3	1.0	1.6 ± 0.2 *			2.6 ± 0.3	5.6
4	2.6	21.8 ± 2.2 *			24.4 ± 2.3	27.4
5	8.8	28.0	5.2 ± 0.5 *		42.0 ± 4.0	40.6
6	0.6	9.7	15.1 ± 1.0 *		25.4 ± 1.7	22.4
7	0.1	0.6	1.9	0.4 ± 0.1 *	3.0 ± 0.8	3.6
Total	13.8 ± 0.8	61.7 ± 3.5	22.2 ± 1.3	0.4 ± 0.1	98.1 ± 5.0	99.9
Observed Total	16.4 ± 0.5	59.7 ± 1.2	23.4 ± 0.7	0.4 ± 0.1	99.9 ± 1.5	
$\langle N_{\pi^0} \rangle$	0.49 ± 0.04	1.09 ± 0.07	0.19 ± 0.02	0.0		
Observed $\langle N_{\pi^0} \rangle$	0.64 ± 0.03	1.05 ± 0.07	0.23 ± 0.04	0.0		

* Observed values.

Table 12 shows the experimental and calculated pion multiplicities for all annihilations.

Table 12

Calculated and Observed Pion Multiplicities for Antiproton-neutron Annihilation.

	Calculated		Observed
	Original scheme	Modified scheme	
$\langle N_{\pi} \rangle$	3.62 ± 0.16	4.90 ± 0.20	5.07 ± 0.09
$\langle N_{\pi^-} \rangle$	1.62 ± 0.07	2.05 ± 0.08	2.07 ± 0.03
$\langle N_{\pi^+} \rangle$	0.89 ± 0.04	1.07 ± 0.04	1.08 ± 0.03
$\langle N_{\pi^0} \rangle$	1.11 ± 0.05	1.78 ± 0.08	1.92 ± 0.08

II-5 Discussion

From the analysis of antiproton annihilation with nucleons, it is apparent that a statistical model can predict the proper frequencies, provided some resonances are included. In principle then, one could start from a Fermi-statistical model and predict all pion final state frequencies. For a statistical model however, it is essential that no resonance dominates. This can be achieved either if there is no resonance possible, or if so many resonances are possible, that none is preferred. The latter appears to be the case here.

In this analysis, it was assumed that the annihilation could occur with equal probability from either the triplet or singlet S state. This is not a necessary condition [21]. In the case of antiproton-proton annihilation this would not affect the results significantly, unless annihilation from either a T=1 or T=0 state also does not occur with equal frequency. However, in the annihilation with neutrons this could be important, and may in fact account for the poor agreement. Thus it might be necessary to include the relative rate of triplet to singlet annihilation as an additional parameter.

It was also found that the charged and neutral

pion multiplicities impose strict conditions on possible variables . In particular, starting from a T=0 state one must end up with equal pion multiplicities for all charge states. But experimentally more neutral pions are observed in antiproton-proton annihilation. Thus this excess must come from the T=1 state. This partially explains why the assumption of a T=1 state going to a pion and a T=0 state gives better results; it ensures an excess of neutral pions. We seem, however, to have too many neutral pions now, indicating that perhaps only some channels follow this assumption.

Finally, variations in the statistical factors, that is the relative rate of α and β production, may affect the results slightly. The inclusion of higher isospin states (such as T=2) will also affect the outcome, but to a much greater degree.

Chapter III

ANTIPROTON-NUCLEUS ANNIHILATION.

III-1 Introduction

When an antiproton annihilates on a nucleus, it annihilates with one of the nucleons at the surface of the nucleus [4]. The annihilation centre emits pions in all directions, and consequently some will traverse the nucleus. Inside the nucleus, these pions have a chance to interact with the remaining nucleons, thus decreasing the total pion multiplicity observed, and adding nucleons to the final products of the annihilation.

Most experiments on antiproton-nucleus annihilation have been performed with emulsion [4,12,16,17,22], although some have also been done in propane bubble chambers [14]. In emulsion one finds a charged pion multiplicity, $\langle N_{\pi^{\pm}} \rangle$, of 2.44±.07 (about 22% less than in antiproton-nucleon annihilation) and a mean pion energy of 365±8 Mev. (about the same as in antiproton-proton annihilation). On the average an antiproton star (annihilation event) will have 3.29±.11 protons, of mean energy 129±6 Mev.

Figure 1 and 2 show the charged pion energy distribution and proton energy distribution respectively; the number of particles per Mev per 1000 annihilations have been plotted, on a log-log scale, versus the energy of the particle. Also shown in figure 1 is the pion energy distribution for antiproton-proton annihilation, determined by the Nevis Laboratories [13]. A surprisingly large difference between the distributions is apparent between 100 and 200 Mev. To illustrate this, the fractional difference between these two distributions, was plotted as a function of energy (Figure 3). In this figure, a peak is very obvious*, and resembles the peaking observed in the pion-nucleon cross-section [23] (Figure 4). In pion-nucleon scattering in free space, the cross-section suddenly increases to a very large value at a pion incident energy of about 180 Mev, which is associated with the resonance production of $N^{*}_{3/2,3/2}$ (1238). This isobar is a meta-stable particle of very short life (10^{-23} seconds), having intrinsic angular momentum 3/2 and isospin 3/2; its mass is centred about 1238 Mev. The pion-nucleon cross-section

---

*Since only half of the pions go through the nucleus, an absorption of 50% indicates that the nucleus is completely opaque to pions of this energy.

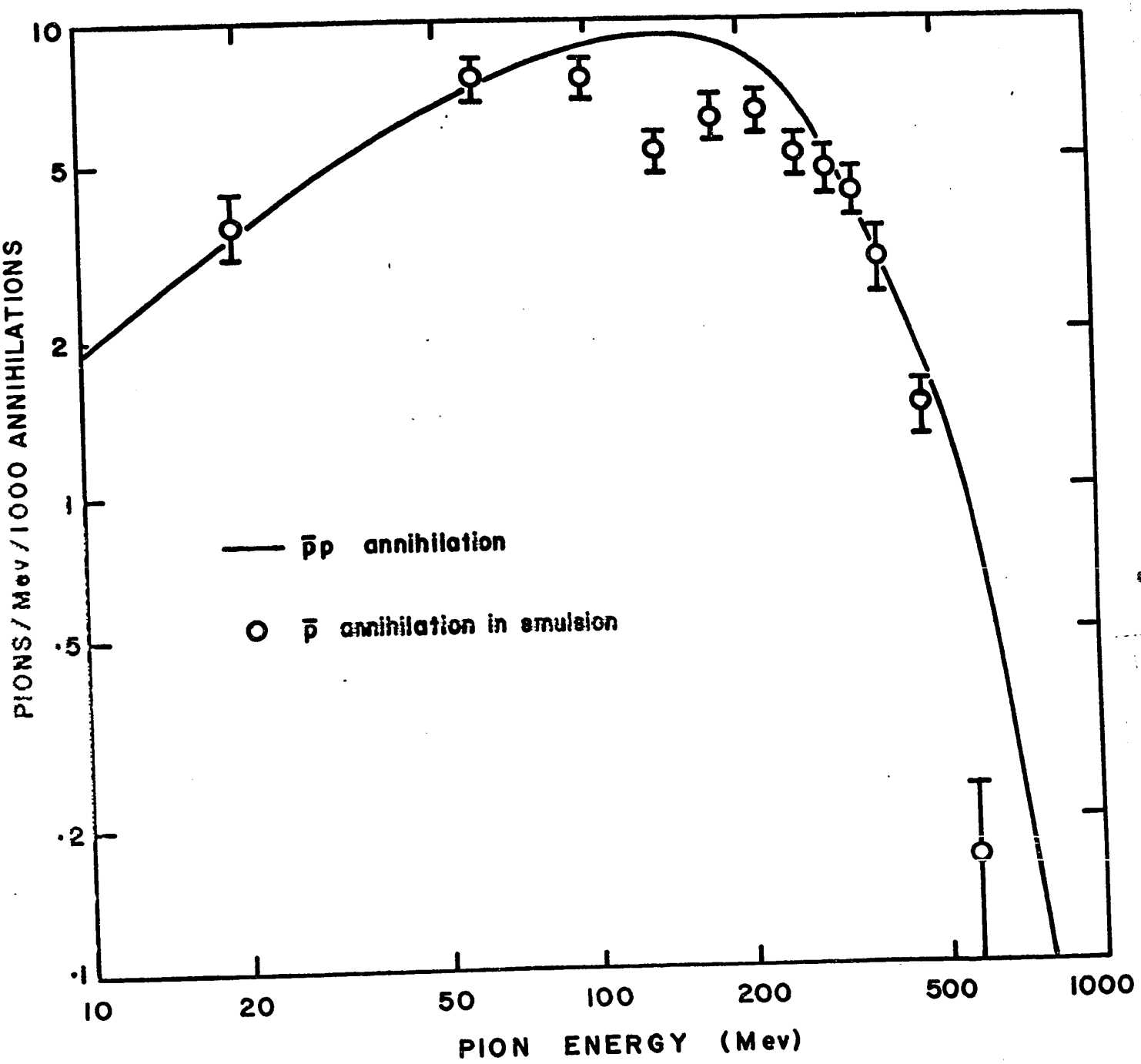

Figure 1- Charged Pion Energy Distribution from $\bar{p}$ Annihilation

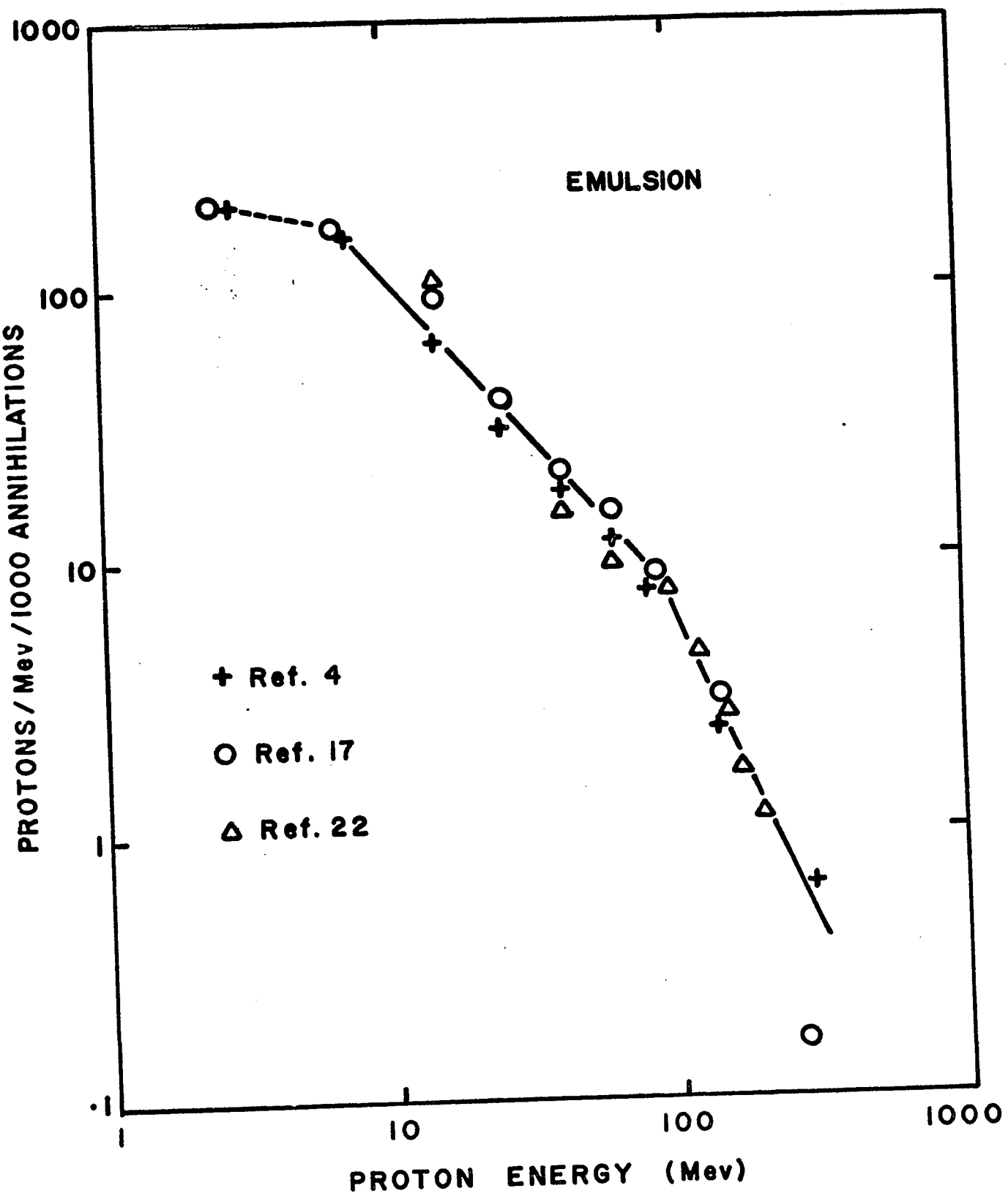

Figure 2 - Proton Energy Distribution from $\bar{p}$ Annihilation in Emulsion

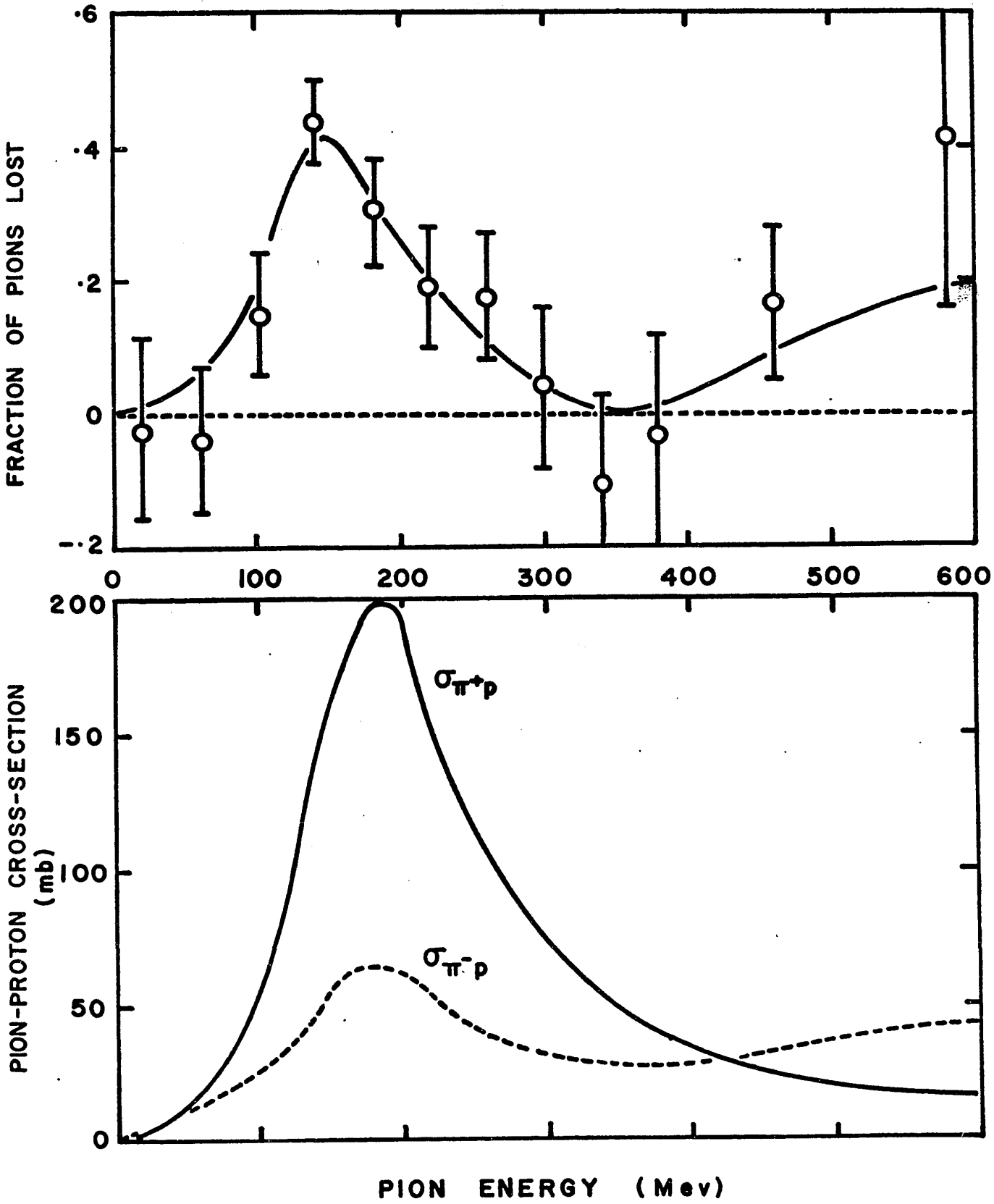

Figure 3- Charged Pions Lost in Nuclear Matter Following $\bar{p}$ Annihilation in Emulsion

Figure 4- Pion-proton Cross-section

shown is, however, for elastic scattering, while figure 3 is a measure of the absorption of pions by the nucleus; this tends to suggest that at this energy absorption proceeds via resonance production [6]. That is, the following process occurs:

$$\pi + N \longrightarrow N^*$$

$$N^* + N \longrightarrow N + N \quad \text{leading to absorption.}$$

The pion and nucleon combine to form the resonance, which subsequently de-excites by colliding with another nucleon. In free space the resonance cannot exist much longer than 10^{-22} seconds, but inside the nucleus many of its decay modes in momentum space are forbidden by the Pauli exclusion principle (PEP) thus prolonging its life; also, the proximity of other nucleons allows interactions with them within a short time (10^{-23} - 10^{-22} seconds). Nonetheless some of the isobars will decay, thus giving:

$$\pi + N \longrightarrow N^*$$

$$N^* \longrightarrow \pi + N$$

which is simply elastic scattering or charge exchange scattering.

The energetic nucleons produced by the interacting pions set up a cascade of secondaries, allowing many nucleons to leave the nucleus, thus producing relatively large stars.

An attempt was made to simulate the pion interactions inside the nucleus by means of a Monte Carlo (MC) calculation. Pions having the energy distribution particular to antiproton-proton annihilation were allowed to radiate isotropically from the annihilation centre at the surface of the nucleus.

If they went into the nucleus they were allowed to interact according to the isobar model. That is, the cross-section of interaction is the same inside as outside the nucleus; an isobar is then formed which can de-excite by colliding with another nucleon, or by re-emitting the pion. The relative rates of these two ways to de-excite was the only parameter of the programme.

When a pion is scattered, it can again interact with another nucleon in the same nucleus. Similarly, the energetic nucleons produced can interact, to set up a secondary cascade.

The final products of these calculations were recorded and analysed as though they were regular experimental data. To normalize the number of pion events to the

actual number of annihilations, the distributions were multiplied by the total pion multiplicity for all annihilations.

III-2 The Monte Carlo Calculation

The work was started on an IBM 1620-II computer and continued on an IBM 360/40G. Only minor changes had to be made to convert the programme; in particular the random number generator had to be changed.

A Monte Carlo calculation is a thought experiment, where a process is imagined to occur according to definite rules. The process is however not completely determined, and thus during the calculation at an appropriate time a choice must be made. This choice is made with the help of random numbers. If the calculation is now repeated many times, each time using different random numbers, the different outcomes can be analysed statistically; that is, an expected distribution can be drawn.

III-2(a) Random Number Generator

Thus of prime importance to a Monte Carlo calculation is a supply of good random numbers. Since in a complex calculation many random numbers are required, it is not practical to store all these numbers in the computer; instead the numbers are generated (calculated according to some specific formula). Of course, if the num-

bers are calculated, they are not truly random, and they are thus called pseudo-random numbers. The design of pseudo-random number generators has, in the last few years, become a highly specialized field; new number generators are being invented, and old ones are being rejected because they have failed some special test.

The generator must produce numbers which at least appear random. That is, one should not be able to predict the approximate value of a number from any previous number, or sequence of numbers. Since in Monte Carlo calculations one often requires a sequence of random numbers to make a decision, this latter is especially important.

The most successfull generators, up till now, are those employing a multiplicative congruential method. Here the last random number generated is multiplied by a fixed constant, and then divided by one plus the largest number allowed. The remainder of this division is the new random number. For the IBM 1620-II, a decimal machine, the following formula was used [24]:

$R_{n+1} = 23R_n \left\{ \text{mod } (10^8+1) \right\}$, where R_n is the n^{th} random number generated. The generator was coded in SPS, rather than FORTRAN, so that it would be sufficiently fast. The generator can produce approximately 5×10^6 numbers, before it repeats itself. The numbers obtained were divided

by 10^8 so that they would have an equal chance to take on any value between zero and one.

For the IBM 360/40G, a binary machine, the programme RANDU, supplied by IBM [25], was used. Basically it is also a multiplicative congruential method, having a period of about 5×10^8 numbers. It is also normalized to take on values between zero and one.

Both generators have been tested [27,25] and found to be sufficiently good; however, the generators may fail more specialized tests [26]. Thus the output obtained was always spot checked for randomness, when possible; these tests never showed any bias.

III-2(b) Programme

For the calculations the nucleus was considered to be a spherical potential well, in which the protons and neutrons form two Fermi gases. The characteristics of these Fermi gases, such as the potential depth and Fermi level, were obtained from Metropolis et al [27]. The latter paper and that of Werbrouck [28] were used as a basis for the programme.

The programme itself may be divided into the following parts:

A) Initialization: The relevant cross-sections, distributions and constants are read in, and all counters are set.

B) Start: By means of random numbers, the incident energy, position and direction of the pions is determined.

C) Penetration: The mean free path of the particle in nuclear matter is calculated, and by means of another random number the distance to the collision is obtained; from the old position, the direction of motion, and this distance, the new position is found. If the new position is inside the nucleus the programme proceeds with the next step; otherwise it continues at step H.

D) Collision: The target nucleon is identified, and its momentum and direction are determined; the type of interaction (that is elastic scattering, charge exchange or absorption) and the

outgoing direction (in the centre of mass) of the scattered particle are found; all these require the use of random numbers.

The outgoing direction and energy of the scattered and target particles (in the laboratory frame) are calculated using relativistic mechanics; both energies are tested to ensure that the Pauli exclusion principle is not being violated; if it is, appropriate action is taken (the exact procedure depends on the programme and will be discussed later).

E) Struck Particle: If the struck nucleon is sufficiently energetic after the collision it is stored in the memory to be followed later.

F) Incident Particle: The energy of the incident particle is tested to determine whether it is sufficiently energetic to be followed; if so, the

programme proceeds with step C; if not, the particle is abandoned and the programme performs step G.

G) Stored Particles: The memory is tested to see whether there are any particles still to be followed; if so, their position, direction and energy become that of a 'new' incident particle, and the programme executes step C; if not, a new event is started with step B.

H) Output: The energy and direction of the outgoing particle are printed and step G is initiated.

At the end of the programme, when the required number of events have been simulated, the energy and angular distribution of all incident and outgoing particles are printed.

A schematic flow chart of the programme is shown in figure 5, and a sample programme and output may be found in appendix 3.

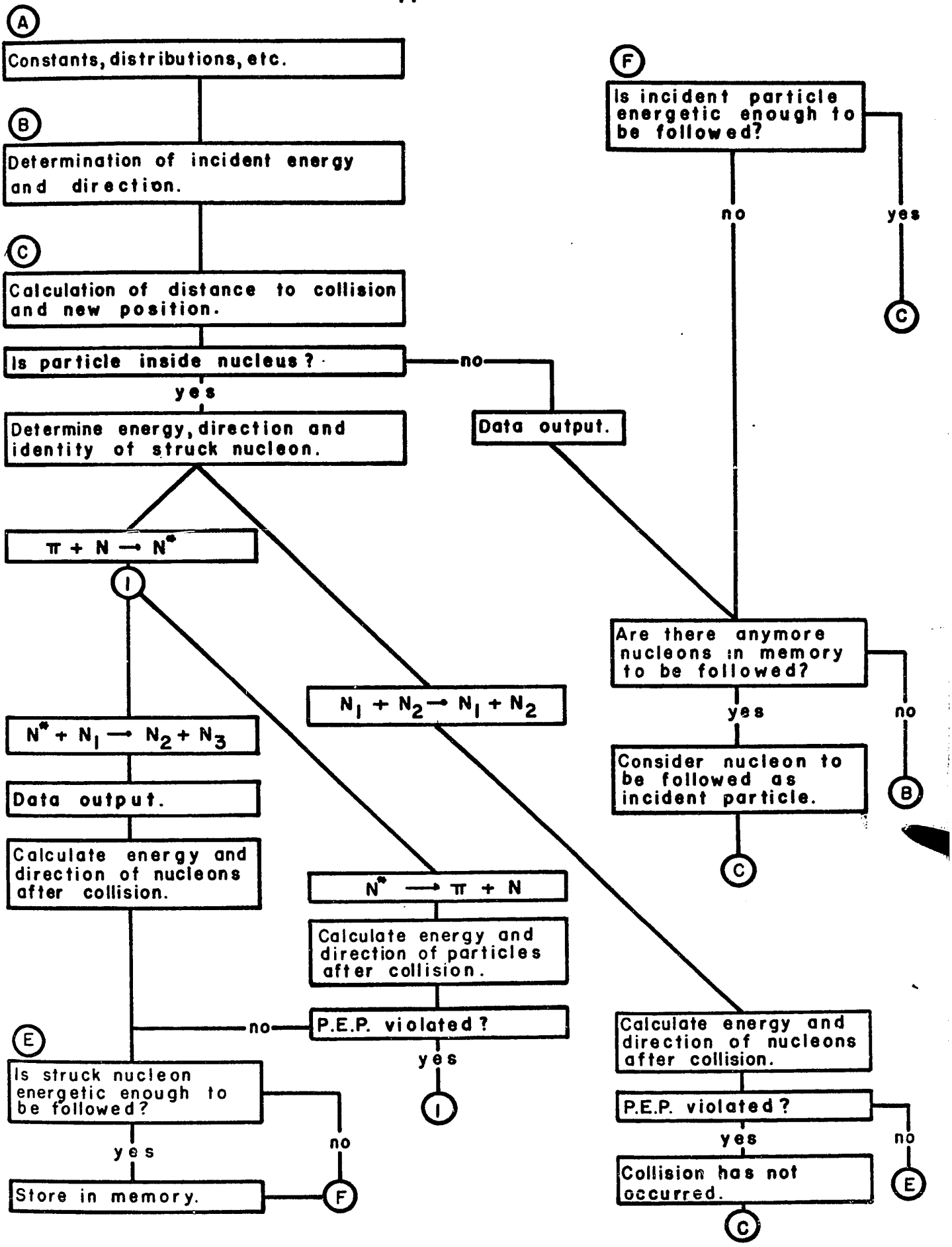

Figure 5 - Schematic Flow Chart of Programme

III-2(c) Use of Random Numbers

As pointed out before, an important part of Monte Carlo calculations is to chose between alternatives. For instance, when the incident particle is to collide, it may be known that the probability of collision with a neutron is x, and with a proton, naturally, 1-x (where $0 \leq x < 1$). If random numbers, which are uniformly distributed between 0 and 1, are available, then these can be used to choose the nucleon struck in any particular case. If the random number (R) is less than x, a neutron will have been struck; if it is greater than x, a proton is the struck particle. Thus, if the choice were made many times, the ratio of neutrons to protons would be the desired value of x to 1-x.

For a multiple choice, for instance n possibilities having probabilities $a_1, a_2 \ldots a_i \ldots a_n$, the i^{th} possibility would be chosen if:

$$\sum_{j=1}^{i-1} a_j \leq R \sum_{j=1}^{n} a_j < \sum_{j=1}^{i} a_j$$

Again, if many choices were made, the different possibili-

ties would occur with the correct frequency.

This last formula can be easily adapted to continuous functions. For instance, let p(x)dx express the probability for a variable to take on a value between x and x+dx, where dx is infinitesimal ; then the summation becomes an integral, and the resulting formula is:

$$R \int_{x_{min}}^{x_{max}} p(y)\,dy = \int_{x_{min}}^{x} p(y)\,dy$$

If the integrals can be found analytically, then for every R selected the value of x may be calculated.

Defining P(x) as:

$$P(x) = \frac{\int_{x_{min}}^{x} p(y)\,dy}{\int_{x_{min}}^{x_{max}} p(y)\,dy}$$

then $$x = P^{-1}(R)$$

A practical example is the calculation of the distance to interaction (L) travelled by a particle in a medium, if the particle has a mean free path λ. In this case the following formulae apply:

$$\int_0^L p(x)\,dx = 1-e^{-L/\lambda}$$

and $$\int_0^\infty p(x)\,dx = 1$$

Thus $$R = 1-e^{-L/\lambda} = P(L)$$

and $$1-R = e^{-L/\lambda}$$

Since (1-R) is also a random number between 0 and 1, it may be replaced by R.

and therefore: $$R = e^{-L/\lambda}$$

and $$L = -\lambda \log_e R$$

III-2(d) Kinematics

Another important part of the programme is the kinematics. The energy and direction of the incident and struck particles are known, and the outgoing direction, in the centre of mass, has also been determined. From this information the energy and direction after the collision must be found. To accomplish this, a series of rotations and relativistic transformations are performed. The rotations are performed to keep the transformation formulae simple. In the laboratory frame both particles are moving, but not generally along the same line, or along any of the axes; thus the first rotation is one such that the struck nucleon moves along the x-axis, followed by a transformation of both particles to the rest frame of the struck nucleon. Now one particle is at rest, while the other approaches from some general direction, which still is not along an axis. Consequently another rotation is performed, in the rest frame of the struck nucleon, to have the incident particle move along the x-axis. The particles are then transformed to the centre of mass system, and will now be approaching each other with equal momentum and along the x-axis. After the collision, they will have equal but opposite momentum and will move off in the pre-

determined directions. The inverse transformations and rotations are applied, and finally the energy and direction of both particles after the collision will have been found. Since all transformations are relativistic, any change in the rest-mass of either of the particles will not cause any difficulty.

The remaining problems in the programme are those of logic and computing language, both of which are predominantly characteristic of the computer and will not be discussed.

III-3 Simulation of Antiproton Annihilation

As mentioned earlier, to simulate the annihilation, pions were considered to be emitted isotropically from the surface of a nucleus. These pions were adjusted to have the charge and energy distribution typical of antiproton-nucleon annihilation.

The nucleus was considered as a spherical potential well of radius $1.3A^{1/3}$ fermis, in which the protons and neutrons form two Fermi gases. Furthermore, the antiproton could annihilate with equal probability on any of the nucleons.

The pions traversing the nucleus could interact with the nucleons and set up a cascade, which generally results in nucleons leaving the nucleus. The outgoing pion and proton energy distributions and multiplicities were compared to the experimental ones.

Different methods for determining when a pion is scattered or absorbed were tried, and the ones giving the best results will be shown.

It should be noted that all scattering was assumed to be isotropic in the centre of mass. At first glance this appears to be a poor assumption. However, a trial was performed in which the scattering was strongly

peaked in the forward and backward direction; this did not produce any significant difference in the energy distribution of the pions or protons. Thus, for simplicity, the differential cross-section was left as a constant.

Two more trials were performed to test the validity of some of our other assumptions. In the first one, the pions were assumed to be emitted from the centre of the nucleus, rather than from the surface. This test gave far too many protons, and an insufficient number of pions. For the second one, it was assumed that pions could not be absorbed, unless they had insufficient energy to leave the nucleus. After all, it is possible that only very low energy pions are absorbed. This test gave too many pions, especially low energy ones,and not sufficient high energy protons. From these two trials it is clear that the anti-proton does indeed annihilate on the surface and that there is some way for fast pions to be absorbed by the nucleus.

For the next trial, then, it was assumed that a constant fraction of the pions was absorbed. The percentage, before the application of the Pauli exclusion principle, was set at 20%; the Pauli exclusion principle will tend to increase the percentage for low energy pions, since, if the isobar cannot decay the first time, the pion has again a 20% change (that is 20% of 80%, or 16%, which

is in addition to the initial 20%) of being absorbed, and so on. The Pauli exclusion principle is not liable to forbid an isobar to de-excite by collision on a nucleon since an additional 140 Mev is available. The agreement of this trial was found to be surprisingly reasonable, however it was felt that an energy dependent absorption rate would give still better results.

Several energy dependent schemes were tried [7], and the most successful one was one in which the absorption rate is inversely proportional to the exponential of the pion energy; the actual formula for the absorption fraction (F_{AB}) was:

$$F_{AB} = e^{-E_\pi/200}$$

where E_π is the incident pion kinetic energy. (The incident pion energy is approximately proportional to the isobar energy and mass). The results of this calculation, denoted by M4, are shown in figures 6 and 7. The graphs are again a log-log plot of the number of particles per Mev per 1000 annihilations versus the particle energy. Figure 6 shows the calculated pion ditribution, and the solid line is the best line through these points; this line is repro-

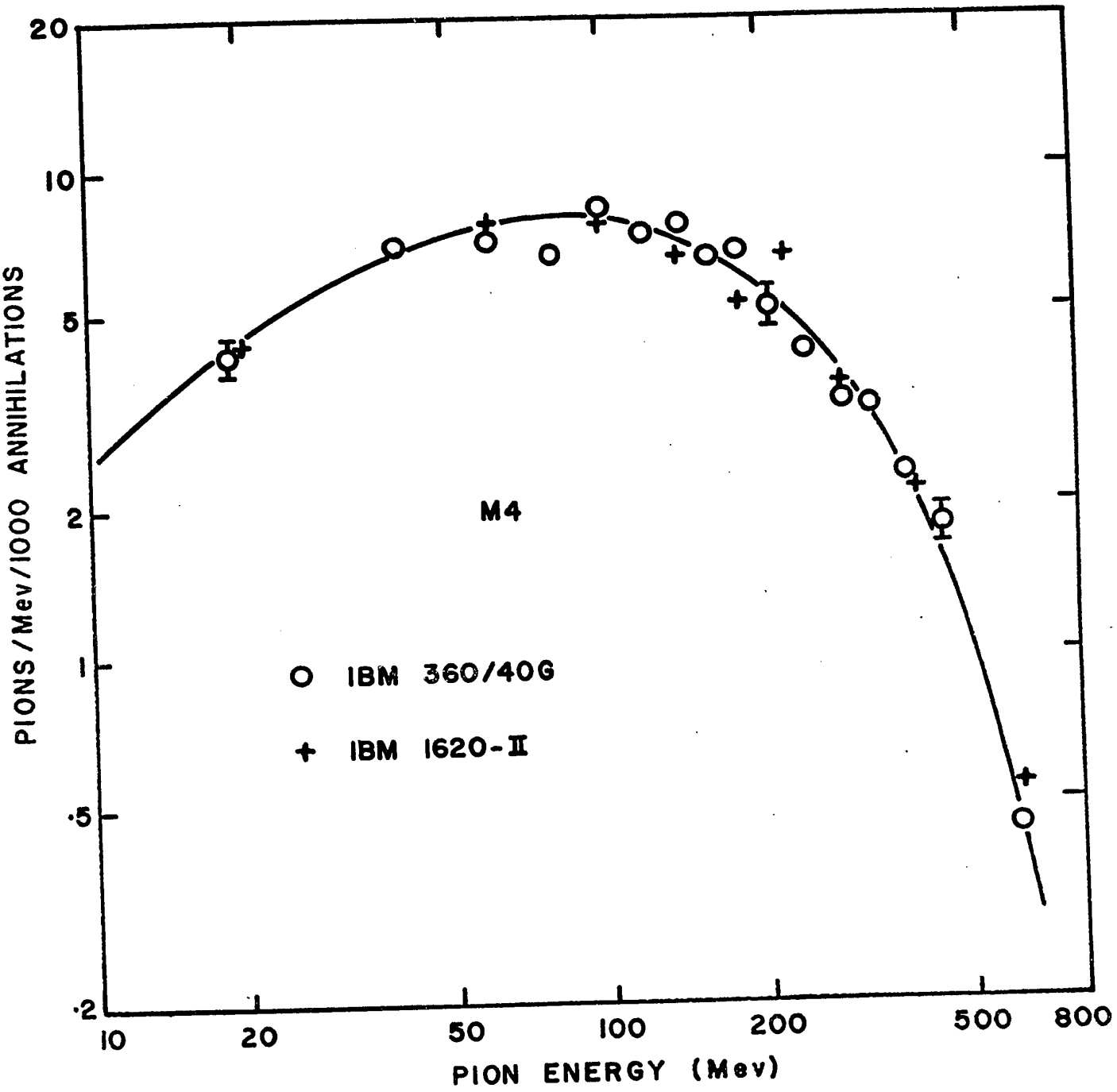

Figure 6 - Calculated Pion Energy Distribution for $\bar{p}$ Annihilation in Emulsion

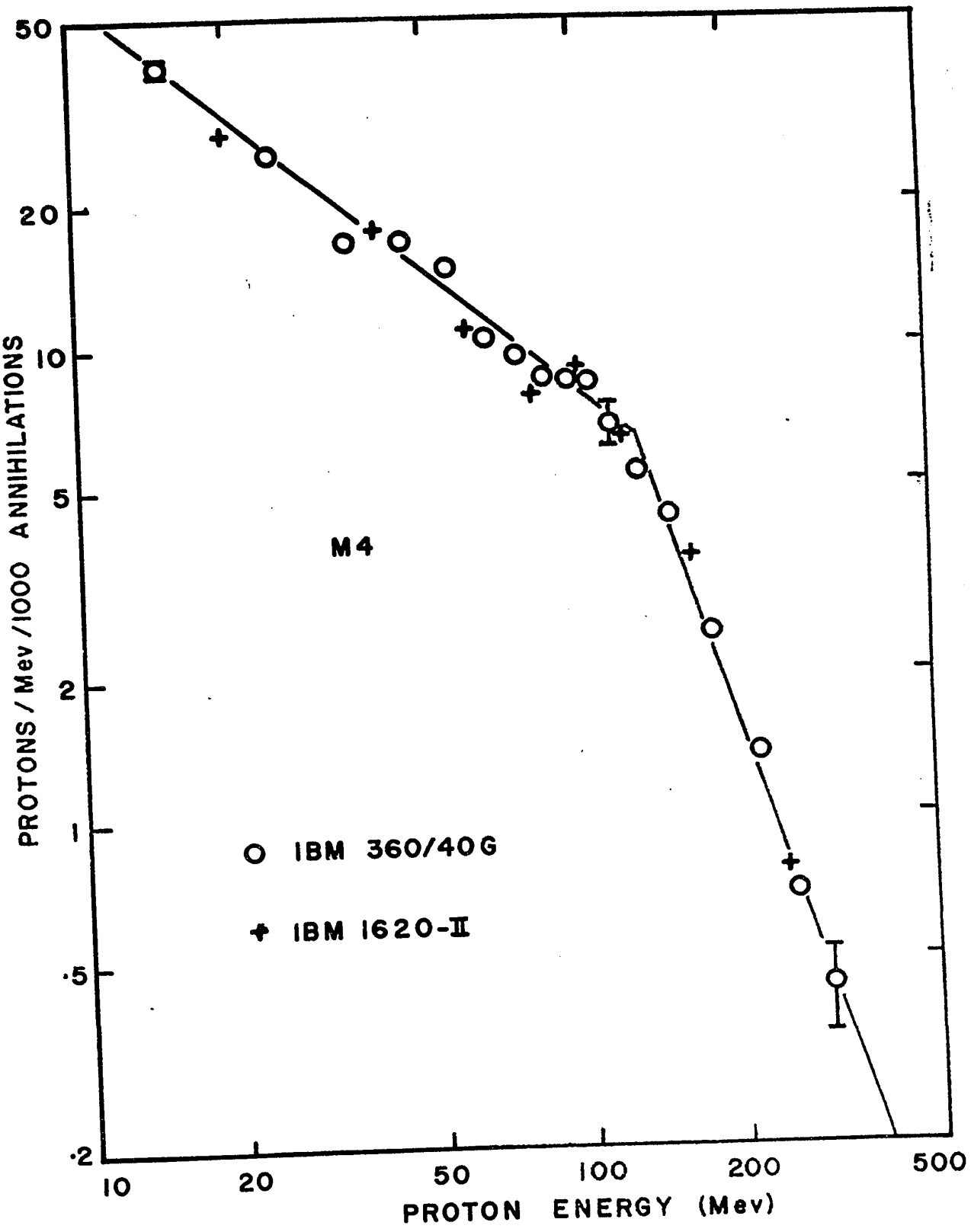

Figure 7 - Calculated Proton Energy Distribution for $\bar{p}$ Annihilation in Emulsion

duced in figure 10, which also shows the experimental points, and an alternate model. Similarly figures 7 and 11 show the proton distribution. The agreement is very reasonable, considering the crudeness of the model; particularly satisfying is the fact that no normalizing constant needs to be introduced.

The alternate model, shown in figures 8,9,10 and 11 involved an entirely different approach. In this calculation, the programme allowed the isobar one attempt at decaying; if, on this first attempt, the particular mode chosen by the programme was forbidden by the Pauli exclusion principle, then the pion had to be absorbed. This method was called one shot (OS), for obvious reasons. The method doesn't have any variables, and it is thus very surprising that the results agree so well with the experimental values.

Finally, table 13 shows the calculated and observed charged pion and proton multiplicities.

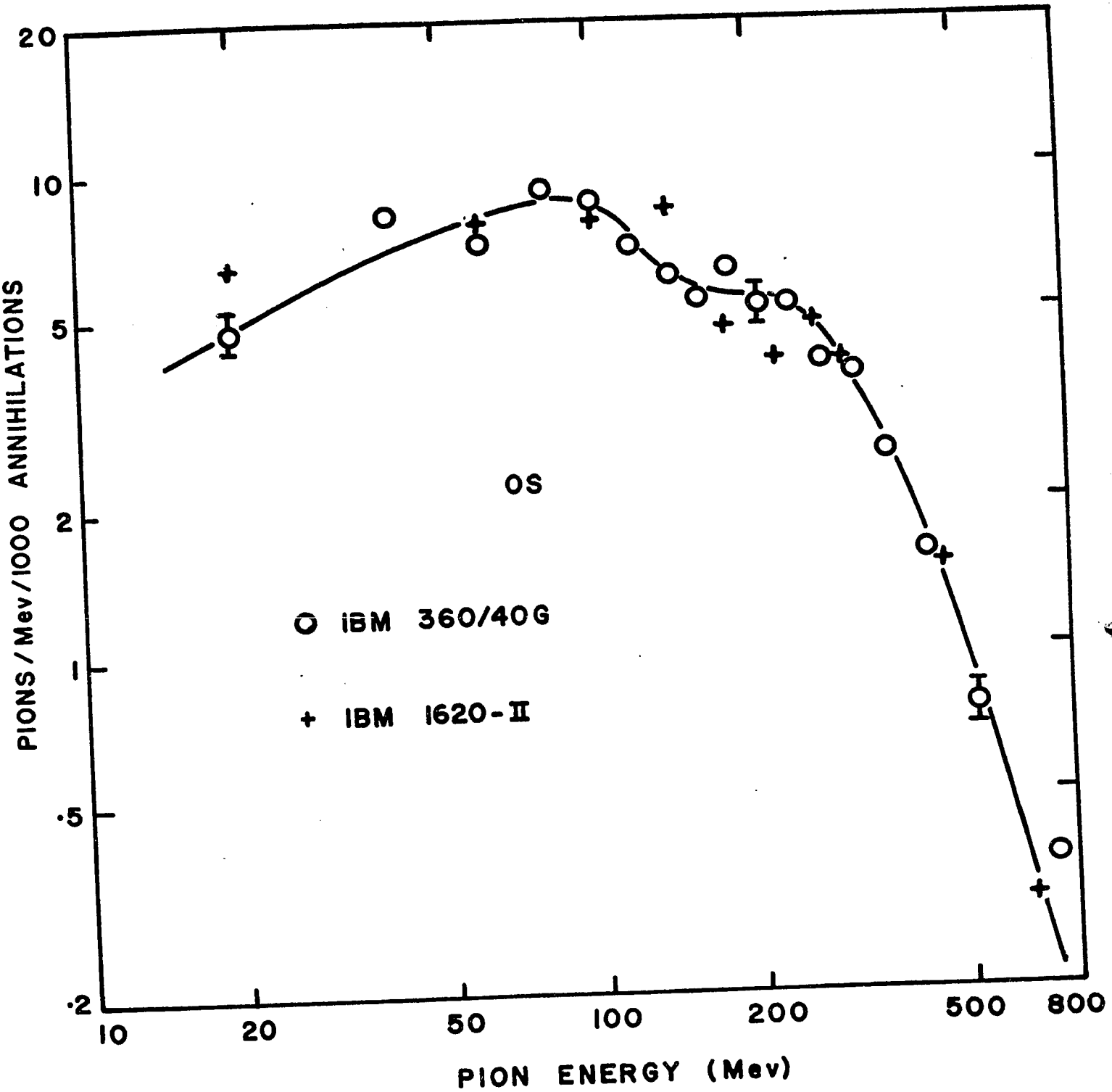

Figure 8 - Calculated Pion Energy Distribution for $\bar{p}$ Annihilation in Emulsion

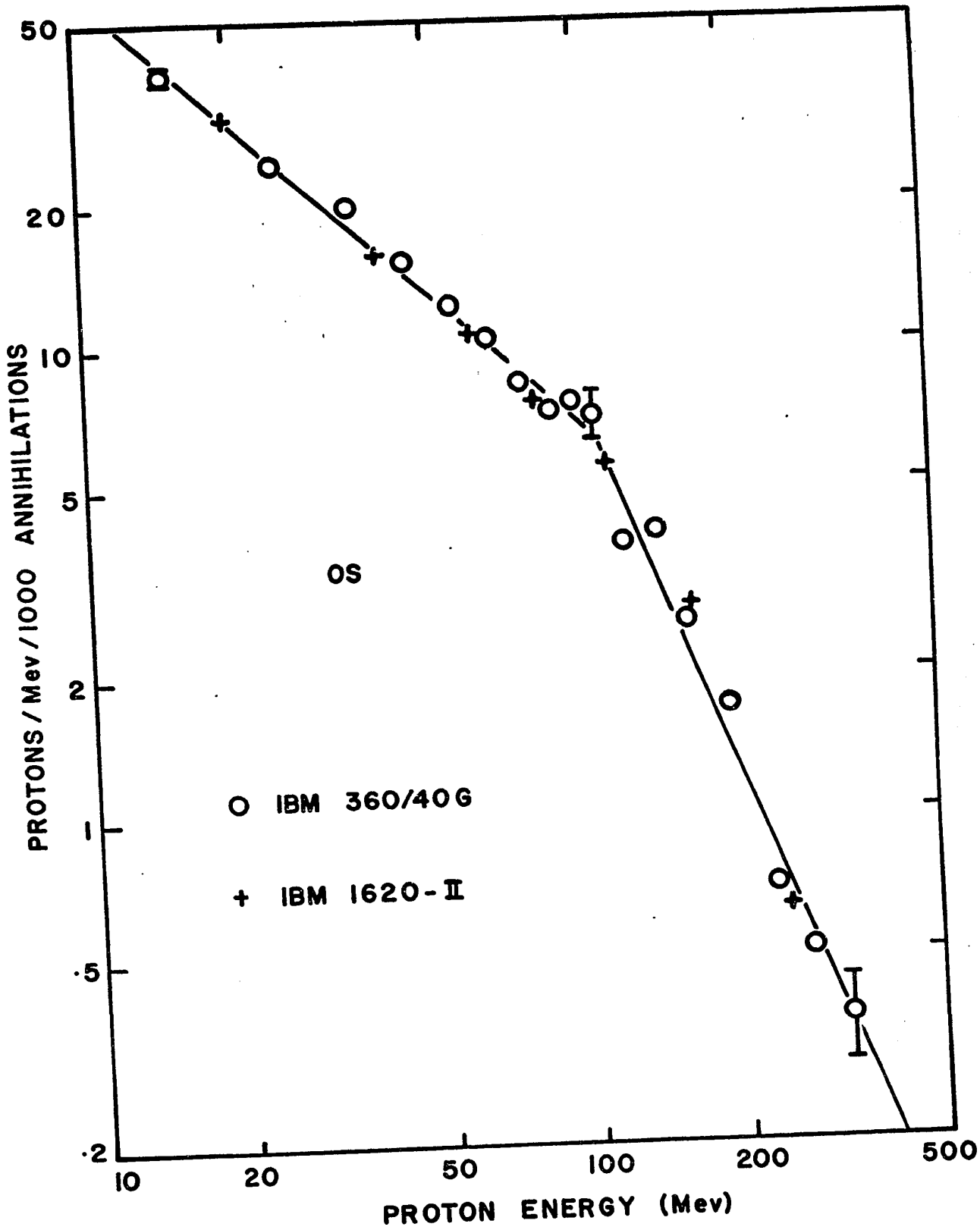

Figure 9 - Calculated Proton Energy Distribution for $\bar{p}$ Annihilation in Emulsion

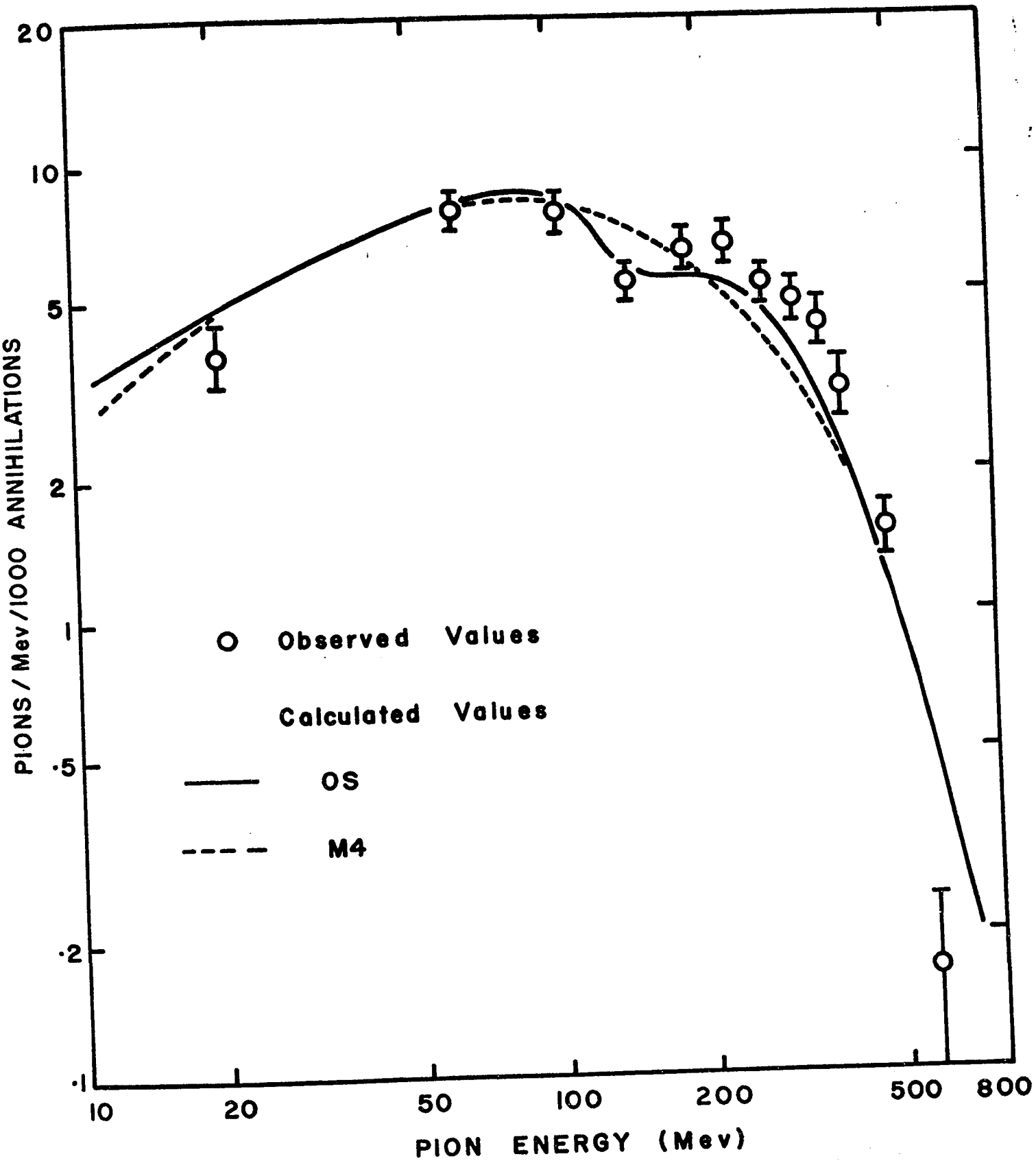

Figure 10 - Observed and Calculated Pion Energy Distribution for $\bar{p}$ Annihilation in Emulsion

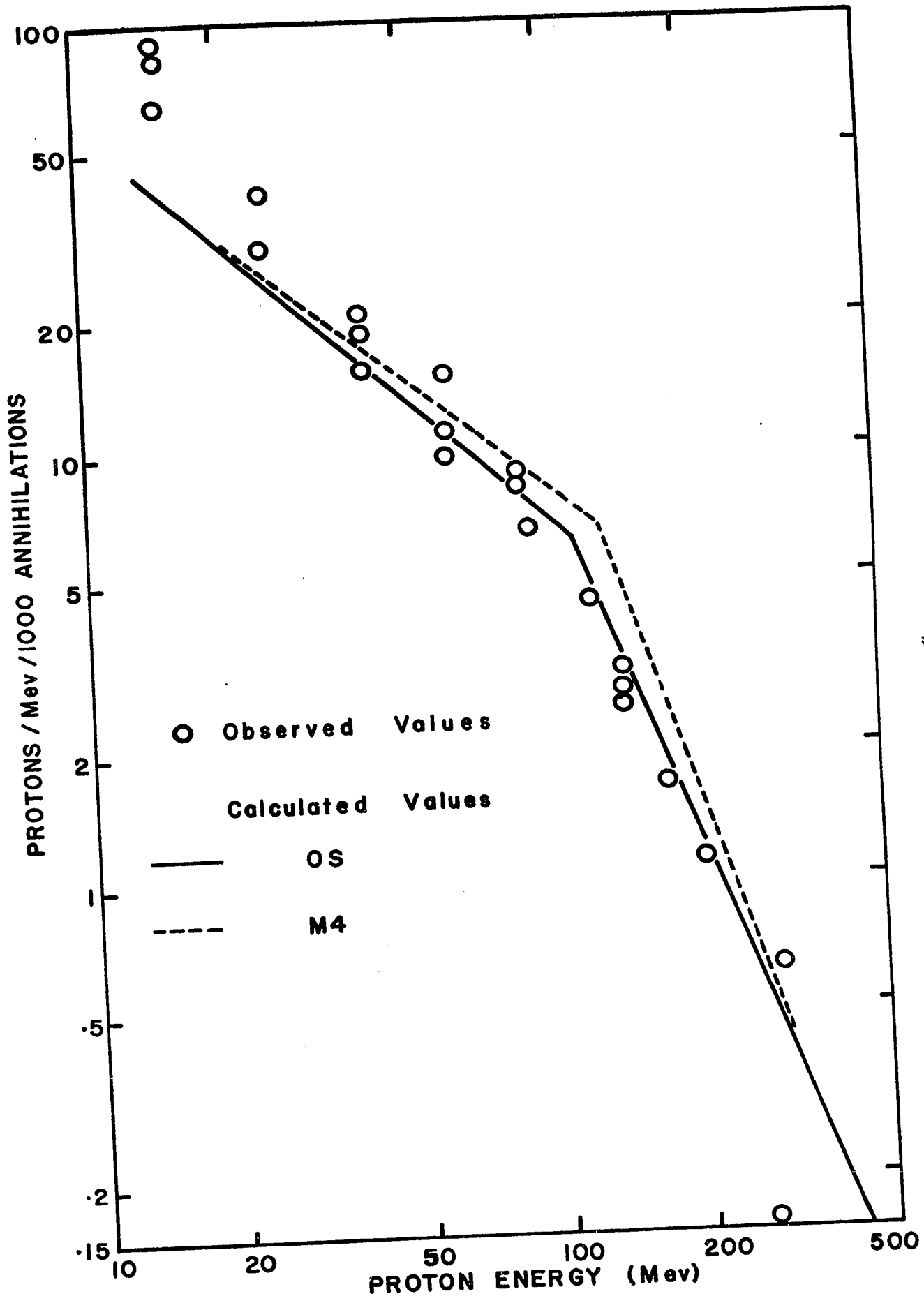

Figure II - Observed and Calculated Proton Energy Distribution

Table 13

Observed and Calculated Proton and Pion Multiplicities for Antiproton Annihilation in Emulsion.

	Observed	Calculated	
		M4	OS
$\langle N_{\pi^{\pm}} \rangle$	2.44 ± 0.07	2.21 ± 0.05	2.31 ± 0.05
$\langle N_p \rangle_{E>30 \text{ Mev}}$	1.3 ± 0.1	1.42 ± 0.04	1.23 ± 0.03

III-4 Discussion

The calculations using the isobar model give surprisingly good results, even though the nuclear model is crude and many simplifying assumptions were made.

The model does not give the correct nucleon energy distribution below 30 Mev, because below this energy evaporation adds to the spectrum. In principle, the average energy remaining in the nucleus after the initial cascade may be found from the programme, and from this the contribution of evaporation can be calculated.

In the calculations it was assumed that the pions see a potential well; this, however, introduces some problems with energy conservation when the pion is absorbed. There is some evidence for the validity of this assumption in figure 3; that is, the peaking, in the graph, occurs at an energy of 140 Mev, rather than 180 Mev. This difference can be attributed to a potential well.

Many improvements can be made to the programme, such as the inclusion of non-isotropic scattering, the effect of nucleon motion on the average pion-nucleon cross-section, inclusion of the nucleon-isobar cross-section to determine F_{AB}, and so on; these are not expected to produce major changes, and until improved experimental data is available, are not considered to be worthwhile.

Chapter IV

NEGATIVE PION CAPTURE IN COMPLEX NUCLEI.

IV-1 Introduction

The study of antiproton annihilation on complex nuclei has yielded some information on the behaviour of pions inside the nucleus, and it seems that the capture of pions by large nuclei should yield more. A considerable amount of experimental and theoretical work has been done on the subject.

The early experiments were done mostly in emulsion[29], but the only information obtained from these experiments is the energy spectrum of the emitted protons. Since neutrons cannot be observed in nuclear emulsions, and since σ-stars (the stars produced by negative pion capture) are mostly neutron yielding stars, a large uncertainty results in the determination of the total number of protons per star; the fast proton multiplicity is also very low. As a result of these two factors, the proton spectra obtained by the various research groups are statistically poor and often very different. Thus, although this data was taken into account, it is not considered to be significant.

The later experiments[30,31,32] are mostly counter experiments, where a neutron is detected, and its

energy measured by time of flight. In some experiments two neutrons, or a neutron and a proton, were detected, and in these an angular correlation could be established. One experiment of particular interest was performed by Ozaki et al. [32]; they measured the ratio of neutron-neutron pairs to neutron-proton pairs emitted back to back, after negative pion capture. The ratio was found to be 5.0±1.5 for carbon and 3.9±1.2 for aluminium, in favour of the neutron-neutron pairs.

This experiment led to a considerable amount of theoretical work [33], however without much success. In these theoretical models the pion is generally assumed to be absorbed on a pair existing as such in a nucleus, and thus the ratio of neutron-neutron pairs to neutron-proton pairs emitted represents the approximate ratio of neutron-proton pairs to proton-proton pairs present in the nucleus. The highest ratio obtainable with these assumptions is 3.5 for carbon, but, taking into account secondary interactions, this ratio is not high enough. These models have however been very successful in reproducing the x-ray spectra from pi-mesic atoms.

Using the isobar model the ratio is easily attainable. In the case of an equal number of neutrons and protons, as in carbon, the pions will interact with a neu-

tron 75% of the time and produce an N^{*-}. This isobar must interact with a proton, to yield a neutron-neutron pair. The remaining 25% produce an N^{*o}, which will have equal chance of interacting with a neutron or proton, to give neutron-neutron or neutron-proton pairs respectively. Thus a maximum ratio of 7 is obtained for neutron-neutron to neutron-proton pairs. The nucleons produced may cause secondary interactions, which will have a tendency to reduce this ratio. Since aluminium is a larger nucleus than carbon, the reduction will be greater, thus explaining why the ratio is less for aluminium.

IV-2 The Monte Carlo Method and Negative Pion Capture

The Monte Carlo calculation was set up to simulate negative pion capture in carbon, aluminium, cadmium (or large emulsion nuclei), lead and uranium. The neutron spectra obtained were compared to those of Anderson et al.[30]

To perform the calculation, it must be known where, inside the nucleus, the pions are absorbed. The experience with antiproton annihilation would suggest that the pion is absorbed on the surface, but the pion nucleon cross-section at low energies is much smaller than that of antiproton-nucleons: thus the pions might be absorbed throughout the nucleus: the pion could also 'sink' to the middle of the nucleus because of the coulomb attraction, and then be absorbed. All three were tried for the cadmium nucleus, but only the last one produced some agreement. Figure 12 shows the calculated distribution for absorption of the pion at the surface and at the centre of the nucleus, and figure 13 shows how the latter calculation compares with the experimental results.

For these calculations it was assumed that the negative pion-neutron cross-section ($\sigma_{\pi^- n}$) and the positive pion-proton cross-section ($\sigma_{\pi^+ p}$) are equal, since

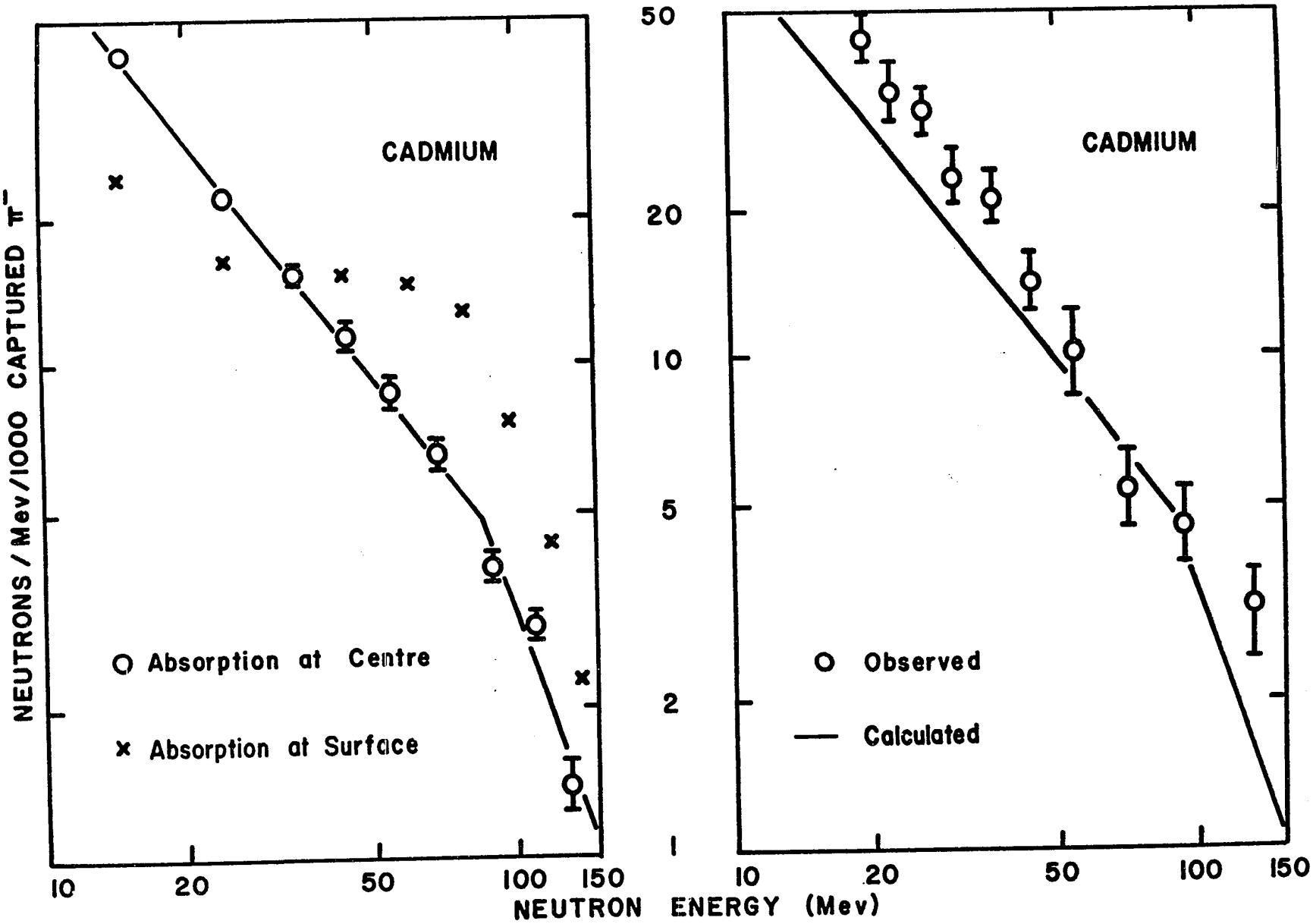

Figure 12 - Calculated Neutron Energy Distribution for π^- Capture in Cadmium

Figure 13 - Observed and Calculated Neutron Energy Distribution for π^- Capture in Cadmium

this is predicted from isospin conservation; however, isospin conservation also predicts that $\sigma_{\pi^- n}$ is three times the negative pion-proton cross-section ($\sigma_{\pi^- p}$). Experimentally it is found that $\sigma_{\pi^+ p} \neq 3\,\sigma_{\pi^- p}$ at low energies, and this is attributed to coulomb interference. Since $\sigma_{\pi^- n}$ cannot be measured directly, it is not certain which assumption, that is $\sigma_{\pi^- n} = \sigma_{\pi^+ p}$ or $\sigma_{\pi^- n} = 3\,\sigma_{\pi^- p}$, is better in this case. Again, the calculation was performed for both cases: this time no difference was found in the neutron spectrum; but the proton spectrum did show some change. Figures 14 and 15 show the proton spectra calculated on the assumption that $\sigma_{\pi^- n} = \sigma_{\pi^+ p}$ and $\sigma_{\pi^- n} = 3x$ $\sigma_{\pi^- p}$ respectively, while figure 16 shows the experimental and the calculated distributions.

Negative pion capture was also simulated for lead, uranium, aluminium and carbon. Figures 17,19,21 and 23 show the calculated distributions, and figures 18,20,22 and 24 show the experimental and calculated results together.

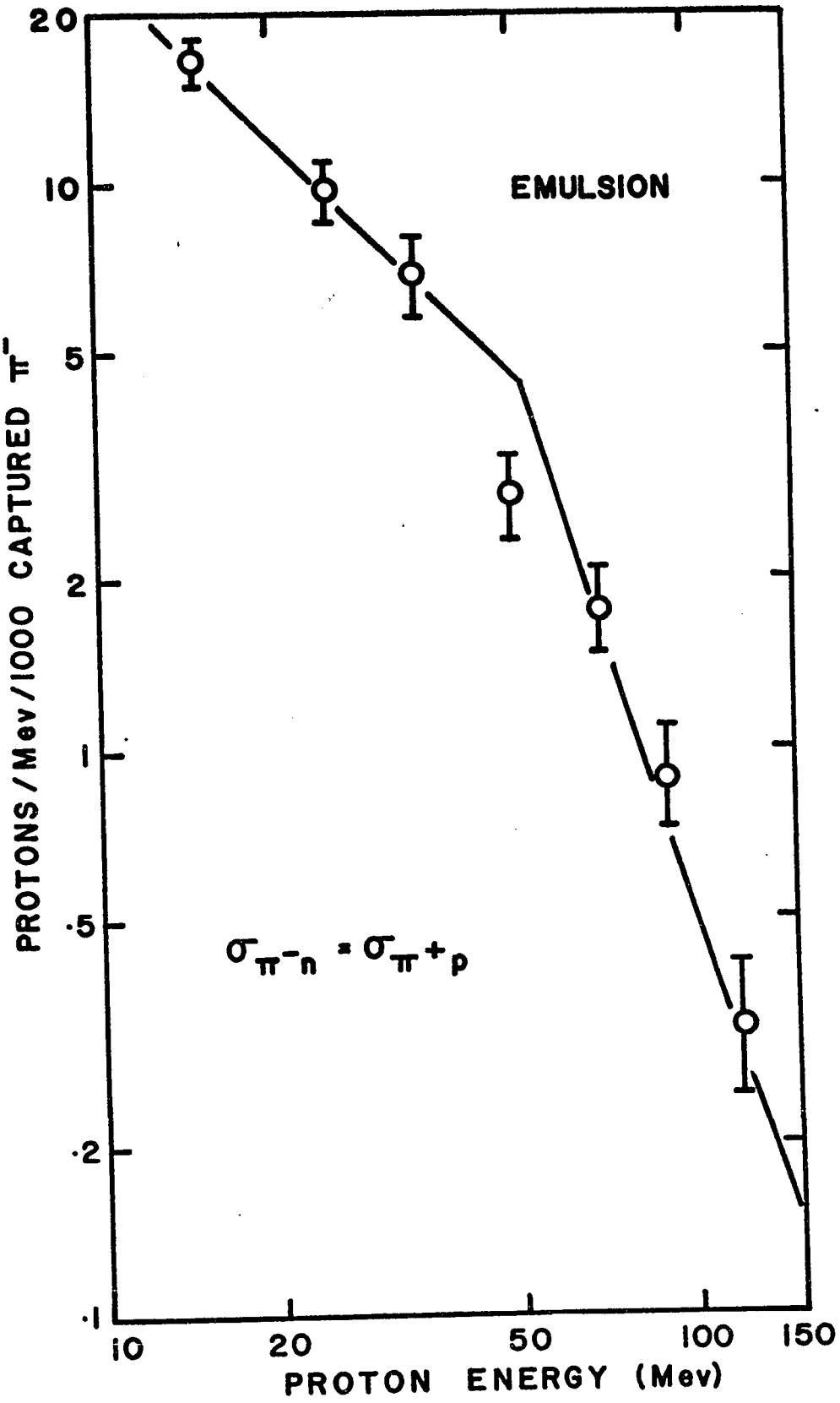

Figure 14 - Calculated Proton Energy Distribution for π^- Capture in Emulsion

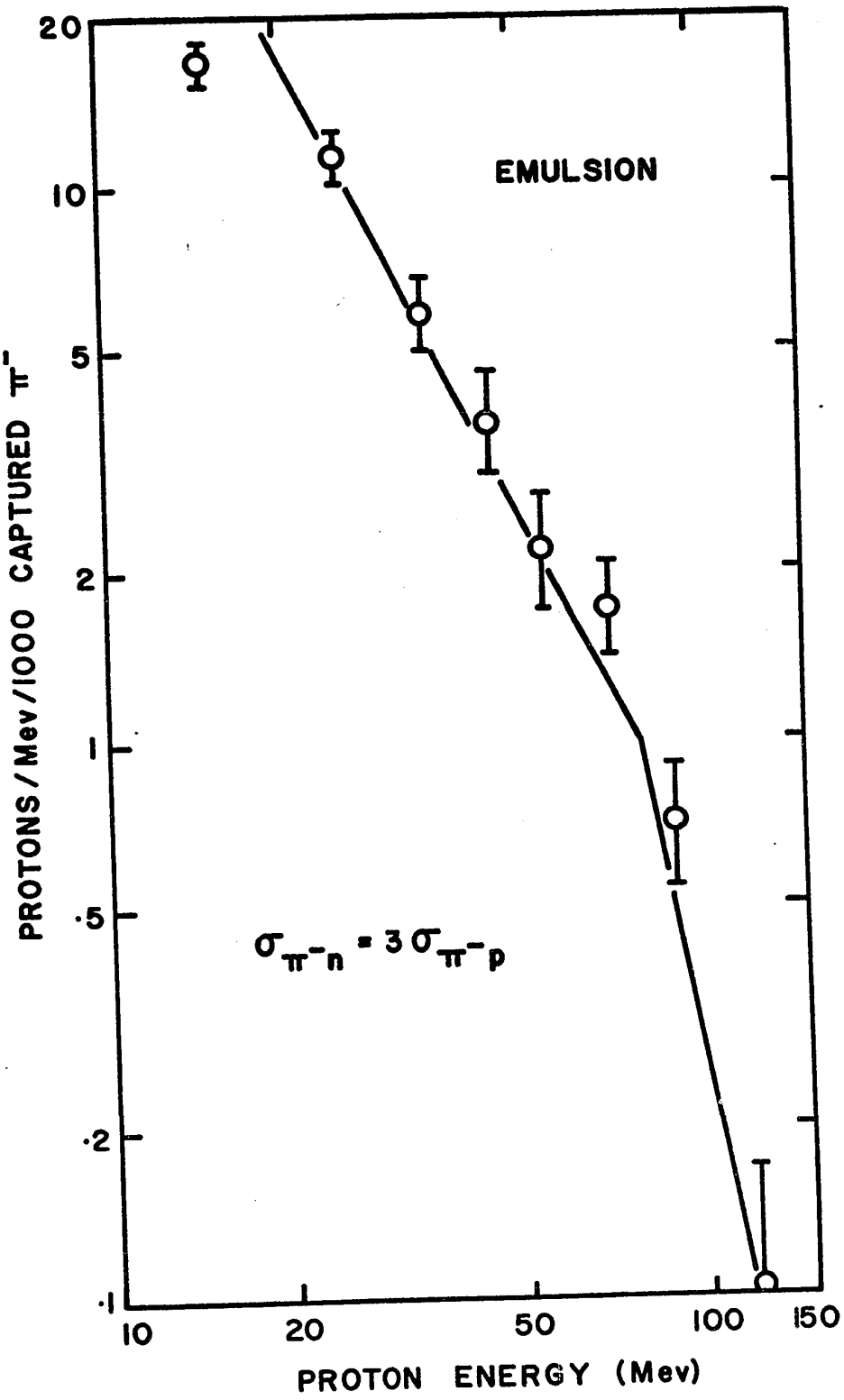

Figure 15 - Calculated Proton Energy Distribution for π^- Capture in Emulsion

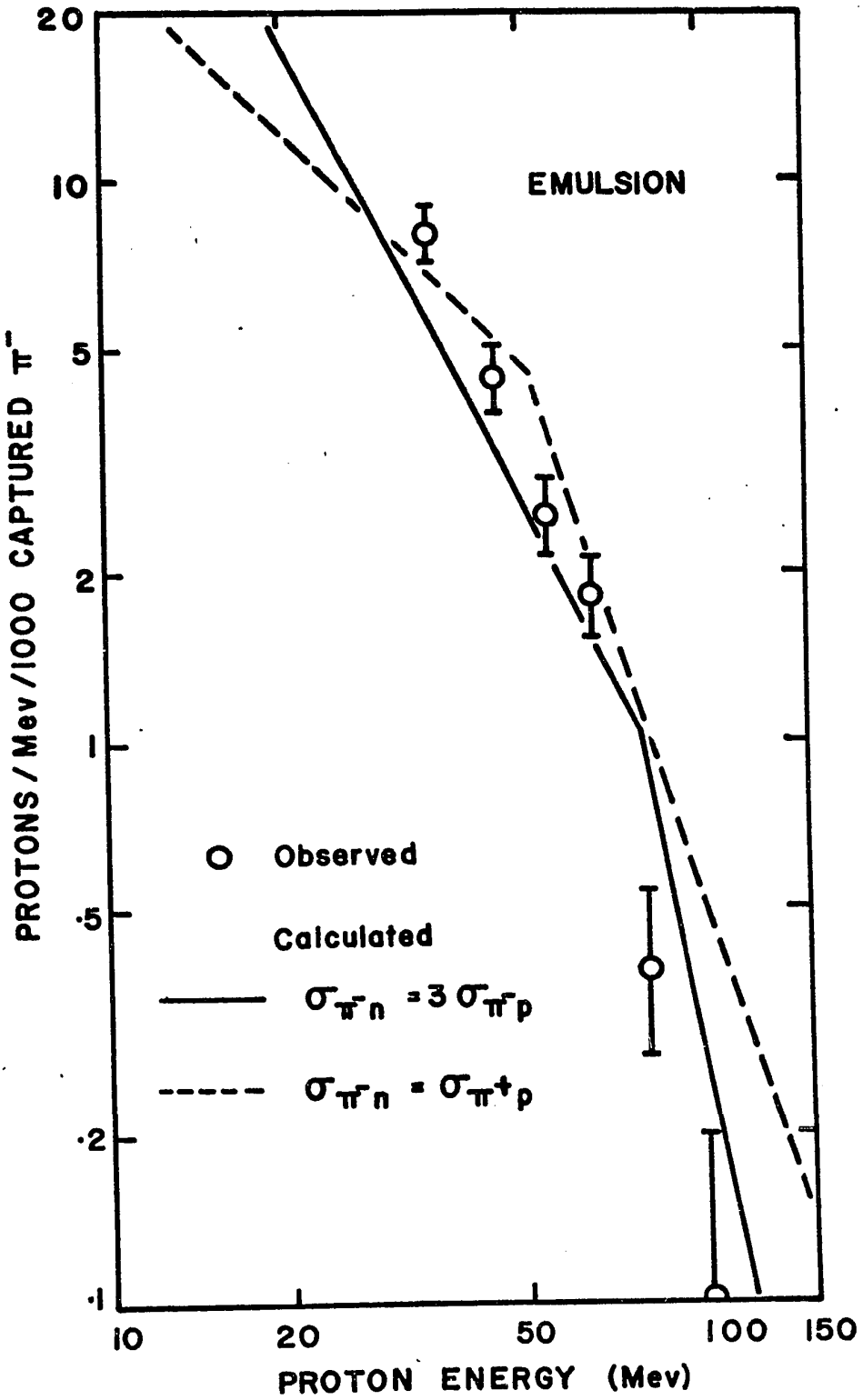

Figure 16 - Observed and Calculated Proton Energy Distribution for π^- Capture in Emulsion

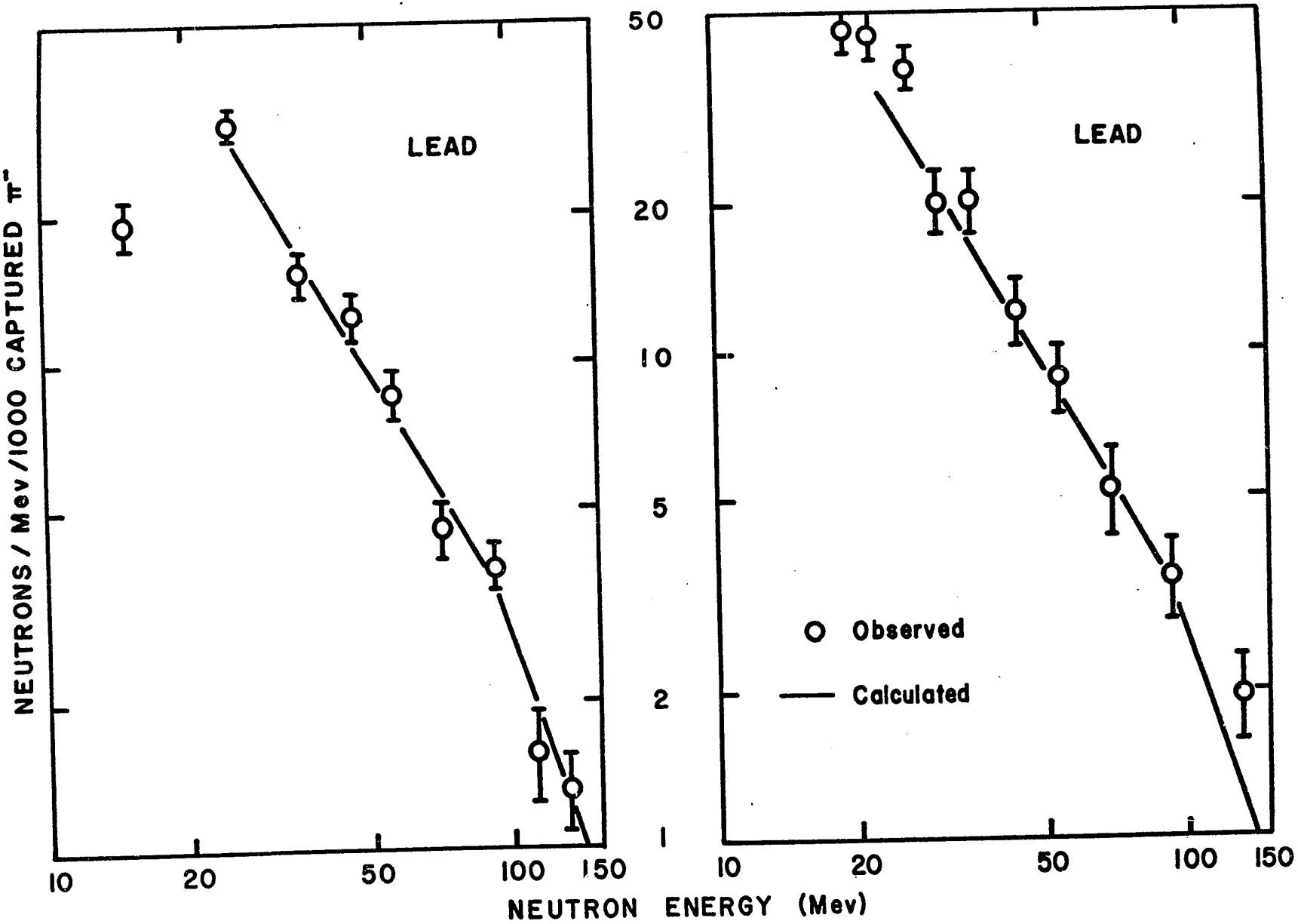

Figure 17 - Calculated Neutron Energy Distribution for π^- Capture in Lead

Figure 18 - Observed and Calculated Neutron Energy Distribution for π^- Capture in Lead

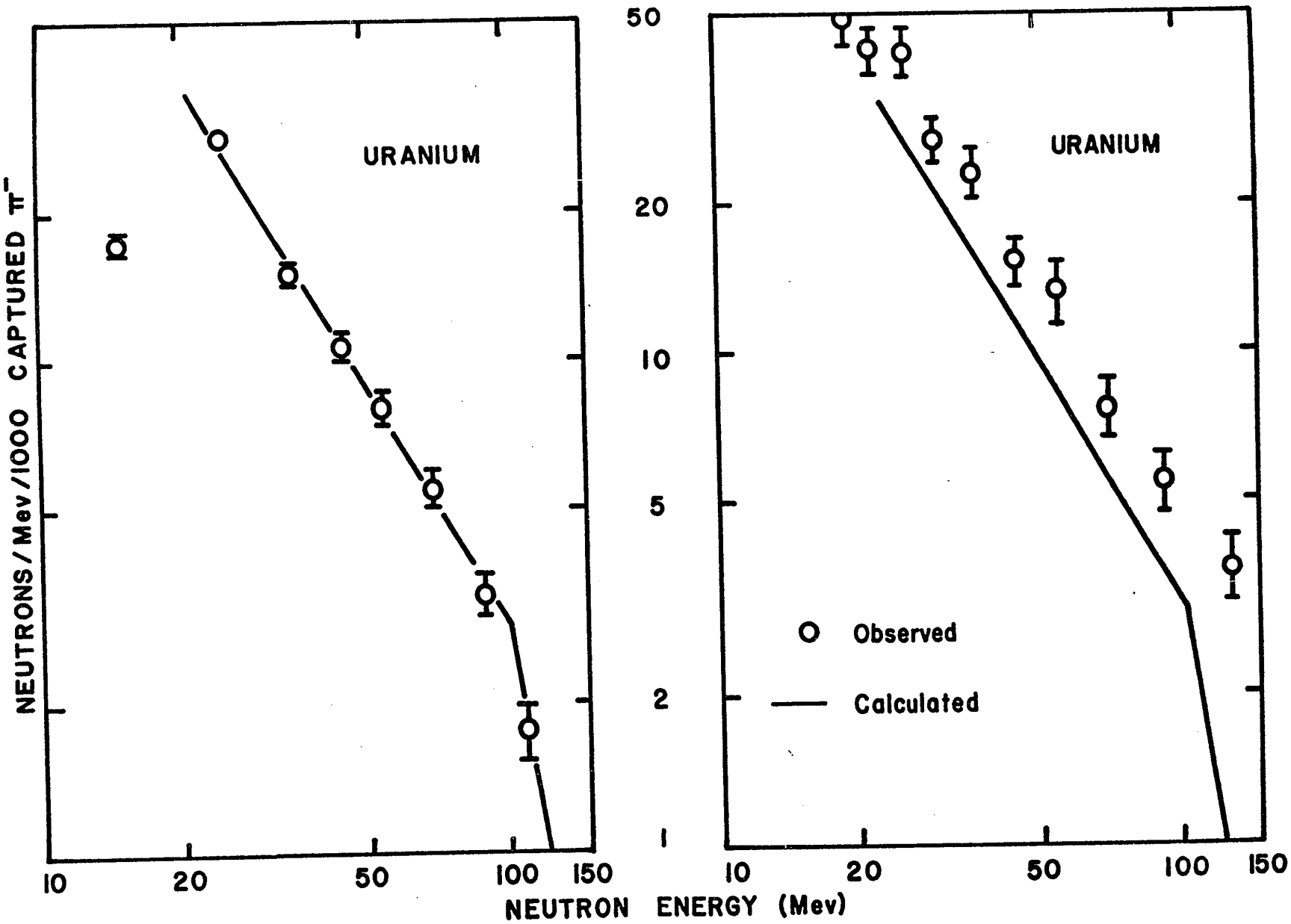

Figure 19 - Calculated Neutron Energy Distribution for π^- Capture in Uranium

Figure 20 - Observed and Calculated Neutron Energy Distribution for π^- Capture in Uranium

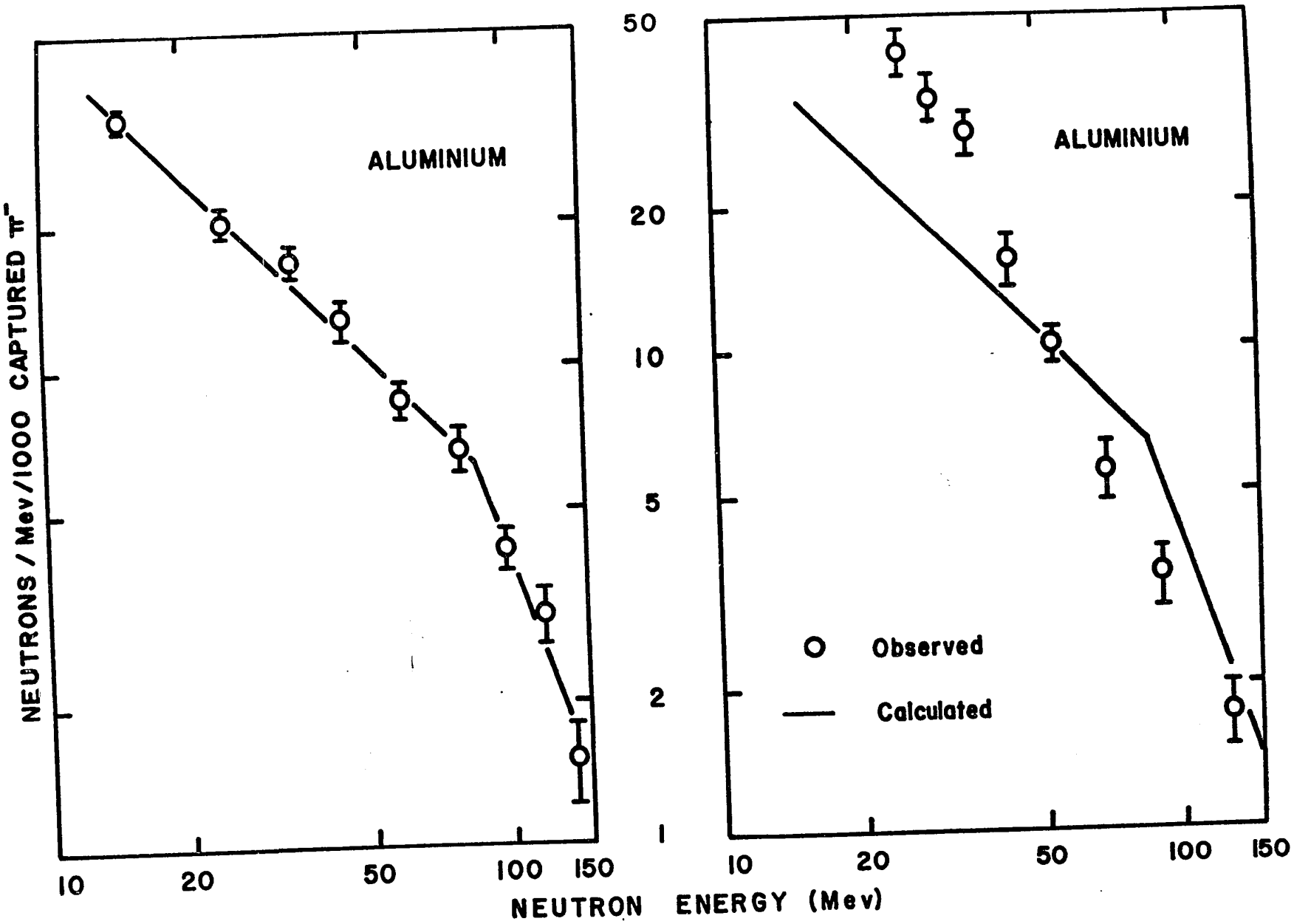

Figure 21 - Calculated Neutron Energy Distribution for π^- Capture in Aluminium

Figure 22 - Observed and Calculated Neutron Energy Distribution for π^- Capture in Aluminium

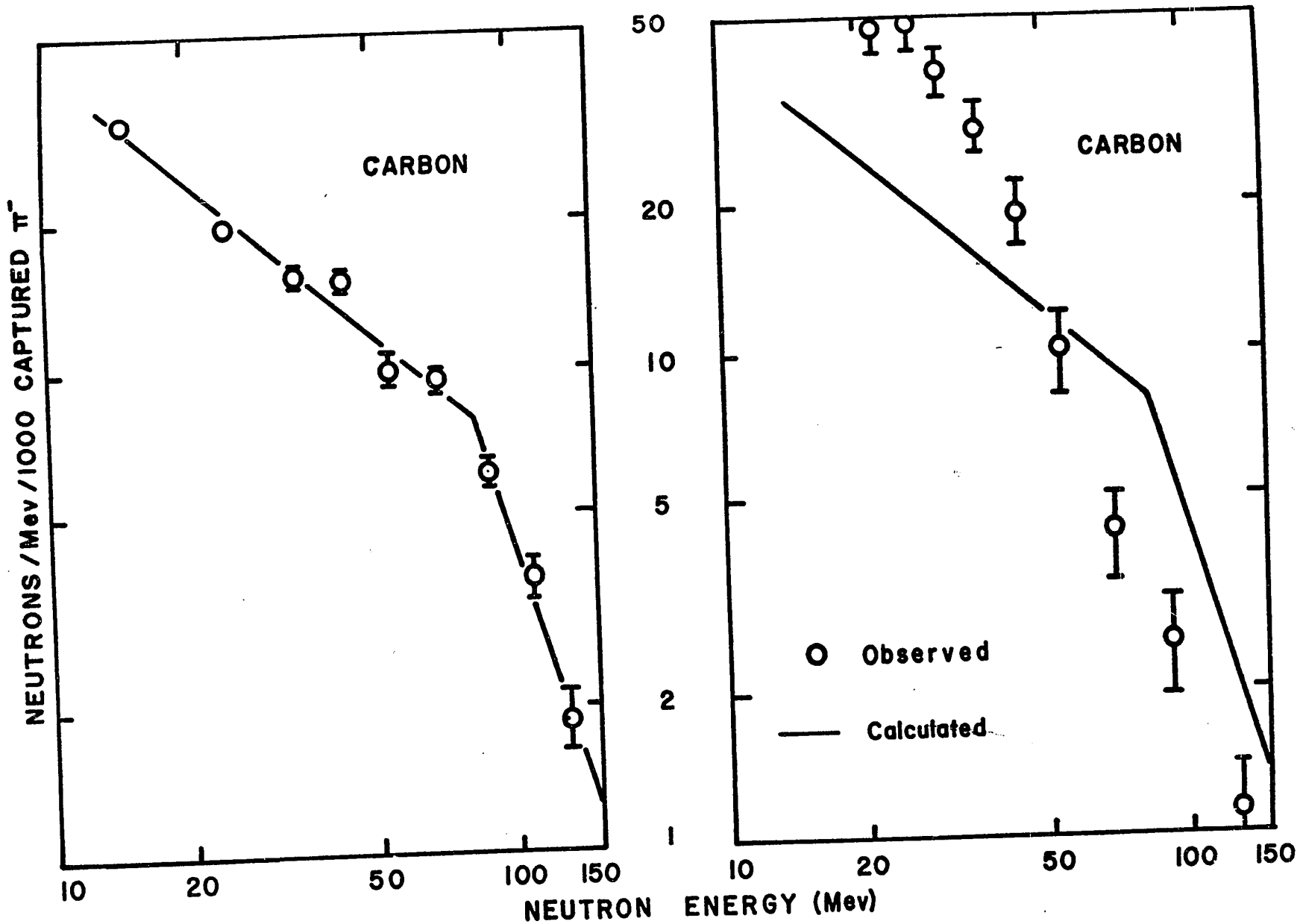

Figure 23- Calculated Neutron Energy Distribution for π^- Capture in Carbon

Figure 24- Observed and Calculated Neutron Energy Distribution for π^- Capture in Carbon

IV-3 Discussion

The experimental distributions were reasonably well reproduced by the calculation. In the case of cadmium and lead, both of which are near spherical nuclei, the agreement was excellent. For uranium and aluminium, however, there is a slight disagreement. In the case of uranium this may be attributed to its non-spherical shape; thus in reality the secondary nucleons, on the average, do not traverse as much nuclear matter as our model assumes, resulting in more fast nucleons. The discrepancy in aluminium is probably because the nucleus is getting small and is no longer well described as a Fermi gas. This would also account for the larger discrepancy observed in carbon.

Chapter V

ENERGETIC PION INTERACTIONS IN EMULSION.

V-1 Introduction

Antiproton annihilation in emulsion and negative pion capture by large nuclei contributed some ideas to the processes governing pion interactions in nuclei. For neither of these, however, is it possible to specify an incident direction; thus no angular distribution can be found. In the interaction of mono-energetic pions it is possible to determine an incident direction, and thus in principle an angular distribution of the scattered pions and of the outgoing protons may be determined, allowing a more comprehensive comparison with calculated results. Unfortunately, at present no such data appears to be available.

This group has thus undertaken a study of the interaction of low energy pions (less than 250 Mev), with complex nuclei. This energy region was selected because it contains the first, and dominant pion nucleon resonance.

To be able to compare the experimental data with theoretical results one must be sure that no bias is introduced. As one is searching for stars, for instance, several

types may be consistently overlooked. To be able to estimate the bias , the pion-nucleus cross-section in emulsion must be found, so that one can calculate how many stars are expected.

In this case the cross-section was estimated from the attenuation of the pion beam as it traversed the emulsion. As a result of the analysis, one also expects to be able to determine the pion flux anywhere in the stack analysed.

V-2 The Irradiation

In December 1966, in a joint experiment between Centre Nucléaire, CNRS at Strasbourg-Cronenbourg and the University of Ottawa, a stack of emulsions was irradiated at the CERN proton synchro-cyclotron by a beam of positive pions. The stack consisted of 70 pellicles of Ilford K5 emulsion, clamped between two slabs of bakelite (figure 25). The stack measured 9.5cm x 4.2cm x 34.7cm, while the whole assembly (stack, bakelite and covering material) measured about 10cm x 10cm x 35cm. The stack was assembled and machined at Strasbourg, and after irradiation the emulsions were also developed and mounted there.

The pion beam* had, at the focus, a nominal energy of 250±20 Mev, an angular spread of 6^{o}, a muon contamination of 15%, and dimensions 2cm x 5cm. The stack was, however, not placed at the focus, but 3 meters behind the focal point (Figure 26). At this point, the maximum angular spread in the stack is 1.5^{o}, and the beam of pions is spread over a large area, so that at the front of the stack the pion flux is fairly uniform. Since the pions have to travel an additional 3 meters, some may decay,

---

*This pion beam was assembled for Dr. N. W. Tanner.

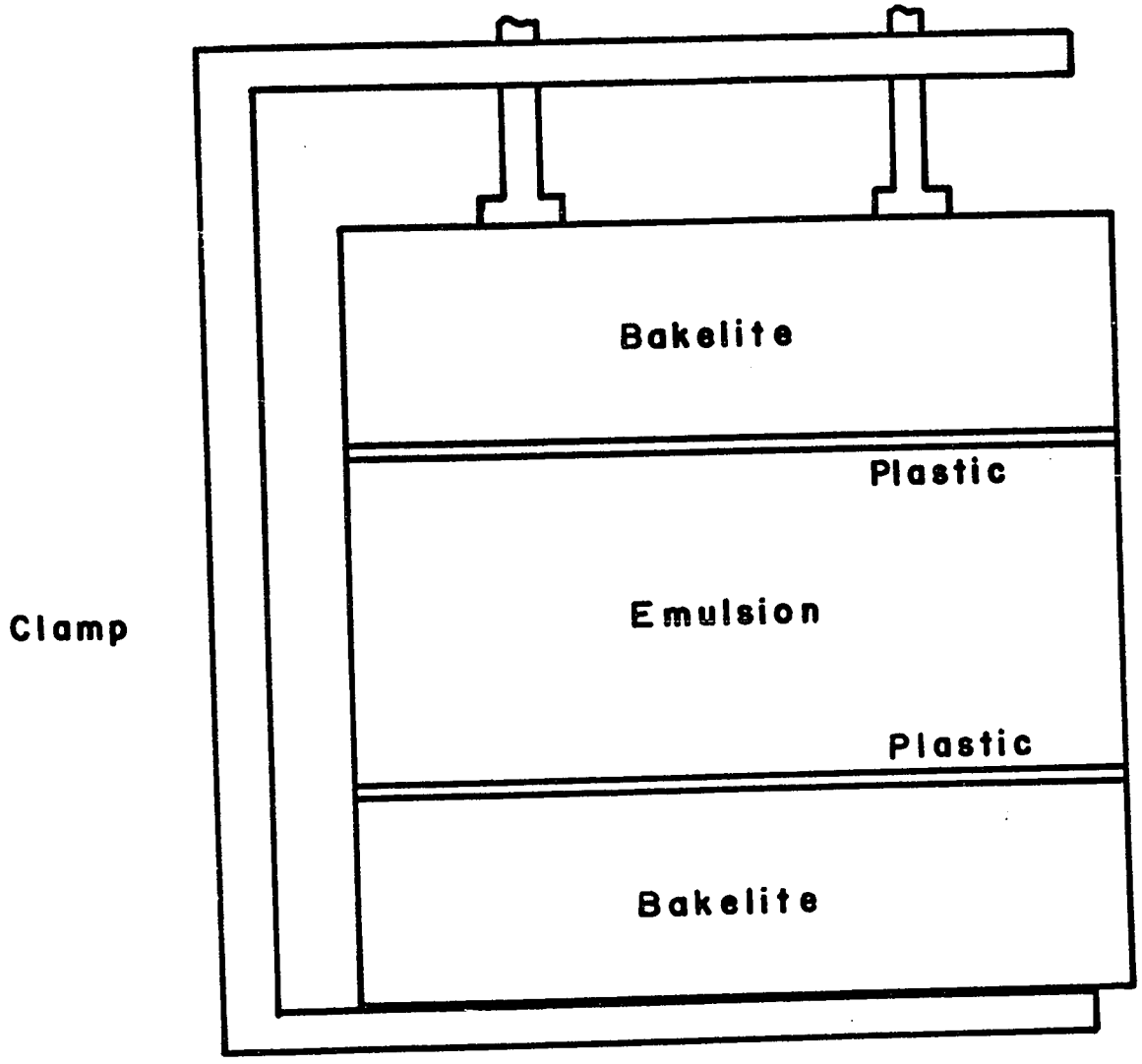

Figure 25 - Schematic Diagram of Emulsion Stack

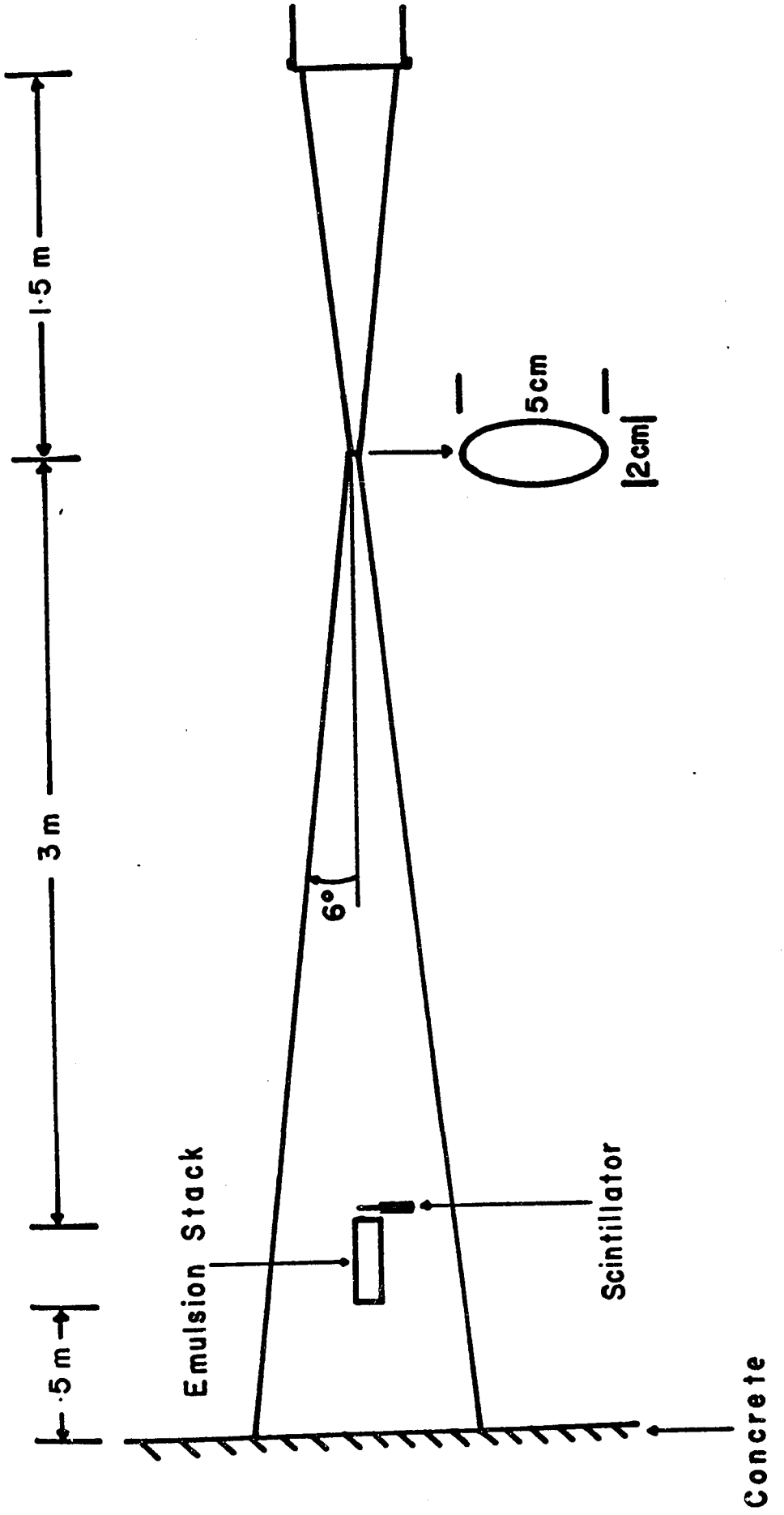

Figure 26 - Schematic Diagram of Irradiation Conditions

increasing the muon contamination to about 18%.

A scintillator was placed in front of the stack, so that the flux could be monitored; the counter measured a total flux, entering the stack, of 7.2×10^3 particles/cm^2.

V-3 Energy Determination

The pion beam had a nominal energy of 250±20 Mev, but since it had to traverse 3 meters of air and a scintillation counter, and since only a small part of the beam was used, the conditions in the stack might be slightly different.

Since positive pions have a definite range, the distribution of stopped pions, in the direction of the beam, is a measure of the incident energy and energy spread. When positive pions stop, they decay into a muon and a neutrino, thus producing a very characteristic event. The number of pion to muon decays per unit interval was found in two plates (P 21 and P 35) as a function of the range in emulsion. The observed distributions were compared to a gaussian test distribution (figure 27) and the χ^2 value was calculated. The parameters of the test distribution were then adjusted till a minimum χ^2 was obtained. These parameters were considered to be the best fit to the experimental data.

Table 14 shows the observed fits, and the corresponding energy. The spread in range is due not only to a spread in energy, but also because of straggling; this was taken into account in the calculation of the energy spread.

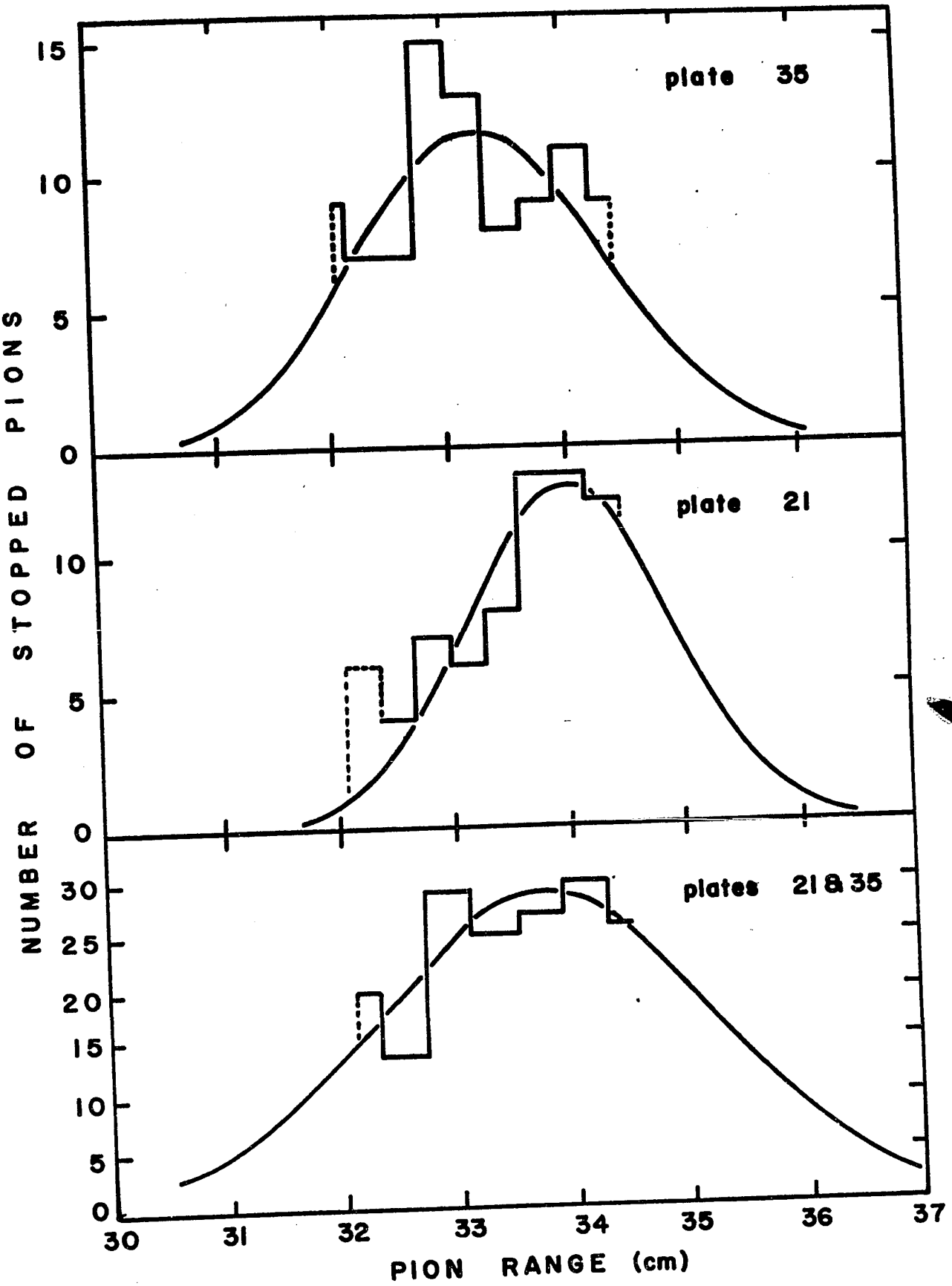

Figure 27 - Observed Stopped Pion Distribution and Gaussian Fit

Table 14: Range of Pions in Emulsion

Plate No.	Range (cm)	Spread in Range (cm)	Observed No. of Pions.	Goodness of Fit. (χ^2)	Energy (Mev)	Spread in Energy (Mev)
35	33.4	1.1	79	40%	235	-
21	34.0	1.0	69	60%	239	-
21&35	33.7	1.43	148	40%	237	6

V-4 Beam Characteristics in the Emulsion

The beam entering the stack was found to have an angular spread less than 1.5°, and to be parallel to the stack within $.5^{\circ}$. As the beam traverses the stack, however, due to multiple scattering, the angular spread of the beam increases. This angular dispersion, σ_θ, may be calculated [34] at any distance, t, in the stack from the following formula:

$$\sigma_\theta = 15 t^{1/2} k/p\beta \quad \text{degrees}$$

where t is measured in cms., and

$$k = (29.5 + 3.2 \log_{10} t)$$

is the scattering constant, p is the momentum of the particle in Mev/c and β is the ratio of the particle velocity to that of the speed of light. In this particular experiment $p\beta$ is not a constant, but decreases with increasing t; thus for the calculation of the angular dispersion the average value of $(1/p\beta)$ over the traversed path was used. The angular dispersion was determined experimentally at several points and these values, together with the theoretical

curve are shown in figure 28

Since there is an angular dispersion of the beam, there will also be a dispersion in its physical dimension, thus causing a decrease in flux as t increases. If a very fine beam of pions had been injected into the emulsion, then after a distance t the beam would have spread, to give a gaussian distribution (figure 29). Letting $\sigma_\perp$ be the standard deviation of this distribution, then the flux, $\phi(y)$, at a distance y from the axis would be given by:

$$\phi(y) = ke^{-y^2/2\sigma_\perp^2}$$

In this experiment, a uniform beam of pions is incident on the stack; decomposing this into many fine beams, and adding the contribution of each to the flux at a point x from the edge of the stack (figure 30) yields the formula:

$$\Phi(x) = k \int_{x-a}^{x} e^{-y^2/2\sigma_\perp^2} dy$$

where a is the width of the plate. $\sigma_\perp$ can be calculated from σ_e, using the formula:

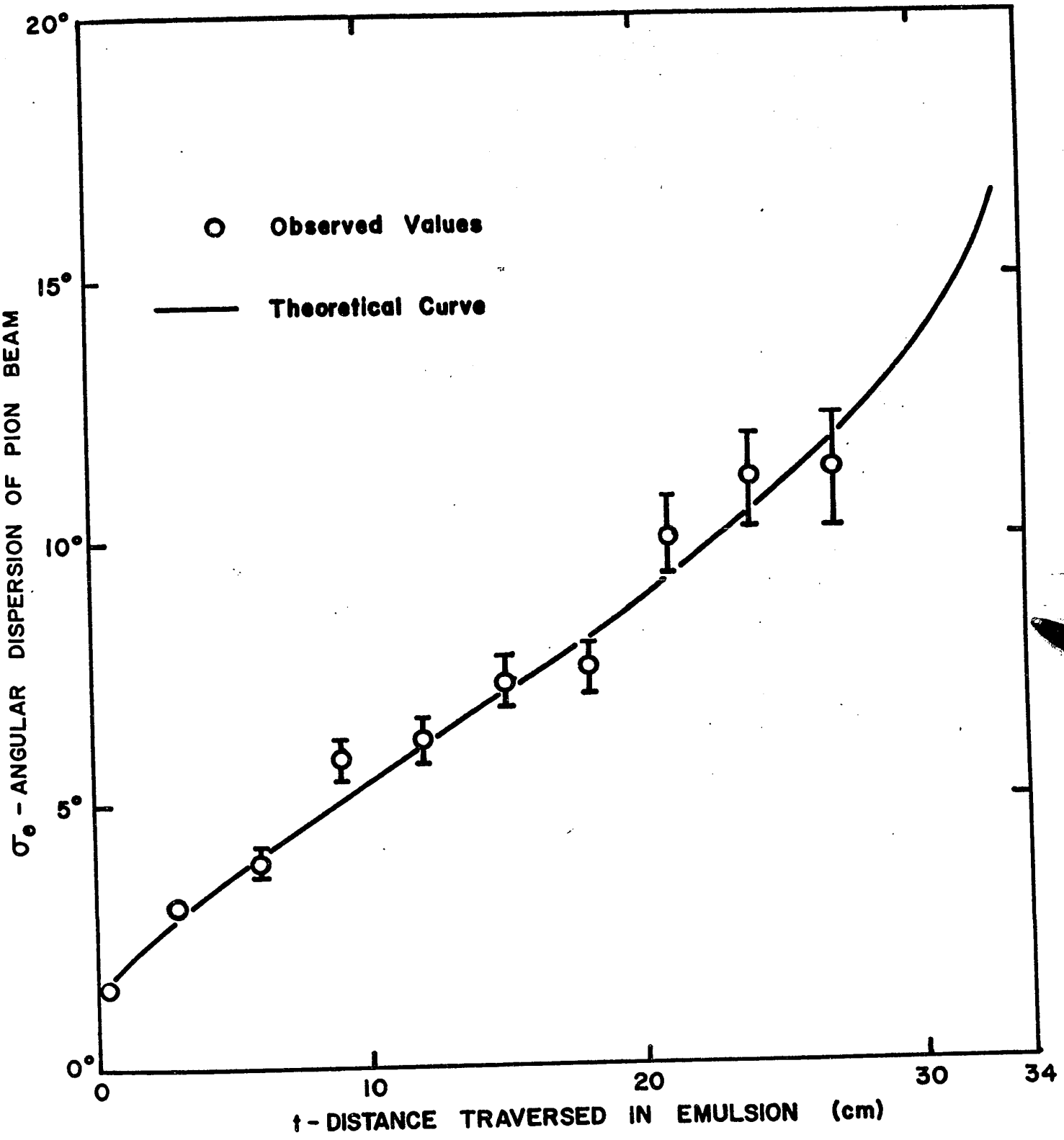

Figure 28 - Observed and Predicted Angular Dispersion of the Pion Beam as a Function of Traversed Distance

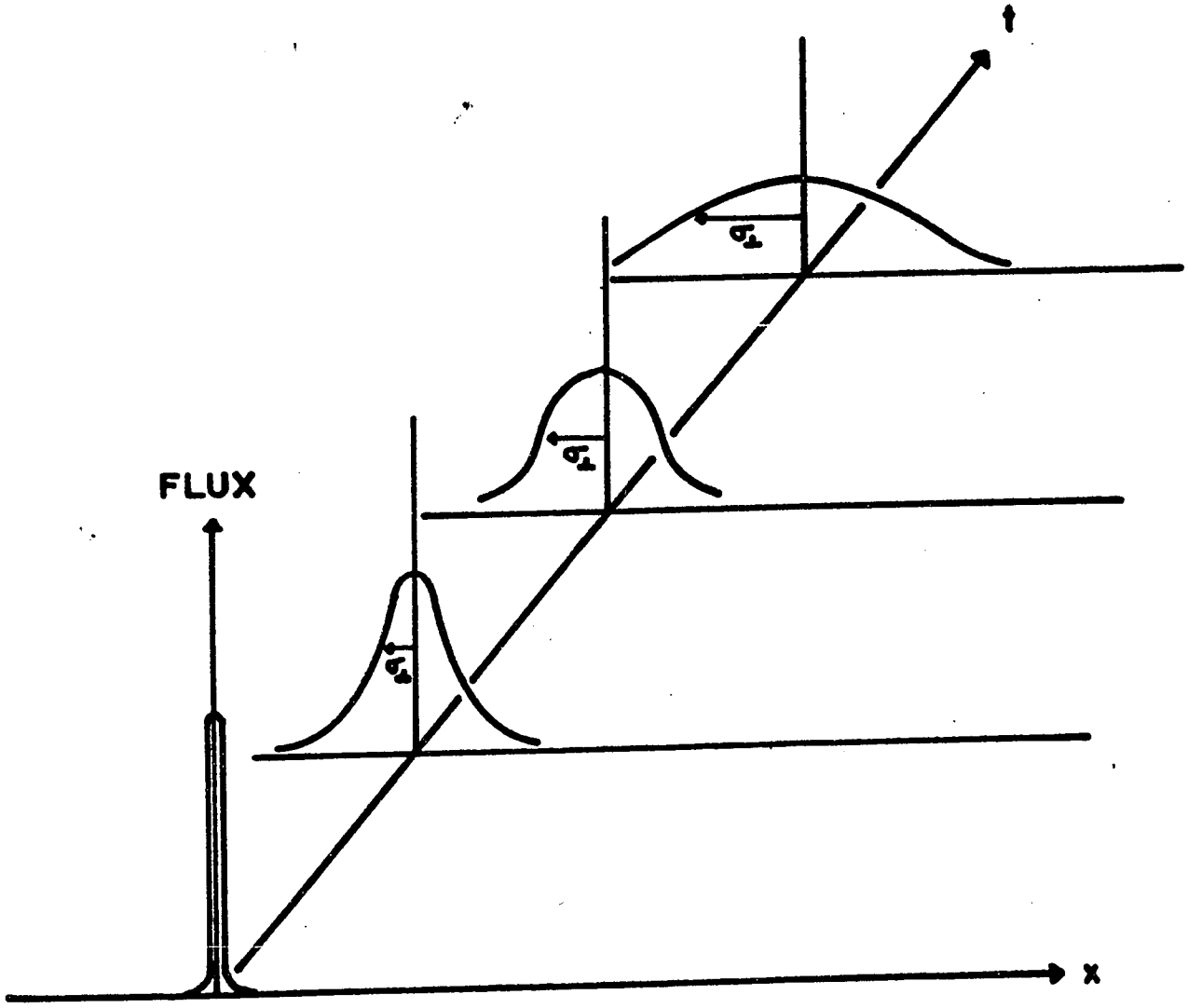

Figure 29-Schematic Diagram of Dispersion of a Fine Beam Injected into a Scattering Material

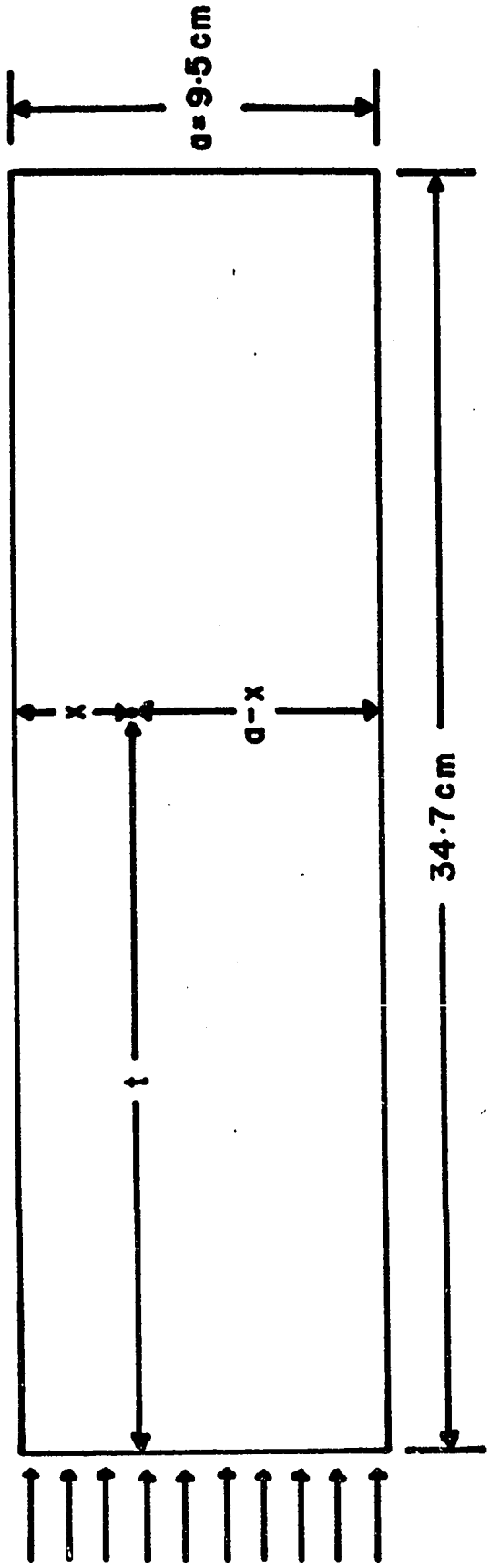

Figure 30 - Geometry Used to Calculate $\bar{\Phi}(x)$

$$\sigma_{\perp} = t \quad \sigma e / \sqrt{(3)}$$

Thus the flux at any point can be calculated, except that the flux also decreases because pions interact with nuclei. Since the pion flux in the central 4 cms of the plate does not decrease appreciably due to multiple scattering for $t \leq 21$ cms, an estimate of the interaction cross-section can be made. The flux, in the central 4 cms, was found at several values of t, and from the observed decrease a mean free path of interaction was determined. Figure 31 is a plot of $\log_{10}(\Phi)$ versus t, and the slope yields an average pion loss of $(3.38 \pm .17) \times 10^{-2}/cm$, assuming a muon contamination of $(18 \pm 2)\%$.

Using this, the flux across the beam at several values of t was calculated, and figure 32 shows the calculated and observed values. One can see that indeed in the central 4 cms the flux is not appreciably changed due to multiple scattering.

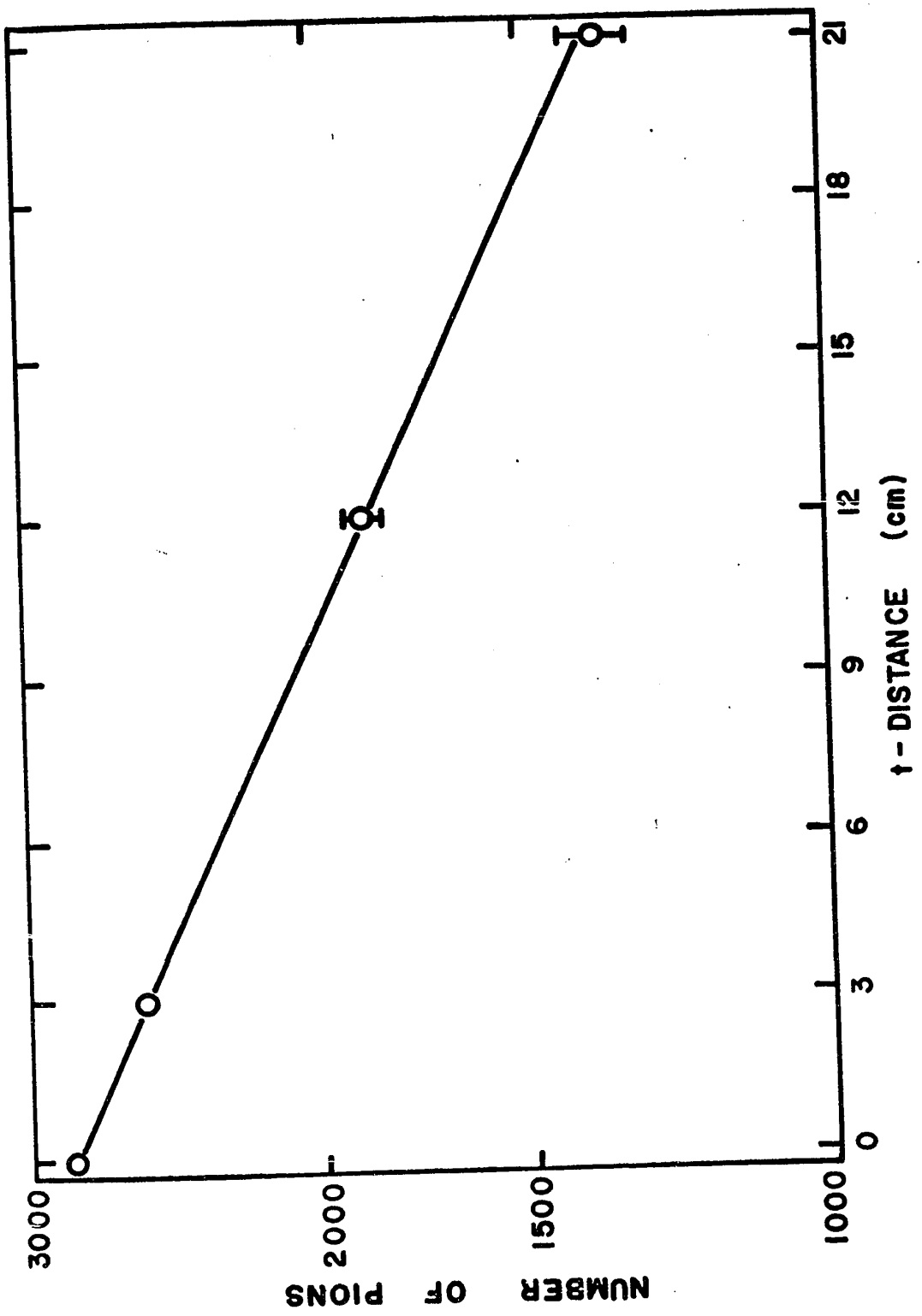

Figure 31 - Decrease in Pion Flux as a Function of Distance

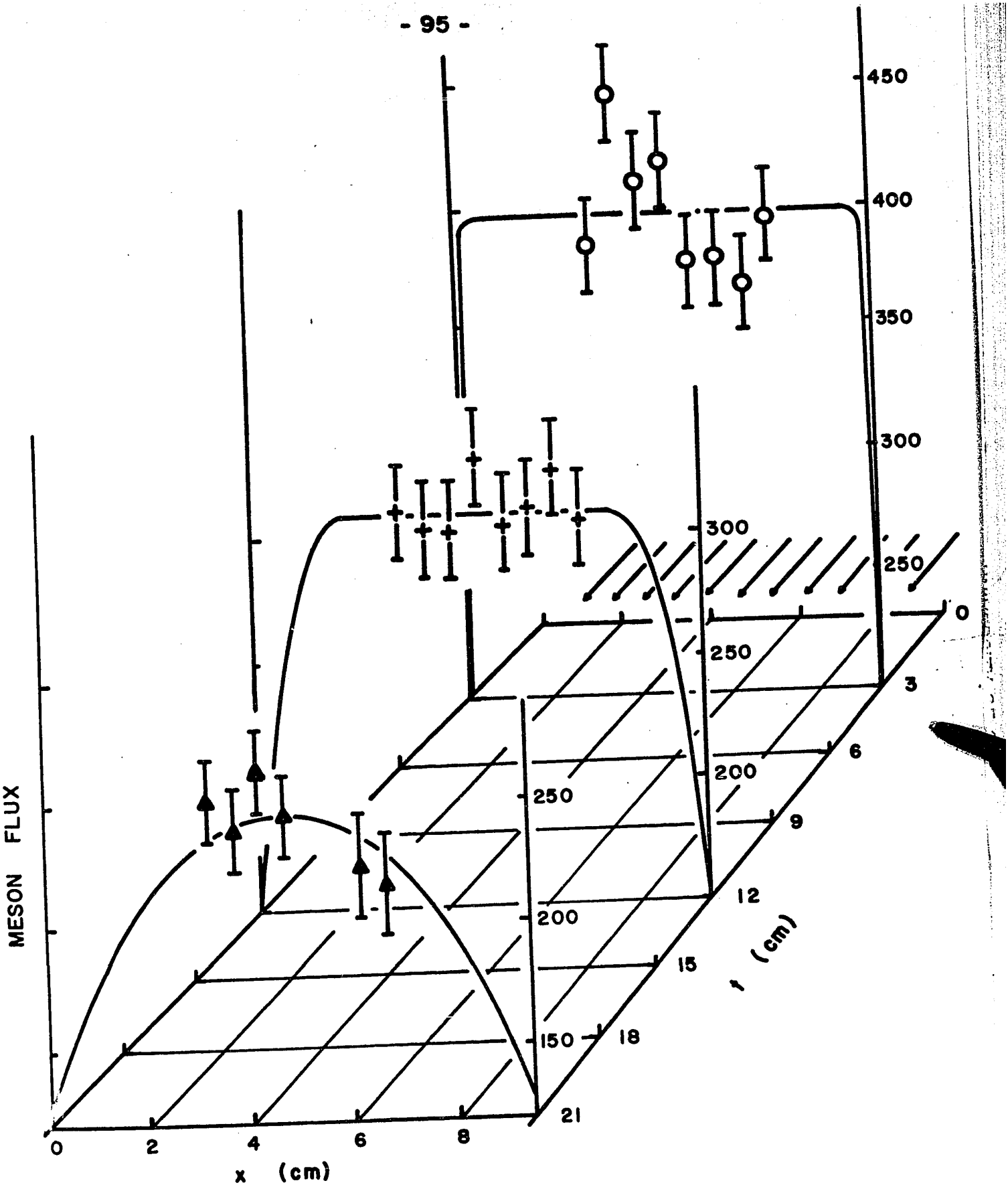

Figure 32- Variation of Meson Flux in Emulsion at Several Distances

V-5 Detection of Stars

Plates 21 and 35 were area scanned for pion induced stars. In both plates nine areas of 1cm x 4cm were scanned at 3cm intervals, from 3cm to 27cm. Stars were accepted as pion induced stars if they had a minimum track in the right direction.

Plate 21 was scanned on a normal flat stage, while plate 35 was scanned on a tilted stage; the latter was done in an attempt to find a more efficient method of area scanning. Normally, with a flat stage, scanning is done by moving the z-motion on the microscope; this is tedious to do, and also causes the motion to wear out quickly. With a tilted stage, the emulsion is not perpendicular to the optical axis,but at a slight angle to the plane (figure 33). As a result, the top and bottom of the emulsion can be seen simultaneously through the microscope. When the plate is moved along this direction, a volume is scanned, rather than an area. Thus in one motion scanning in depth, as well as along a line, is performed; and to view any point in the emulsion only two motions, rather than three, are required. In principle, then, this method should be more efficient*.

---

* It should be noted that this is another application of a tilted stage, which are at present being used extensively by this laboratory.(See M.-A. Vincent, M.Sc. thesis, University of Ottawa)

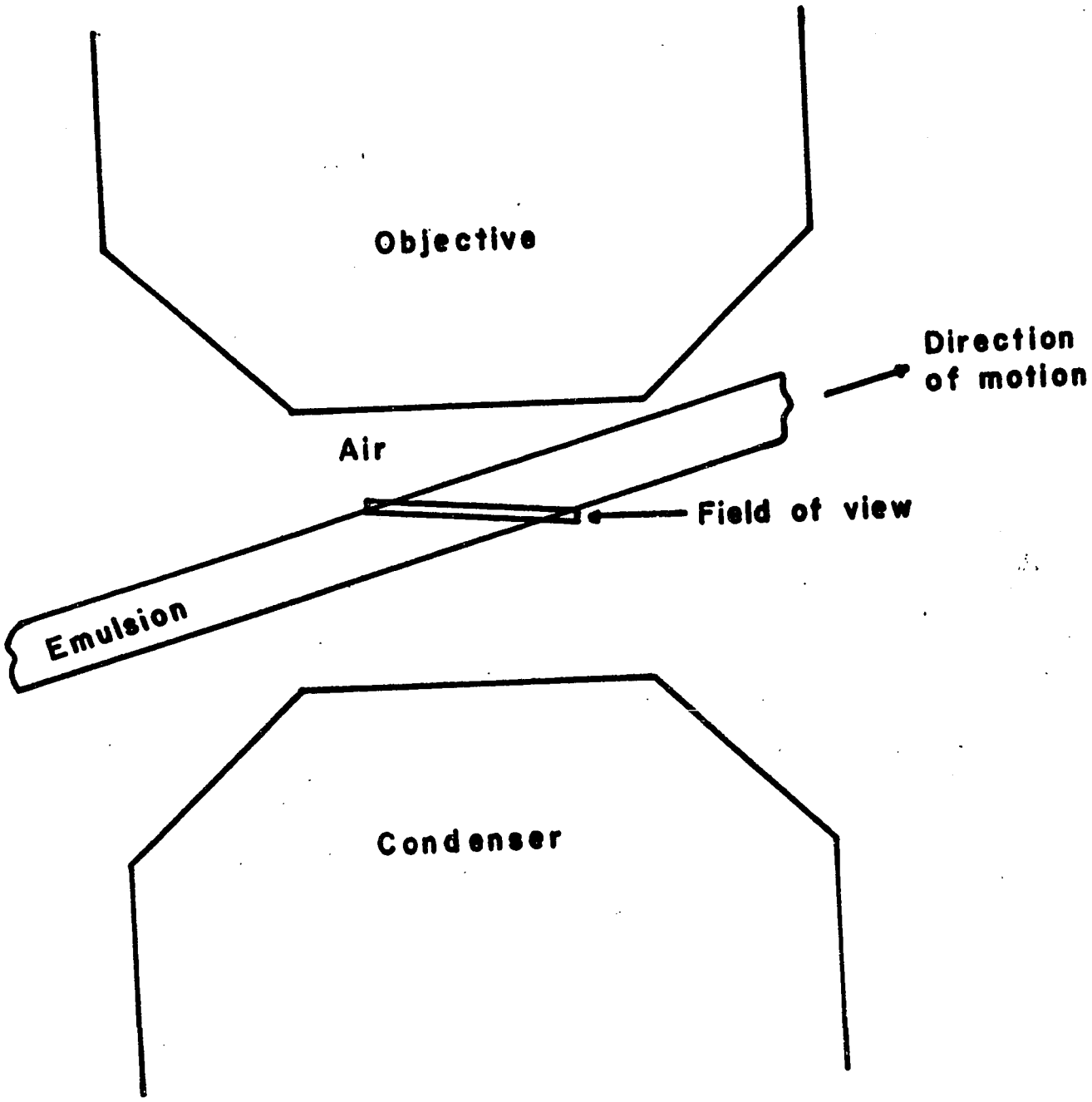

Figure 33- Schematic Diagram of Tilted Stage

However, there are some difficulties. Since a larger volume is scanned in a period of time, scanning this way requires more concentration. Then also, since scanning has to be done while the emulsion is moving from left to right, one has a tendency at first to become motion sick; however, with practice this may be overcome*. These difficulties would not be present for an automatic scanning device, such as the flying spot microscope.

Another problem is due to the thickness of the emulsion. The stage needs to be tilted enough, so that the top and bottom of the emulsion are visible through the microscope. For scanning, a total magnification of 300x is considered to be desirable; for this magnification, the field of view is about 550μ x 550μ. The original emulsion was 600μ thick, but because of shrinkage it is presently only 250μ thick. Since a dry objective was used, and the refractive index of air and emulsion differ, the apparent depth of the emulsion is at most 170μ. Thus the stage needs

---

* It was found to be especially important that the stage be moved smoothly.

to be tilted at an angle θ given by:

$$\tan \theta = 170\mu / 550\mu$$

or:

$$\theta = 17^{\circ}$$

The actual angle used was 17.7°.

With such a large angle the regular objective could not be used, because its working distance is too short; thus an objective of inferior quality, with a longer working distance had to be employed. This, plus the fact that the condenser also had to be modified, resulted in an image of relatively poor quality. At optimum conditions, however, a minimum track could be resolved.

When scanning for stars, in both plates, black or grey tracks ending in the emulsion were looked for; these are generally the results of stars, and thus pion induced stars will be found. (Since there are many electron tracks, looking for minimum tracks to produce stars is a near impossible task.) This method is not totally efficient: any pion producing a star having only minimum or almost minimum tracks will be missed. Add to these the neutron stars and the visible stars missed, and the total efficiency is poor. However, an estimate of this efficiency may be made from the

observed pion flux, and the appropriate corrections can be introduced.

V-6 The Pion Interaction Cross-section

A cross-section may be determined in two ways: first by measuring the attenuation of the beam as it passes through matter, and second by measuring the number of interactions per unit volume per unit flux.

The attenuation of the pion beam as it passes through the emulsion was measured and a mean free path of 29.1 ±1.0cm was found (figure 31). This is an average value in the energy interval from 120 Mev to 230 Mev. The value compares well to data for positive and negative pion mean free paths at various energies in emulsion (table 15). (It is expected that the negative pion mean free path will be less than that for positive pions because of the coulomb barrier).

The interaction cross-section can be calculated, if it is assumed that the pion nucleon cross-section inside and outside the nucleus are the same. In that case, if σ_{coul} is the geometrical cross-section, then:

$$\sigma = \sigma_{coul}\left[1-(E_{coul}/E_{\pi})\right]\left[1-e^{-(A^{1/3}\,\overline{\sigma_{\pi N}}/\pi r_o^2)}\right]$$

is the actual cross-section. The second term is the cor-

Table 15: Mean Free Path of Pions in Emulsion

Particle	Energy Interval (Mev)	Mean Free Path (cm)	Reference
π^-	190-230	27.4	35
π^-	295	26.8±1.4	36
π^+	70-80	25.5±3	37
π^+	35-50	38 ±4.5	37
π^+	144-196	31.7±3.3	38
π^+	151±7	31.8±1.9	39
π^+	217±6	27.1±1.3	40
π^+	120-230	29.1±1.0	This work

rection for the coulomb repulsion, where E_{coul} is the coulomb barrier and E the pion incident energy, and can be derived from the Rutherford scattering formula. The last term accounts for the opacity of the nucleus to pions; A is the atomic mass number, $\overline{\sigma_{\pi N}}$ is the average pion-nucleon cross-section, and r_o is taken as 1.3f.

Figure 34 shows the effect of each of these terms on the total cross-section for pion interactions with small and large nuclei in emulsion. Since there are many types of nuclei in emulsion, the collision probability, rather than the cross-section, was plotted; that is, the percentage of pions that interact per centimeter traversed. Also shown is the collision probability due to the hydrogen in emulsion; for the total collision probability in emulsion, this last factor must be added.

Using the calculated cross-sections, the expected number of pions lost per centimeter is 3.40%, which is to be compared to the experimental value of 3.38± .17%, which was previously found.

Since the calculated cross-section appears to be sufficiently accurate, it was used to calculate the total flux along the beam, and this is compared to the observed values in figure 35. The calculations were performed assuming the limiting cases of 15% and 20% muon contamination.

Finally, the cross-section was calculated from the

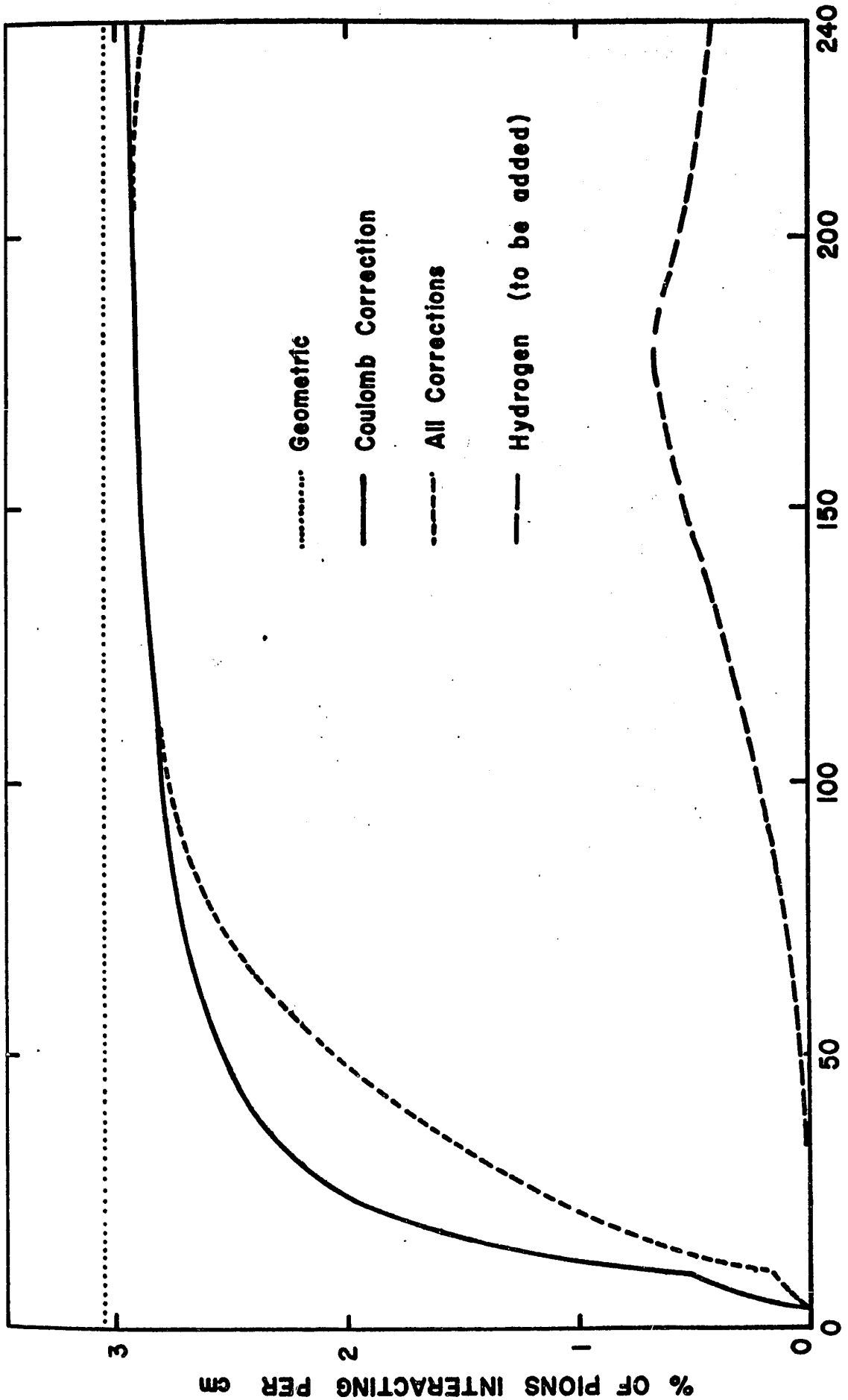

Figure 34-Predicted Pion Interaction Probability

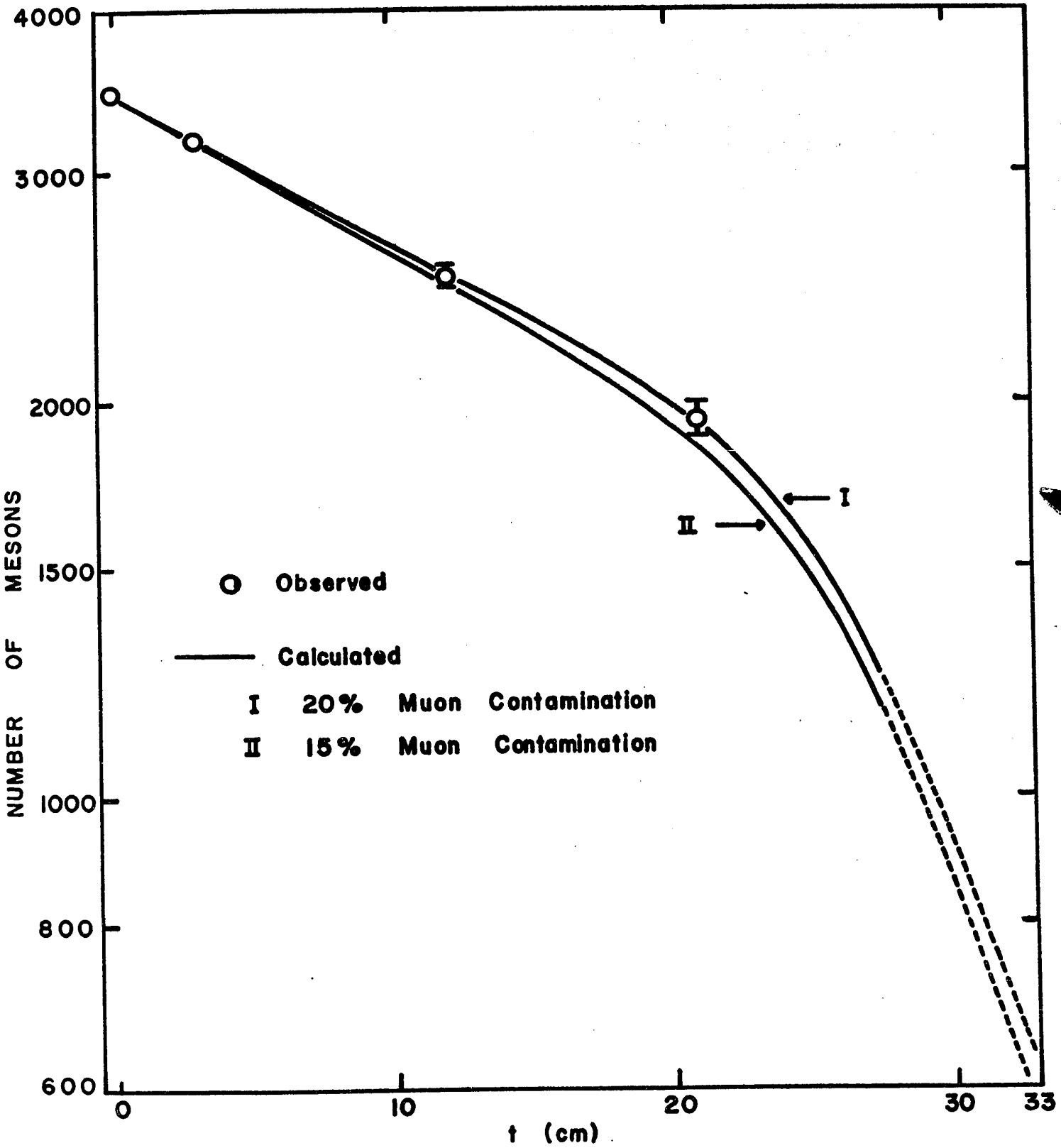

Figure 35 - Observed and Calculated Meson Flux

number of pion induced stars found. A total number of 166 and 154 stars were found in plates 21 and 35 respectively. From the number of stars found and the attenuation of the beam, a detection efficiency of 73±7% was found for the first 12cm, and an efficiency of 59±8% for the next 15cm. The decrease in efficiency is probably because in the last 15cm there were less stars per unit volume, and more secondaries. Correcting for the efficiency, the collision probability was calculated at several energies. The experimental results, as well as the calculated collision probabilities, are shown in figure 36. $\overline{\sigma_{\pi N}}$ inside the nucleus had been calculated on the assumption that the pion saw a 30 Mev potential well; if this is not assumed, the dashed curve is obtained. At the energies in this experiment no difference can be seen.

The error bars, listed in order of magnitude, include:

a) uncertainty in the number of stars,

b) uncertainty in the efficiency of detecting stars,

c) uncertainty in the muon contamination, and

d) uncertainty in the total flux.

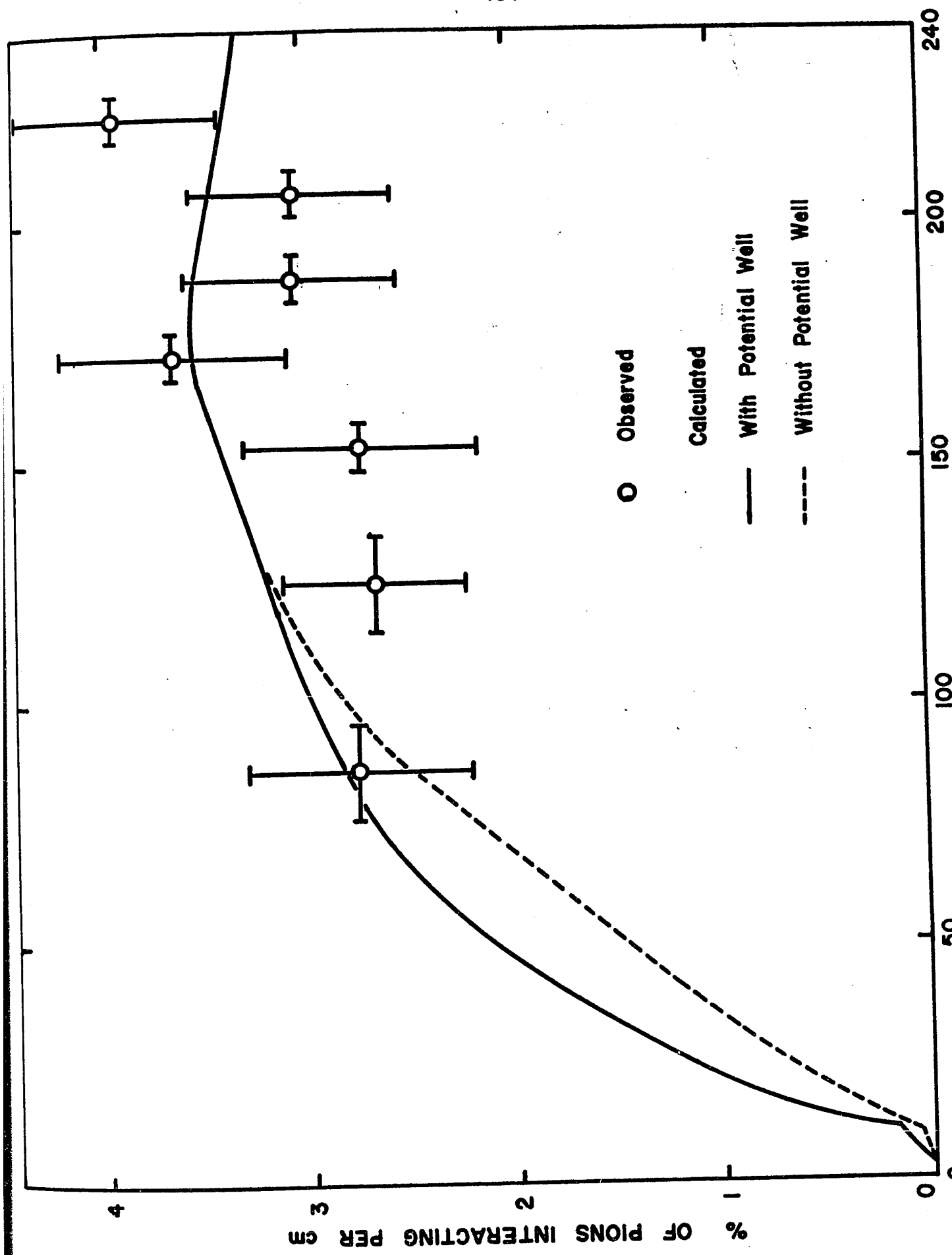

Figure 36- Observed and Calculated Pion Interaction Probability

V-7 Discussion

The tilted stage was used to find pion to muon decays as well as pion induced stars. In both cases it was found to have the same efficiency for detecting stars as a flat stage, while the scanning speed was better by a factor of two to three. With some improvements in the optics, this method is to be considered more efficient.

Our overall efficiency of star detection was found to be very low; however, this low efficiency was primarily due to our method of scanning. That is, we only looked for stars that had a black or grey track attached to it. Our efficiency for detecting these was estimated at 85% to 90%; thus the remaining stars missed must have had only white tracks. Missing these stars may introduce a bias in the experimental distributions, which will have to be corrected for.

The good agreement between the cross-section found and calculated using the isobar model is again encouraging. It should be noted that the BSW model [5] would predict a higher transparency [41] and thus a smaller cross-section.

Finally, the cross-sections below 70 Mev should give an indication as to whether or not the pion needs to see a potential well.

Chapter VI

CONCLUSION

It was found that the isobar model is very convenient to use, and by far simpler than the BSW model of pion absorption. The isobar model can explain the relative ratio of neutron-neutron to neutron-proton pairs produced in negative pion capture, while the method of absorption on correlated pairs cannot. The isobar model does not require a nucleon pair to be close together for fast pion absorption, and thus pion absorption can occur in the required short time (10^{-22} seconds), while the pion crosses the nucleus. The isobar model, however, need not be the only process by which pions are scattered inelastically from nuclei, as is indicated by recent data [42].

The analysis has shown that in our nuclear model the pion may see a potential well, resulting in a shift of the peak in the pion-nucleus cross-section. The cause of the potential well is not exactly understood.

The analysis of antiproton annihilation into pions has shown that a statistical model, incorporating isospin conservation, gives a reasonable description of the annihilation process. It should be realized that the statistical model is a simplification and the actual processes

occurring are probably far more complex.

Appendix 1 Some Quantum Numbers

All strongly interacting particles have an intrinsic parity, p, which determines their behaviour under reflection in physical space. By definition the proton and neutron have p=+1. The parity of all other particles are determined from this. Thus, for instance, since antiprotons and antineutrons have opposite parity to protons and neutrons, they have a parity of -1. Pions also have a negative parity. The parity, P, of a system of two particles of relative angular momentum L, and intrinsic parities p_1 and p_2 is:

$$P = p_1 p_2 (-1)^L$$

so that in the case of a nucleon and antinucleon:

$$P = (-1)^{L+1}$$

In strong interactions parity is conserved, and thus must be considered in nucleon-antinucleon annihilation.

C-parity is defined only for particles which transform into themselves under charge conjugation, and are thus their own antiparticles. Nucleons, strange mesons and charg-

ed mesons do not have a C-parity, while photons, neutral pions and the antineutron-neutron and antiproton-proton system do. The neutral pion has C=+1. For the antineutron-neutron and antiproton-proton system, C depends on their relative angular momentum and their spin orientation. Since both particles in the system are fermions, they must be anti-symmetric under the exchange of all space variables (charge conjugation, angular momentum and spin). Thus:

$$C\,(-1)^{L}\,(-1)^{S+1} = -1$$

where S, the total spin, is one when the spins are aligned, and zero when they are opposite. From this one gets:

$$C = (-1)^{L+S}$$

in the case of the antineutron-neutron and antiproton-proton systems. C is also conserved in strong interactions, and must be considered when the systems decay into neutral pions.

It is also possible to define a quantity, called G-parity, for all non-strange mesons. One finds that, like parity, the G-parity is the same for all particles in an isospin multiplet. It may be shown that for a meson, which

has a C-parity, the G-parity is given by:

$$G = C(-1)^T$$

where T is the isospin of the multiplet. Thus, for instance, in the case of pions, the G-parity is found to be -1, since $C=+1$ for π^o and $T=1$ for pions. For the antinucleon-nucleon system, recalling that:

$$C = (-1)^{L+S}$$

in the case of the antiproton-proton system, it is easy to see that:

$$G = (-1)^{T+L+S}$$

Again, G-parity is conserved in strong interactions. Thus, if the annihilation centre has $G=-1$, it can only decay into an odd number of pions, while if $G=+1$, it can lead to an even number of pions.

Finally, the intrinsic angular momentum of a particle, as well as the intrinsic angular momentum of a system of particles, is denoted by J in elementary particle physics. For a system of particles, their relative angular

momentum and their spin orientation are commonly denoted using the spectroscopic notation. When considering the interactions of elementary particles with a nucleus this can lead to some confusion, and care must thus be taken.

ADDENDUM

P101 - to obtain the opacity of the nucleus from the known average pion nucleus cross-section $\overline{\sigma_{\pi n}}$, the sphere is replaced by a disk of thickness 4/3 R. This gives the average thickness of the sphere, and gives a good approximation to the opacity. The density of nuclear matter is:

$$(4/3\ \pi r_o^3)^{-1}$$

so that the mean free path λ is:

$$\lambda = \frac{4/3\ \pi r_o^3}{\overline{\sigma_{\pi n}}}$$

The fraction of pions traversing a thickness $4/3R = 4/3\ A^{1/3} r_o$ is given by:

$$e^{-\frac{4/3\ A^{1/3} r_o\ \overline{\sigma_{\pi n}}}{4/3\ \pi r_o^3}}$$

$$= e^{-A^{1/3}\ \overline{\sigma_{\pi n}}\ /\ \pi r_o^2}$$

so that the opacity is:

$$1 - e^{-A^{1/3}\ \overline{\sigma_{\pi n}}\ /\ \pi r_o^2}$$

Appendix 2 Use of Clebsch-Gordan Coefficients

Adopting the same notation as in the text, that is: $|T=1, T_3=1\rangle = \alpha^+$, $|1,0\rangle = \alpha^0$, $|1,-1\rangle = \alpha^-$, and $|0,0\rangle = \beta$, the α^0 can be decomposed into two α states as follows:

$$\alpha^0 = 1/\sqrt{2}\ \alpha^+\alpha^- + 1/\sqrt{2}\ \alpha^-\alpha^+$$

However, if β states are also allowed, then it may also be decomposed into the following two ways:

$$\alpha^0 = \alpha^0 \beta$$

$$\alpha^0 = \beta\, \alpha^0$$

To calculate the relative frequency for the α^0 state to go to $\alpha^-\alpha^+$, for instance, the product squared is taken:

$$|\langle \alpha^0 | \alpha^-\alpha^+ \rangle|^2 = |1/\sqrt{2}\ \langle \alpha^+\alpha^- | \alpha^-\alpha^+ \rangle + 1/\sqrt{2}\ \langle \alpha^-\alpha^+ | \alpha^-\alpha^+ \rangle|^2$$

$$= |0 + 1/\sqrt{2}\ |^2$$

$$= 1/2$$

Similarly:

$$|\langle \alpha^0 | \alpha^+\alpha^- \rangle|^2 = 1/2$$

$$|\langle \alpha^0 | \alpha^0\ \beta \rangle|^2 = 1$$

$$|\langle \alpha^0 |\ \beta\, \alpha^0 \rangle|^2 = 1$$

sothat the probability for α^0 to go to $\alpha^-\alpha^+$ is 1/6.

From the relations:

$$\alpha^{\pm} = 1/\sqrt{2}\,\alpha^{\pm}\alpha^0 + 1/\sqrt{2}\,\alpha^0\alpha^{\pm}$$

$$\alpha^{\pm} = \alpha^{\pm}\beta$$

$$\alpha^{\pm} = \beta\,\alpha^{\pm}$$

$$\beta = 1/\sqrt{3}\,\alpha^+\alpha^- - 1/\sqrt{3}\,\alpha^0\alpha^0 + 1/\sqrt{3}\,\alpha^-\alpha^+$$

$$\beta = \beta\,\beta$$

the probabilities for the other modes can be easily calculated.

Appendix 3 **Sample Programme**

Following is a copy of the programme (OS) for antiproton annihilation in emulsion; also shown, on the last page, is a sample of the output obtained.

In the coding the conventions used were: all symbols starting or ending in X,Y,Z, refer to space positions or directions; all symbols starting in T,E, or W refer to kinetic energy in Mev, momentum in Mev/c and mass in Mev/c^2, respectively; all symbols starting with NUCL refer to pions if their value is negative, neutrons if their value is zero and protons if their value is positive; all symbols starting with SEC or SIG refer to cross-sections measured in millibarns; and all symbols ending in CHAR refer to the charge of the pion.

In the subroutine CMSLOB, symbols starting with U refer to total energy in Mev, and symbols starting with P refer to a component of momentum measured in Mev/c.

```
            C BEGIN
            C*****DIMENSIONS,COMMON,ARITHMETHIC FUNCTIONS AND CONSTANTS
S.0001            DIMENSION XSTORE(20),YSTORE(20),ZSTORE(20),ESTORE(20),CAPX(20)
S.0002            DIMENSION CAPY(20),CAPZ(20)
S.0003            DIMENSION  NUCLST(20)
S.0004            DIMENSION  TINT(21)
S.0005            DIMENSION SECII(11),SECIJ(9)
S.0006            DIMENSION NPIIN(21,100),NPIOUT(21,100),NNOUT(21,100)
S.0007            DIMENSION  NSCN(21)
S.0008            COMMON W1C2,W2C2,BETA,GAMMA,PN
S.0009            COMMON  WAFT
S.0010            TTOE(T,W)=(T*T&2.*W*T)**.5
S.0011            ETOT(E,W)=(E*E&W*W)**.5-W
S.0012            PI=3.141593
S.0013            RZERO=1.3
S.0014            IPAGE=0
            C*****READ DATA
            C READ 1
S.0015            READ (1,13) TINT
S.0016         13 FORMAT (7(F6.1,2X))
S.0017            READ (1,3)SECII
S.0018          3 FORMAT (11(F6.1,1X))
S.0019            READ (1,11) SECIJ
S.0020         11 FORMAT (9(F6.1,1X))
S.0021            READ (1,1) W1,W2,W3
S.0022          1 FORMAT (3(E10.3,2X))
            C READ 2
S.0023        100 READ (1,2) IRN,IN
S.0024          2 FORMAT (I10,I6)
S.0025            IF(IRN)118,118,119
S.0026        118 IRN=JRN
S.0027        119 CONTINUE
S.0028            READ (1,6) TCOUL,TMIN,TPAULP,TPAULN,AA,AN,AP
S.0029          6 FORMAT (4(E10.3,2X),3(F4.0,2X))
S.0030            READ (1,17) KCHAR
S.0031         17 FORMAT (I2)
S.0032            WRITE (3,20)
S.0033         20 FORMAT('* P MASS * N MASS*PION MASS*   A   *   N    *   Z    *COUL
           1. E.*MIN. E. *PAULI P *PAULI N *RANDOM NO*NO OF PART.*INC. CHAR.*'
           2)
S.0034            WRITE (3,19)W1,W2,W3,AA,AN,AP,TCOUL,TMIN,TPAULP,TPAULN,IRN,IN,
           1KCHAR
S.0035         19 FORMAT (1H0,10E9.2,3I10)
            C*****SET CONSTANTS FROM DATA
S.0036            ISKIP=50
S.0037            W2C2=W2
S.0038            EMINPI=TTOE(TMIN,W3)
S.0039            EMIN=TTOE(TMIN,W1)
S.0040            EPAULP=TTOE(TPAULP,W1)
S.0041            EPAULN=TTOE(TPAULN,W2)
            C*****SET INITIAL CONDITIONS
S.0042            DO 43 I=1,21
S.0043            DO 43 J=1,100
```

```
S.0044            NPIOUT(I,J)=0
S.0045            NPIIN(I,J)=0
S.0046         43 NNOUT(I,J)=0
S.0047            DO 40 L=1,IN
S.0048        103 IF(ISKIP-40) 301,302,302
S.0049        302 WRITE (3,303)
S.0050        303 FORMAT(98H1*PART.* INC  *INC. PION* OUT  *OUT  PION* ISOBAR  *  IS
                 1OBAR  * PROTON  * NEUTRON * NO *   OUT   */1H ,97H*  NO *CHARGE*
                 2ENERGY *CHARGE*  ENERGY *MASS(MEV)* PC (MEV) *  ENERGY *  ENERGY *
                 3COL.*DIRECTION*)
S.0051            IPAGE=IPAGE&1
S.0052            WRITE (3,304) IPAGE
S.0053        304 FORMAT(T120,'PAGE  ',I4)
S.0054            ISKIP=0
              C START
S.0055        301 ICOL=0
S.0056            NO=0
S.0057            CALL RANDU(IRN,JRN,RN)
S.0058             IRN=JRN
S.0059            INT=20.*RN&1.
S.0060            CALL RANDU(IRN,JRN,RN)
S.0061             IRN=JRN
S.0062            TINIT=TINT(INT)&RN*(TINT(INT&1)-TINT(INT))
S.0063            TINI =TINIT-TCOUL&TMIN
S.0064            EINIT=TTOE(TINI ,W3)
S.0065            E=EINIT
S.0066            W1C2=W3
S.0067            WAFT=W1C2
S.0068            NUCL=-1
S.0069            ICHAR=KCHAR
S.0070            I=1
S.0071            K=1
                  C
                  C     SELECT IMPACT POSITION
S.0072            XPOS=0.
S.0073            YPOS=0.
S.0074            ZPOS=1.
S.0075            CALL RANDU(IRN,JRN,RN)
S.0076             IRN=JRN
S.0077            ZDIR=1.-2.*RN
S.0078            YDIR=SQMXSB(ZDIR)
S.0079            XDIR=0.
              C*****FOLLOW PARTICLE TILL IT STRIKES AND FIND NEW CONDITIONS
              C FOLLOW
S.0080            INT=.1*TINIT+1.
S.0081            IMT=10.*(ZDIR+1.)+1.
S.0082            NPIIN(IMT,INT)=NPIIN(IMT,INT)+1
                  C
              C PION OR NUCLEON
S.0083        116 IF (NUCL) 28,106,106
                  C     CALCULATE X-SECTION FOR PIONS
S.0084         28 T=ETOT(E,W3)
S.0085            IF (T-720.) 130,131,131
S.0086        131 SIGIJ=50.
S.0087            GO TO 132
```

```
S.0088      130 INT=T/90.&1.
S.0089          AINT=INT-1
S.0090          SIGIJ=SECIJ(INT)&((T-AINT*90.)/90.)*(SECIJ(INT&1)-SECIJ(INT))
S.0091      132 IF (T-580.) 133,134,134
S.0092      134 SIGII=20.
S.0093          GO TO 135
S.0094      133 INT=T/58.&1.
S.0095          AINT=INT-1
S.0096          SIGII=SECII(INT)&((T-AINT*58.)/58.)*(SECII(INT&1)-SECII(INT))
S.0097      135 IF (ICHAR) 136,137,138
S.0098      136 PS=AP*SIGIJ
S.0099          SN=AN*SIGII
S.0100          GO TO 38
S.0101      137 PS=AP*(SIGII&SIGIJ)*.5
S.0102          SN=AN*(SIGII&SIGIJ)*.5
S.0103          GO TO 38
S.0104      138 PS=AP*SIGII
S.0105          SN=AN*SIGIJ
S.0106          GO TO 38
            C     CALCULATE X-SECTION FOR NUCLEONS
S.0107      106 ESQ=E*E
S.0108          BETSQ=ESQ/(ESQ&W1*W1)
S.0109          BET=BETSQ**.5
S.0110          SIGII=(10.63-29.92*BET&42.9*BETSQ)/BETSQ
S.0111          SIGIJ=(34.10-82.2*BET&82.2*BETSQ)/BETSQ
S.0112          IF (NUCL) 34,34,33
S.0113       33 PS=AP*SIGII
S.0114          SN=AN*SIGIJ
S.0115          GO TO 38
S.0116       34 PS=AP*SIGIJ
S.0117          SN=AN*SIGII
S.0118       38 SIGMA=(PS&SN)/AA
S.0119       37 AMBDA=41.888*RZERO*RZERO/(SIGMA*AA**.3333333)
S.0120          PROBP=PS/(PS&SN)
S.0121      101   CALL RANDU(IRN,JRN,RN)
S.0122              IRN=JRN
            C     DETERMINE IF COLLISION IS WITH A PROTON OR A NEUTRON
S.0123          IF (PROBP-RN) 36,35,35
S.0124       35 NUCL2=1
S.0125          GO TO 102
S.0126       36 NUCL2=0
S.0127      102   CALL RANDU(IRN,JRN,RN)
S.0128              IRN=JRN
            C     NOW CALCULATE THE PENETRATION
S.0129          DIST=-AMBDA*ALOG(RN)
            C PION OR NUCLEON
S.0130          IF (NUCL) 320,321,321
S.0131      320 IF (E-EMINPI) 322,321,321
S.0132      322 DIST=0.
            C     CALCULATE THE NEW POSITION
S.0133      321 XPOS=XPOS&XDIR*DIST
S.0134          YPOS=YPOS&YDIR*DIST
S.0135          ZPOS=ZPOS&ZDIR*DIST
            C
            C     CHECK IF STILL INSIDE THE NUCLEUS
```

```
S.0136          0=XPOS*XPOS&YPOS*YPOS&ZPOS*ZPOS
S.0137          IF(1.0000001-0)  21,152,152
C GO TO OUTPUT 1 IF OUTSIDE OF NUCLEUS
C
C PION OR NUCLEON
C       DECIDE IF CHARGE EXCHANGE OCCURS
S.0138      152 IF (NUCL) 140,22,22
S.0139      140 CALL RANDU(IRN,JRN,RN)
S.0140          IRN=JRN
S.0141          RNG=RN-.3333333
S.0142          NN=ICHAR&NUCL2
S.0143          NNU=NN&2
S.0144          GO TO (22,144,146,22),NNU
S.0145      144 IF(RNG) 145,147,147
S.0146      145 ICHAR=-1
S.0147          GO TO 154
S.0148      147 ICHAR=0
S.0149          GO TO 154
S.0150      146 IF(RNG) 148,147,147
S.0151      148 ICHAR=&1
S.0152      154 NUCL2=NN-ICHAR
C
C       SELECT ANGLES IN CM
S.0153       22 CALL RANDU(IRN,JRN,RN)
S.0154          IRN=JRN
S.0155          QDIR=1.-2.*RN
S.0156          CALL RANDU(IRN,JRN,RN)
S.0157          IRN=JRN
S.0158          PHICM=2.*PI*RN
S.0159      171 ICOL=ICOL&1
S.0160          X1=XDIR
S.0161          Y1=YDIR
S.0162          Z1=ZDIR
S.0163          E1=E
C
C       FIND THE ENERGY AND DIRECTION OF STRUCK NUCLEON
S.0164          IF (NUCL2) 123,123,122
S.0165      122 EPAULI=EPAULP
S.0166          GO TO 124
S.0167      123 EPAULI=EPAULN
S.0168      124 CALL RANDU(IRN,JRN,RN)
S.0169          IRN=JRN
S.0170          EFERMI=EPAULI*RN**.3333333
S.0171          CALL RANDU(IRN,JRN,RN)
S.0172          IRN=JRN
S.0173          ZRST=1.-2.*RN
S.0174          QRST=SQMXSB(ZRST)
S.0175          CALL RANDU(IRN,JRN,RN)
S.0176          IRN=JRN
S.0177          TETA=2.*PI*RN
S.0178          XIQ=COS(TETA)
S.0179          YIQ=SIN(TETA)
S.0180          IF(W2C2)169,169,161
C
C       NOW FIND THE ENERGY AND DIRECTION IN LAB SYSTEM
```

```
S.0181      190  CALL RANDU(IRN,JRN,RN)
S.0182             IRN=JRN
S.0183           QDIR=1.-2.*RN
S.0184           CALL RANDU(IRN,JRN,RN)
S.0185             IRN=JRN
S.0186           PHICM=2.*PI*RN
                 C     PION ABSORBED
S.0187       162 CALL RANDU(IRN,JRN,RN)
S.0188             IRN=JRN
                 C     DETERMINE IF THIRD PARTICLE IS A PROTON OR A NEUTRON
S.0189           IF (RN-AP/AA) 163,164,164
S.0190       163 NNO=NN&3
S.0191           GO TO 173
S.0192       164 NNO=NN&2
S.0193       173 GO TO (162,165,166,166,162),NNO
S.0194       165 NUCL2=0
S.0195           GO TO 168
S.0196       166 NUCL2=1
S.0197       168 CALL LBRSTB (QRST,XIO,YIO,ZRST,EFERMI,X1,Y1,Z1,E1)
S.0198           NUCL3=NNO-NUCL2-2
                 C     CALCULATE THE MASS AND THE VELOCITY OF THE ISOBAR
S.0199           UPRIM=W2C2&SSTSOB(E1,W1C2)
S.0200           BCM1=E1/UPRIM
S.0201           W4=(UPRIM-BCM1*E1)/SOMXSB(BCM1)
S.0202           W1C2=W4
S.0203           W2C2=0.
S.0204           CALL RSTLAB (QRST,XIO,YIO,ZRST,X1,Y1,Z1,E1)
                 C OUTPUT 2
S.0205           WRITE (3,4) L,KCHAR,TINIT,NN,W4,E1,ICOL
S.0206         4 FORMAT(1H0,2X,I4,3X,I2,3X,F9.2,2X,1H*,I2,13X,F9.2,1X,F10.2,21X,I3)
S.0207           ISKIP=ISKIP&2
S.0208           ICOL=0
S.0209           IF (NUCL3) 123,123,122
S.0210       169 CONTINUE
S.0211       172 W2C2=W2
                 C     CALCULATE THE ENERGY AND DIRECTION OF THE OUTCOMING NUCLEONS
S.0212           CALL LBRSTB (QRST,XIO,YIO,ZRST,EFERMI,X1,Y1,Z1,E1)
S.0213           WAFT=W2C2
S.0214           CALL CMSLOB (X1,Y1,Z1,E1,QDIR,PHICM,X2,Y2,Z2,E2)
S.0215           W1C2=W2C2
S.0216           CALL RSTLAB (QRST,XIO,YIO,ZRST,X1,Y1,Z1,E1)
S.0217           CALL RSTLAB (QRST,XIO,YIO,ZRST,X2,Y2,Z2,E2)
S.0218           NUCL=NUCL3
                 C GO TO STORE
S.0219           GO TO 32
                 C     ELASTIC COLLISIONS
S.0220       161 CALL LBRSTB (QRST,XIO,YIO,ZRST,EFERMI,X1,Y1,Z1,E1)
S.0221           CALL CMSLOB (X1,Y1,Z1,E1,QDIR,PHICM,X2,Y2,Z2,E2)
S.0222           CALL RSTLAB (QRST,XIO,YIO,ZRST,X1,Y1,Z1,E1)
S.0223           W5=W1C2
S.0224           W1C2=W2C2
S.0225           CALL RSTLAB (QRST,XIO,YIO,ZRST,X2,Y2,Z2,E2)
S.0226           W1C2=W5
                 C*****AND CHECK IF PARTICLES ARE WORTHWHILE TO FOLLOW
                 C
```

```
C     CHECK IF ENERGY OF SECONDARY IS GREATER THAN EPAULY AND EMIN
      IF (NUCL2) 109,109,108
  108 EPAULI=EPAULP
      GO TO 110
  109 EPAULI=EPAULN
  110 IF (E2-EPAULI) 180,23,23
  180 IF (NUCL) 190,102,102
   23 IF (NUCL) 32,112,111
  111 EPAULI=EPAULP
      GO TO 113
  112 EPAULI=EPAULN
  113 IF(E1-EPAULI) 102,32,32
   32 IF(E2-EMIN)117,25,25
C
C     CHECK IF WITHIN DIMENSION
C STORE
   25 IF(I-20) 31,31,30
C
C     AND STORE THE SECONDARY
   31 XSTORE(I)=X2
      YSTORE(I)=Y2
      ZSTORE(I)=Z2
      ESTORE(I)=E2
      CAPX(I)=XPOS
      CAPY(I)=YPOS
      CAPZ(I)=ZPOS
      NUCLST(I)=NUCL2
      I=I&1
C
C     FOLLOW  INCIDENT PARTICLE
C PION OR NUCLEON
  117 IF (NUCL)  27,104,104
  104 IF(E1-EMIN) 26,27,27
   26 ICOL=0
      GO TO 105
   27 E=E1
      XDIR=X1
      YDIR=Y1
      ZDIR=Z1
C GO TO FOLLOW
      GO TO 116
C*****OUTPUT AND FOLLOW NEXT PARTICLE
C
C     OUT ROUTINE
   21 TFIN=ETOT(E,WIC2)
      TFIN=TFIN&TCOUL-TMIN
C OUTPUT 1
  115 IF (NUCL) 150,120,39
  150 WRITE (3,16) L,KCHAR,TINIT,ICHAR,TFIN,ICOL,XDIR,YDIR,ZDIR
   16 FORMAT(1H0,I6,I5,F12.2,I5,F12.2,42X,I3,F10.4,F10.4,F10.4)
      IMT=10.*(ZDIR+1.)+1.
      INT=.1*TFIN+1.
      IF(ICHAR)141,142,143
  141 NPIOUT(IMT,INT)=NPIOUT(IMT,INT)+1
      GO TO 139
```

```
S.0268      142 NPIOUT(IMT,INT)=NPIOUT(IMT,INT)+1000
S.0269          GO TO 139
S.0270      143 NPIIN(IMT,INT)=NPIIN(IMT,INT)+1000
S.0271      139 CONTINUE
S.0272          ISKIP=ISKIP&1
S.0273          GO TO 300
S.0274       39 WRITE (3,14) TEIN,ICOL,XDIR,YDIR,ZDIR
S.0275       14 FORMAT(1H ,62X,F9.2,11X,I3,F10.4,F10.4,F10.4)
S.0276          IF(TEIN-0.) 300,311,311
S.0277      311 INT=.1*TEIN+1.
S.0278          IMT=10.*(ZDIR+1.)+1.
S.0279          NNOUT(IMT,INT)=NNOUT(IMT,INT)+1
S.0280          GO TO 300
S.0281      120 WRITE (3,15) TEIN,ICOL,XDIR,YDIR,ZDIR
S.0282       15 FORMAT(1H ,72X,F9.2,I4,F10.4,F10.4,F10.4)
S.0283          IF(TEIN-0.) 300,312,312
S.0284      312 INT=.1*TEIN+1.
S.0285          IMT=10.*(ZDIR+1.)+1.
S.0286          NNOUT(IMT,INT)=NNOUT(IMT,INT)+1000
S.0287      300 ISKIP=ISKIP&1
S.0288          ICOL=0
            C     CHECK IF ANY PARTICLES ARE LEFT IN STORAGE
S.0289      105 IF (I-K)40,40,29
S.0290       29 E=ESTORE(K)
S.0291          XDIR=XSTORE(K)
S.0292          YDIR=YSTORE(K)
S.0293          ZDIR=ZSTORE(K)
S.0294          XPOS=CAPX(K)
S.0295          YPOS=CAPY(K)
S.0296          ZPOS=CAPZ(K)
S.0297          NUCL=NUCLST(K)
S.0298          WIC2=W2
S.0299          WAFT=WIC2
S.0300          K=K&1
            C GO TO FOLLOW
S.0301          GO TO 106
            C
            C     REJECTION  ROUTINE
S.0302       30 WRITE (3,10)
S.0303       10 FORMAT (1HC,19HTOO MANY COLLISIONS)
            C GO TO START
S.0304       40 CONTINUE
            C OUTPUT 3
S.0305       18 FORMAT(1X,I4,20I6,I7)
S.0306       62 FORMAT('0TOT ',21I6)
S.0307        9 FORMAT('0 -1.0  -0.9  -0.8  -0.7  -0.6  -0.5  -0.4  -0.3  -0.2  -0
                1.1   0.0   0.1   0.2   0.3   0.4   0.5   0.6   0.7   0.8   0.9   1
                2.0  TOT'//)
S.0308       12  FORMAT('1')
S.0309          WRITE (3,8)
S.0310          WRITE(3,9)
S.0311        8 FORMAT(74H1INPUT PION E-A DIST.(UNITS) AND POSITIVE OUTPUT PION E-
                1A DIST.(THOUSANDS))
S.0312          DO 50 I=1,21
S.0313       50 NSOM(I)=0
```

```
S.0314          DO 47 J=1,100
S.0315          JEN=J*10-10
S.0316          NSUM=0
S.0317          DO 53 I=1,21
S.0318          NSOM(I)=NSOM(I)+NPIIN(I,J)
S.0319       53 NSUM=NSUM+NPIIN(I,J)
S.0320          IF(J-51) 47,45,47
S.0321       45 WRITE(3,12)
S.0322          WRITE(3,9)
S.0323       47 WRITE (3,18) JEN,(NPIIN(I,J),I=1,20),NSUM
S.0324          WRITE (3,62) (NSOM(I),I=1,21)
S.0325          WRITE (3,5)
S.0326          WRITE(3,9)
S.0327        5 FORMAT(60H1OUTPUT PION E-A DIST.NEGATIVE(UNITS) AND NEUTRAL(THOUSA
               1NDS))
S.0328          DO 51 I=1,21
S.0329       51 NSOM(I)=0
S.0330          DO 48 J=1,100
S.0331          JEN=J*10-10
S.0332          NSUM=0
S.0333          DO 54 I=1,21
S.0334          NSOM(I)=NSOM(I)+NPIOUT(I,J)
S.0335       54 NSUM=NSUM+NPIOUT(I,J)
S.0336          IF(J-51)48,44,48
S.0337       44 WRITE (3,12)
S.0338          WRITE(3,9)
S.0339       48 WRITE (3,18) JEN,(NPIOUT(I,J),I=1,20),NSUM
S.0340          WRITE (3,62) (NSOM(I),I=1,21)
S.0341          WRITE (3,7)
S.0342        7 FORMAT(56H1OUTPUT PROTONS(UNITS) AND NEUTRONS(THOUSANDS) E-A DIST.
               1)
S.0343          WRITE(3,9)
S.0344          DO 52 I=1,21
S.0345       52 NSOM(I)=0
S.0346          DO 49 J=1,100
S.0347          JEN=J*10-10
S.0348          NSUM=0
S.0349          DO 55 I=1,21
S.0350          NSOM(I)=NSOM(I)+NNOUT(I,J)
S.0351       55 NSUM=NSUM+NNOUT(I,J)
S.0352          IF (J-51) 49,46,49
S.0353       46 WRITE (3,12)
S.0354          WRITE(3,9)
S.0355       49 WRITE (3,18) JEN,(NNOUT(I,J),I=1,20),NSUM
S.0356          WRITE (3,62) (NSOM(I),I=1,21)
             C GO TO READ 2
S.0357          GO TO 100
S.0358     1191 IN=IN-L&1
S.0359          WRITE (2,2) IRN,IN
S.0360          STOP
S.0361          END

          SIZE OF COMMON  000024   PROGRAM  036112

                    END OF COMPILATION  MAIN
```

```
LEVEL0  10CT67                    IBM OS/360 BASIC FORTRAN IV (E) COMPILATION

S.0001          SUBROUTINE LBRSTB (Q,XIQ,YIQ,Z2,ES,X,Y,Z,E)
S.0002          COMMON W1,W2,BETA,GAMMA
                C
                C       ROTATE AXIS INTO DIRECTION OF MOTION
S.0003          XP=Q*(XIQ*X&YIQ*Y)&Z2*Z
S.0004          YP=XIQ*Y-YIQ*X
S.0005          ZP=Q*Z-Z2*(XIQ*X&YIQ*Y)
                C       FIND THE MOMENTA
                C       FIND RELATIVISTIC CONSTANTS BETA ,GAMMA AND U
S.0006          BETA=ES/SSTSQR(ES,W2)
S.0007          GAMMA=1./SQMXSR(BETA)
S.0008          U=SSTSQR(E,W1)
                C       DO RELATIVISTIC TRANSFORMATION ON MOMENTA
S.0009          XP=GAMMA*(XP-BETA*U/E)
                C       CALCULATE NEW E,X,Y,Z
S.0010          SUM=SUMSQR(XP,YP,ZP)
S.0011          E=SUM*E
S.0012          SINV=1./SUM
S.0013          X=XP*SINV
S.0014          Y=YP*SINV
S.0015          Z=ZP*SINV
S.0016          RETURN
S.0017          END

                  SIZE OF COMMON   000016    PROGRAM  000756

                                END OF COMPILATION  LBRSTB

LEVEL0  10CT67                    IBM OS/360 BASIC FORTRAN IV (E) COMPILATION

S.0001          SUBROUTINE RSTLAB (Q,XIQ,YIQ,Z2,X,Y,Z,E)
S.0002          COMMON W1,W2,B,G
S.0003          U=SSTSQR(E,W1)
S.0004          X=G*(X&B*U/E)
S.0005          SUM=SUMSQR(X,Y,Z)
S.0006          E=SUM*E
S.0007          SUMINV=1./SUM
S.0008          X=X*SUMINV
S.0009          Y=Y*SUMINV
S.0010          Z=Z*SUMINV
S.0011          COM=Q*X-Z2*Z
S.0012          Z=Z2*X&Q*Z
S.0013          X=XIQ*COM-YIQ*Y
S.0014          Y=YIQ*COM&XIQ*Y
S.0015          RETURN
S.0016          END

                  SIZE OF COMMON   000016    PROGRAM  000652

                                END OF COMPILATION  RSTLAB
```

```
S.0001          SUBROUTINE CMSLOB (X,Y,Z,E,ODIR,PHICM,X2,Y2,Z2,E2)                HM000011
                C   THIS SUBROUTINE IS DESIGNED TO CALCULATE THE EXIT ENERGY AND   HM000011
                C   DIRECTION OF A PARTICLE OF GIVEN INCIDENT ENERGY AND DIRECTION HM000011
                C   WHICH IS SCATTERED THROUGH ANGLES TETA AND PHI IN THE CM SYSTEM. HM000011
                C   THE RECOIL ENERGY AND DIRECTION OF THE TARGET ARE ALSO CALCULATED.HM000011
S.0002          COMMON W1C2,W2C2,ABC,ABD,RN,W                                     HM000011
                C   CALCULATE THE MOMENTUM OF THE PARTICLE IN THE CM BEFORE COLLISION.HM000011
S.0003          U=SSTSQB(E,W1C2)                                                  HM000011
S.0004          BETACM=E/(U&W2C2)
S.0005          GAMACM=1./SQMXSB(BETACM)
S.0006          PCMBEF=BETACM*W2C2*GAMACM
S.0007          UCM1=SSTSQB(PCMBEF,W1C2)
S.0008          UCM2=SSTSQB(PCMBEF,W2C2)
S.0009          IF (W1C2-W) 32,33,32
S.0010       32 UCM1=(UCM1&UCM2)*.5
S.0011          UCM2=UCM1
S.0012          PCMBEF=(UCM1*UCM1-W*W)**.5
                C   CALCULATE THE MOMENTUM IN CM AFTER COLLISION.                  HM000011
S.0013       33 PCMAFX=PCMBEF*ODIR
S.0014          PCMAYZ=PCMBEF*SQMXSB(ODIR)
S.0015          PAFY=PCMAYZ*SIN(PHICM)
S.0016          PAFZ=PCMAYZ*COS(PHICM)
                C   TRANSFORM TO LAB PRIMED SYSTEM.                               HM000011
S.0017          PAFX=GAMACM*(BETACM*UCM1&PCMAFX)                                  HM000011
                C   NOW CALCULATE E,X,Y,Z                                         HM000011
S.0018          I=0
S.0019          Q=SSTSQB(X,Y)
S.0020       21 IF (Q) 31,31,30
S.0021       30 PX=PAFX*X-(PAFY*Y&PAFZ*Z*X)/Q                                     HM000011
S.0022          PY=PAFX*Y&(PAFY*X-PAFZ*Z*Y)/Q                                     HM000011
S.0023          PZ=PAFX*Z&PAFZ*Q                                                  HM000011
S.0024          GO TO 20                                                          HM000011
S.0025       31 PX=-PAFZ*Z                                                        HM000011
S.0026          PY=PAFY                                                           HM000011
S.0027          PZ=PAFX*Z                                                         HM000011
S.0028       20 PSQR=SUMSQB(PX,PY,PZ)
S.0029          I=I&1                                                             HM000011
S.0030          GO TO (22,23),I                                                   HM000011
S.0031       22 E1=PSQR
S.0032          X1=PX/PSQR
S.0033          Y1=PY/PSQR
S.0034          Z1=PZ/PSQR
                C   AND CALCULATE E2,X2,Y2,Z2                                     HM000011
S.0035          PAFY=-PAFY                                                        HM000011
S.0036          PAFZ=-PAFZ                                                        HM000011
S.0037          PAFX=GAMACM*(BETACM*UCM2-PCMAFX)                                  HM000011
S.0038          GO TO 21
S.0039       23 E2=PSQR                                                           HM000011
S.0040          X2=PX/PSQR                                                        HM000011
S.0041          Y2=PY/PSQR                                                        HM000011
S.0042          Z2=PZ/PSQR
S.0043          E=E1
S.0044          X=X1
```

```
S.0045          Y=Y1                                                    HM000011
S.0046          Z=Z1                                                    HM000011
S.0047          RETURN
S.0048          END
```

SIZE OF COMMON 000024 PROGRAM 001356

END OF COMPILATION CMSLOB

LEVEL0 10CT67 IBM OS/360 BASIC FORTRAN IV (E) COMPILATION

```
S.0001          SUBROUTINE RANDU(IX,IY,YFL)                             RANDU040
S.0002          IY=IX*65539                                             RANDU041
S.0003          IF(IY)5,6,6                                             RANDU042
S.0004        5 IY=IY&2147483647&1                                      RANDU043
S.0005        6 YFL=IY                                                  RANDU044
S.0006          YFL=YFL*.4656613E-9                                     RANDU045
S.0007          RETURN                                                  RANDU046
S.0008          END                                                     RANDU047
```

SIZE OF COMMON 000000 PROGRAM 000400

END OF COMPILATION RANDU

LEVEL0 10CT67 IBM OS/360 BASIC FORTRAN IV (E) COMPILATION

```
S.0001          FUNCTION SOMXSB(X)
S.0002          DOUBLE PRECISION SOM
S.0003          SOM=(0.1D+01-X*X)**.5
S.0004          SOMXSB=SOM
S.0005          RETURN
S.0006          END
```

SIZE OF COMMON 000000 PROGRAM 000344

END OF COMPILATION SOMXSB

LEVEL0 10CT67 IBM OS/360 BASIC FORTRAN IV (E) COMPILATION

```
S.0001          FUNCTION SUMSQR(X,Y,Z)
S.0002          SUMSQR=(X*X&Y*Y&Z*Z)**.5
S.0003          RETURN
S.0004          END
```

SIZE OF COMMON 000000 PROGRAM 000356

END OF COMPILATION SUMSQR

LEVEL 0 10CT67 IBM OS/360 BASIC FORTRAN IV (E) COMPILATION

```
S.0001          FUNCTION SSTSQR(X,Y)
S.0002          SSTSQR=(X*X&Y*Y)**.5
S.0003          RETURN
S.0004          END
```

SIZE OF COMMON 000000 PROGRAM 000316

END OF COMPILATION SSTSQR

PART. NO	*INC. CHARGE*	*INC. PION* ENERGY	*OUT CHARGE*	*OUT PION* ENERGY	ISOBAR *MASS(MEV)*	ISOBAR * PC (MEV)	PROTON * ENERGY	NEUTRON * ENERGY	NO *COL.	OUT *DIRECTION*	
31	0	166.75	0	166.75					0	0.0	0.5983
32	0	433.47	* 0		1170.33	386.95			5		
								167.47	0	0.6658	-0.0010
								24.85	2	-0.9213	0.1524
							48.30		0	-0.0827	0.7153
								9.73	1	0.1654	0.8695
								33.51	2	-0.7583	0.2033
								8.40	5	0.5960	-0.4613
								89.37	1	-0.4060	-0.4950
33	0	334.19	0	226.50					1	0.7876	0.5607
								6.19	5	-0.4163	0.1541
								6.56	3	-0.0471	-0.8117
34	0	52.84	0	52.84					0	0.0	0.9877
35	0	29.69	0	29.69					0	0.0	0.
36	0	311.50	0	311.50					0	0.0	0.
37	0	27.50	0	27.50					0	0.0	0.
38	0	217.86	* 1		1121.93	296.44			5		
								3.55	5	0.4169	-0.7147
							43.27		0	-0.3063	-0.7969
							3.27		1	0.2188	-0.7770
							173.04		0	-0.0196	-0.7705
								11.07	0	0.5368	0.5309
								12.74	2	0.9724	-0.1072
39	0	147.20	* 1		1237.47	320.29			1		
								17.64	3	0.0312	0.1892
							106.27		0	-0.8598	-0.2688
							152.50		0	0.6890	0.1051
40	0	189.58	0	189.58					0	0.0	0.3692
41	0	137.15	0	137.15					0	0.0	0.3394

Appendix 4 **Kinematics**

In this appendix, the explicit rotation and relativistic transformation matrices used in the subroutines LBRSTB, CMSLOB and RSTLAB are described. With the help of these subroutines the final momenta of two particles involved in a collision may be calculated.

The first subroutine, LBRSTB, transforms the incident particle to the rest frame of the target nucleon. This is accomplished by a rotation of the laboratory frame so that the target particle moves along the x-axis, followed by a relativistic transformation. Figure 37 shows the direction of the target nucleon in the laboratory frame, before and after the rotation.

The total rotation (R_1) consists of a rotation about the z-axis through an angle ϕ, followed by a rotation about the new y-axis through an angle $(\pi/2 - \theta)$. The two rotations are:

$$R_1 = \begin{pmatrix} \sin\theta & 0 & \cos\theta \\ 0 & 1 & 0 \\ -\cos\theta & 0 & \sin\theta \end{pmatrix} \begin{pmatrix} \cos\phi & \sin\phi & 0 \\ -\sin\phi & \cos\phi & 0 \\ 0 & 0 & 1 \end{pmatrix}$$

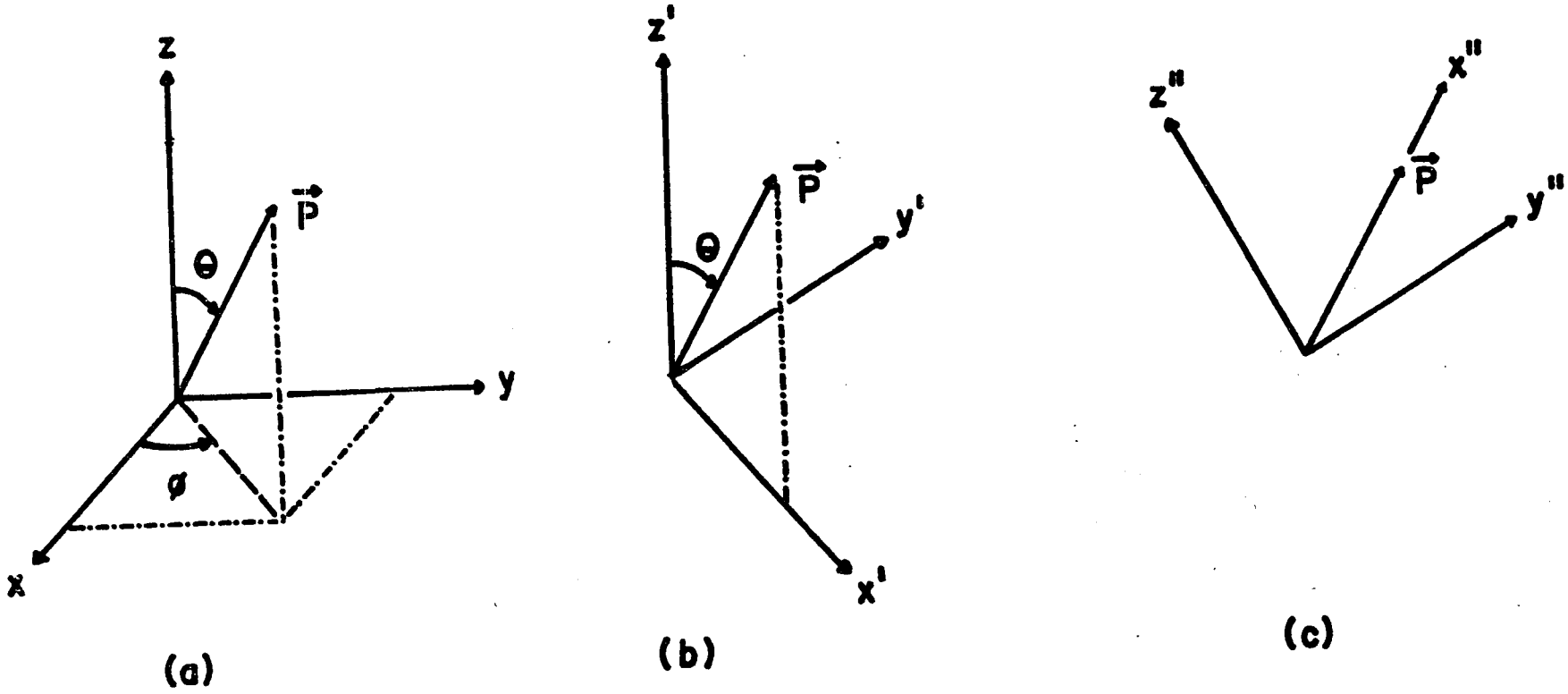

Figure 37- Geometry Used in Kinematic Subroutines

(a) Particle with Momentum $\vec{P}$ in Laboratory Frame

(b) Rotation of Laboratory Frame Through an Angle ø About the z-axis

(c) Additional Rotation Through an Angle $\pi/2 - \Theta$ About New y-axis (y')

$$R_1 = \begin{pmatrix} \sin\theta\cos\phi & \sin\theta\sin\phi & \cos\theta \\ -\sin\phi & \cos\phi & 0 \\ -\cos\theta\cos\phi & -\cos\theta\sin\phi & \sin\theta \end{pmatrix}$$

The quantities $\sin\theta$, $\cos\theta$, $\sin\phi$ and $\cos\phi$ are obtained from the main programme. This rotation is only applied to the momentum $\vec{R}_1$,

$$\vec{P}_1 = \begin{pmatrix} p_{x_1} \\ p_{y_1} \\ p_{z_1} \end{pmatrix}$$

of the incident particle, since the struck particle will be along the x-axis.

This rotation is followed by a relativistic transformation to the rest frame of the struck nucleon. The transformation is applied to the momentum four-vector $\overleftarrow{P}_1$,

$$\overleftarrow{P}_1 = \begin{pmatrix} p_{x_1} \\ p_{y_1} \\ p_{z_1} \\ iU_1 \end{pmatrix}$$

where U_1 , given by*:

$$U_1 = (\vec{P}_1^{\,2} + M_1^{\,2})^{1/2}$$

is the total energy of the particle, and M_1 is the rest mass.

The velocity, β_1, of the moving frame is the velocity of the struck particle, given by:

$$\beta_1 = \frac{|\vec{P}_2|}{(\vec{P}_2^{\,2} + M_2^{\,2})^{1/2}}$$

where $\vec{P}_2$ and M_2 are the momentum and mass of the struck particle. Also required is γ_1, given by:

$$\gamma_1 = \frac{1}{(1 - \beta_1^{\,2})^{1/2}}$$

Then the transformation (T_1) is given by:

---

*Units, such that the velocity of light equals unity (c = 1), were used throughout the programme.

$$T_1 = \begin{pmatrix} \gamma_1 & 0 & 0 & i\,\gamma_1\beta_1 \\ 0 & 1 & 0 & 0 \\ 0 & 0 & 1 & 0 \\ -i\,\gamma_1\beta_1 & 0 & 0 & \gamma_1 \end{pmatrix}$$

This transformation is again only applied to the incident particle, since the struck particle will be at rest.

The two transformations may be combined, but in computing it is more efficient to do them individually.

At the end of subroutine LBRSTB, the incident particle will have been transformed to the appropriate rest frame of the struck nucleon. This information is supplied to the next subroutine CMSLOB, which transforms both particles to their centre of mass, determines their new direction and momentum in the centre of mass after the collision and then transforms them back to the original rest frame of the struck nucleon.

First a rotation is again performed. This time the frame is rotated so that the incident particle moves along the x-axis. The rotation is identical to R_1, except that now the values of $\cos\theta$, $\sin\theta$, $\cos\phi$ and $\sin\phi$ are calculated from the direction cosines (x,y,z) of the incident particle in the rest frame of the struck nucleon. The expressions are:

$$\cos\theta = z$$

$$\sin\theta = (1-z^2)^{1/2} = (x^2+y^2)^{1/2} = Q$$

$$\cos\phi = x/Q$$

$$\sin\phi = y/Q$$

so that the rotation* R_2 is:

$$R_2 = \begin{pmatrix} x & y & z \\ -y/Q & x/Q & 0 \\ -zx/Q & -zy/Q & Q \end{pmatrix}$$

The rotation is not actually applied to either particle, since it is known that the incident particle will be moving

---

*If the particle is moving along the z-axis, Q will be zero, so that x/Q and y/Q are indeterminate. In that case, ϕ is chosen to be zero, and thus x/Q = 1 and y/Q = 0 giving the transformation:

$$R_2 = \begin{pmatrix} 0 & 0 & z \\ 0 & 1 & 0 \\ -z & 0 & 0 \end{pmatrix}$$

along the x-axis, while the struck particle is stationary. However, R_2 will be used later, to obtain the inverse transformation, R_2^{-1}.

Next a relativistic transformation is performed to the centre of mass frame of the two particles. If

$$U_1' = (\vec{P}_1'^{\,2} + M_1^{\,2})^{1/2}$$

is the total energy of the incident particles in the rest frame of the struck particle, where $\vec{P}_1'$ and M_1 are its momentum and mass, and if M_2 is the mass of the struck particle, then the velocity of the centre of mass, β_2, is given by:

$$\beta_2 = \frac{|\vec{P}_1'|}{U_1' + M_2}$$

and

$$\gamma_2 = \frac{1}{(1 - \beta_2^{\,2})^{1/2}}$$

In the centre of mass, the momenta, $\vec{P^*}$, are equal but opposite, and are given by:

$$|\vec{P^*}| = \beta_2 \gamma_2 M_2$$

since the velocity of the struck particle in the centre of mass is β_2. (This can also be obtained by using a transformation similar to T_1, where β_2 and γ_2 have been substituded for β_1 and γ_1, and applying this transformation, (T_2), to the momentum four-vectors of either of the particles).

The total energy, U^*, in the centre of mass system is given by:

$$U^* = (\vec{P^*}^2 + M_1^2)^{1/2} + (\vec{P^*}^2 + M_2^2)^{1/2}$$

and this quantity must be conserved.

Since both particles are now in the centre of mass and moving along the x-axis, the collision can proceed. The programme determines the new directions in the centre of mass and the new momenta are calculated. If the masses do not change, the momentum before and after will be the same; however, if the masses after are different, and given by M_3 and M_4, and the momentum is $\vec{P_A^*}$, then:

$$U^* = (\vec{P_A^*}^2 + M_3^2)^{1/2} + (\vec{P_A^*}^2 + M_4^2)^{1/2}$$

so that:

$$\left| \overrightarrow{P_A^*} \right| = \left\{ \left(\frac{U^{*2} + M_4^2 - M_3^2}{2U^*} \right)^2 - M_4^2 \right\}^{1/2}$$

In our case, the masses are often equal, so that:

$$\left| \overrightarrow{P_A^*} \right| = \left\{ \left(\frac{U^*}{2} \right)^2 - M_4^2 \right\}^{1/2}$$

This portion, which essentially describes the collision, may be represented by a transformation C. This transformation rotates and transforms the momenta of the particles; all other transformations rotate and transform the frame of reference.

The new momentum four-vectors are transformed back to the original rest frame of the struck nucleon by T_2^{-1} given by:

$$T_2^{-1} = \begin{pmatrix} \gamma_2 & 0 & 0 & -i\beta_2\gamma_2 \\ 0 & 1 & 0 & 0 \\ 0 & 0 & 1 & 0 \\ i\beta_2\gamma_2 & 0 & 0 & \gamma_2 \end{pmatrix}$$

and rotated back, using R_2^{-1}:

$$R_2^{-1} = \begin{pmatrix} x & -y/Q & -zx/Q \\ y & x/Q & -zy/Q \\ z & 0 & Q \end{pmatrix}$$

These transformations are applied to both outcoming particles, and when completed the data is passed on to the subroutine RSTLAB.

The subroutine RSTLAB transforms both particles back to the original laboratory frame. This is accomplished by the inverse transformation T_1^{-1}:

$$T_1^{-1} = \begin{pmatrix} \gamma_1 & 0 & 0 & -i\beta_1\gamma_1 \\ 0 & 1 & 0 & 0 \\ 0 & 0 & 1 & 0 \\ i\beta_1\gamma_1 & 0 & 0 & \gamma_1 \end{pmatrix}$$

and the inverse rotation R_1^{-1}:

$$R_1^{-1} = \begin{pmatrix} \sin\theta\cos\phi & -\sin\phi & -\cos\theta\cos\phi \\ \sin\theta\sin\phi & \cos\phi & -\cos\theta\sin\phi \\ \cos\theta & 0 & \sin\theta \end{pmatrix}$$

These transformations are again applied to both particles.

The resultant momenta and directions are made available to the main programme.

In summary, the following transformations are applied (explicitly or implicitly):

$$R_1^{-1}\ T_1^{-1}\ R_2^{-1}\ T_2^{-1}\ CT_2\ R_2\ T_1\ R_1$$

That is, first R_1, then T_1, etc.

This method differs from that of Werbrouck [28]; however, both methods require the same number of transformations to be applied explicitly.

REFERENCES

1- E. Fermi, Prog. Theor. Phys. 5, 570 (1950)

2- F. Cerulus, Nuovo Cim. 14, 827 (1959)

3- K. Zalewski and J. Danysz, Nucl. Phys. B2, 249 (1967)
J. Hébert and H. Mes, Nucl. Phys. B4, 244 (1968)

4- W.H. Barkas et al., Phys. Rev. 105, 1037 (1957)
O. Chamberlain et al., Phys. Rev. 113, 1615 (1959)

5- K.A. Brueckner et al, Phys. Rev. 84, 258 (1951)

6- Z. Fraenkel, Phys. Rev. 130, 2407 (1963)

7- H. Mes et al., Prog. Theor. Phys. 35, 566 (1966)
J. Hébert et al., Antiproton Annihilation in Complex Nuclei, Conference on Nuclear Structure and Elementary Particles, Oxford (1966)

8- H. Mes and J. Hébert, π^- Capture in Complex Nuclei, Conference on Nuclear Structure and Elementary Particles, Oxford (1966)

9- C. Baltay et al., Phys. Rev. 145, 1103 (1966)

10- M. Cresti et al., Proceedings of the Sienna Conference on High Energy Physics, 263 (1963)

11- J. Vandermeulen, on the Annihilation of the Protonium, Ecole Internationale de la Physique des Particules Elémentaires, Herceg Novi (1966)

12- A.J. Apostolakis et al., Nuovo Cim. 37, 1364 (1965)

13- D. Tycko, Nevis Laboratories, Columbia University, private communications.

14- L.E. Agnew et al., Phys. Rev. 118, 1371 (1960)

15- H. Horwitz et al., Phys. Rev. 115, 472 (1959)

16- E. Amaldi et al., Nuovo Cim. 14, 977 (1959)

17- A.G. Ekspong et al., Nucl. Phys. 22, 353 (1961)

18- T.D. Lee and C.N. Yang, Nuovo Cim. 3, 749 (1956)

19- B.R. Desai, Phys. Rev. 119, 1390 (1960)

20- A. Bettini et al., Nuovo Cim. 38, 1495 (1965); 42, 695 (1966); 47, 642 (1967)

21- R. Bizzari, Nuovo Cim. 53, 956 (1968)

22- I. Ahmad, University of Ottawa, unpublished.

23- M.N. Focacci and G. Giacomelli, CERN 66-18 NPD (1966)
L.D. Roper et al., Phys Rev. 138, B190 (1965)

24- O. Taussky and J. Todd, Symposium on Monte Carlo Methods, University of Florida, p 15 (1954)

25- IBM Reference Manual C20-8011 (1959)

26- R.P. Chambers, I.E.E.E. Spectrum 4, 48 (Feb. 1967)
M.Greenberger, Commun. A.C.M. 8, 177 (1965)

27- N. Metropolis et al., Phys. Rev. 110, 185 (1958)

28- A. Werbrouck, Proceedings of the 1964 Easter School for Physicists (Volume I), Herceg Novi, CERN 64-13 (1964)

29- F.L. Adelman, Phys. Rev. 85, 249 (1952)
S.A. Azimov et al., Soviet Physics JETP 4, 632 (1957)
W.B. Cheston and L.J.B. Goldfarb, Phys. Rev. 78, 683 (1950)
M.G.K. Menon et al., Phil. Mag. 41, 583 (1950)
D.H. Perkins, Phil. Mag. 40, 601 (1949)

30- H.L. Anderson et al., Phys. Rev. 133, B392 (1964)

31- G. Campos Venuti et al., Nuovo Cim. 34, 1446 (1964);
Phys. Lett. 9, 45 (1964)
H. Davies et al., Nucl. Phys. 78, 663 (1966)

32- S. Ozaki et al., Phys. Rev. Lett. 4, 533 (1960)

33- R.I. Jibuti and I.I. Kopaleiskvili, Nucl. Phys. 55, 337 (1964)
M. Ericson, Phys. Nucl. 258, 1471 (1964)
P. Huguenin, Nucl. Phys. 41, 534 (1963)
M. Jean, Suppl. Nuovo Cim. 2, 400 (1964)

T. Ericson, Phys. Lett. 2, 278 (1962)
J. le Tourneux, Nucl. Phys. 81, 665 (1966)

34- B. Rossi and K. Greisen, Rev. Mod. Phys. 13, 240 (1941)

35- A.H. Morrish, Phys. Rev. 90, 674 (1953)

36- B. Willot-Chemel, Ann. Phys. 6, 703 (1961)

37- G. Bernadini et al., Phys. Rev. 84, 610 (1951)

38- G. Homa et al., Phys. Rev. 93, 554 (1954)

39- R.Z. Grandez and A.F. Clark, Phys. Rev. 97, 791 (1955)

40- H.D. Taft. Phys. Rev. 101, 1116 (1956)

41- Y. Kimura and Y. Nagashima, Prog Theor. Phys. 33, 43 (1965)

42- D.T. Chivers et al., Phys. Lett. 26B, 573 (1968)

Curriculum Vitae

Name: Johannes (Hans) Antoine François Mes

Born: Eindhoven, N.B., The Netherlands, July 1944

Education:

Primary: St. Bergman's R.K.L.S., Bandung, Republic of Indonesia, 1950-1956

Secondary: University of Ottawa High School, Ottawa, Canada, 1956-1960

University: University of Ottawa, Ottawa, Canada, 1960-1968

Degree: B.Sc. (Honours in Experimental Physics) May 1965

Publications:
-H. Mes, I. Ahmad and J. Hébert, Prog. Theor. Phys. 35, 566 (1966)
-J. Hébert and H. Mes, Nucl. Phys. B4, 244 (1968)
-J. Hébert, I. Ahmad and H. Mes, Antiproton Annihilation in Complex Nuclei, Conference on Nuclear Structure and Elementary Particles, Oxford (1966) (ZAED, Gmelin Institute, Frankfurt, Germany)
-H. Mes and J. Hébert, π^- Capture in Complex Nuclei, Conference on Nuclear Structure and Elementary Particles, Oxford (1966) (ZAED, Gmelin Institute, Frankfurt, Germany)

Papers Presented at Meetings:

ACFAS:
-La Résonance (3,3) dans les Noyaux Complexes, I. Ahmad, J. Mes et J. Hébert, (1965)
-Contributions à l'étude de l'Annihilation de l'Antiproton, H. Mes. S. Chakravartty et J. Hébert, (1966)
-Etude des Collisions Inélastiques π^+ - noyau, S. Chakravartty, H. Mes et J. Hébert, (1967)

CAP:
-Antiproton Annihilation in Complex Nuclei, J.

Hébert, I. Ahmad and H. Mes, (1966)

Document for the transfer from M.Sc. status to Ph.D. status.

-Pion Interactions in Complex Nuclei at Intermediate Energies, H. Mes (1966)
Presented to the Department of Physics University of Ottawa.